

Marshall University

Marshall Digital Scholar

Theses, Dissertations and Capstones

2020

Mechanisms of Dopamine-Induced Methamphetamine Neurotoxicity

Melinda L. Asbury
mindyasbury@gmail.com

Follow this and additional works at: <https://mds.marshall.edu/etd>



Part of the [Neuroscience and Neurobiology Commons](#), [Pharmacy and Pharmaceutical Sciences Commons](#), and the [Toxicology Commons](#)

Recommended Citation

Asbury, Melinda L., "Mechanisms of Dopamine-Induced Methamphetamine Neurotoxicity" (2020). *Theses, Dissertations and Capstones*. 1322.
<https://mds.marshall.edu/etd/1322>

This Dissertation is brought to you for free and open access by Marshall Digital Scholar. It has been accepted for inclusion in Theses, Dissertations and Capstones by an authorized administrator of Marshall Digital Scholar. For more information, please contact zhangj@marshall.edu, beachgr@marshall.edu.

MECHANISMS OF DOPAMINE-INDUCED METHAMPHETAMINE NEUROTOXICITY

A dissertation submitted to
the Graduate College of
Marshall University
In partial fulfillment of
the requirements for the degree of
Doctor of Philosophy

In

Biomedical Sciences

by

Melinda L. Asbury, MD

Approved by

Dr. Richard Egleton, Committee Chairperson

Dr. Kelley Kinningham

Dr. Richard Niles

Dr. Gary Rankin

Dr. Monica Valentovic

Marshall University
December 2020

APPROVAL OF DISSERTATION

We, the faculty supervising the work of Melinda Lea Asbury affirm that the dissertation, *Mechanisms of Dopamine-Induced Methamphetamine Neurotoxicity*, meets the high academic standards for original scholarship and creative work established by the Biomedical Sciences and the Marshall University Joan C. Edwards School of Medicine. This work also conforms to the editorial standards of our discipline and the Graduate College of Marshall University. With our signatures, we approve the manuscript for publication.

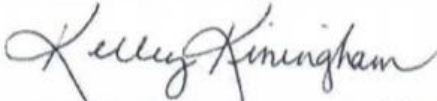
Dr. Richard Egleton, Department of Biomedical Sciences
Committee Chairperson



Date

10/26/20

Dr. Kelley Kinningham, Department of Pharmaceutical Sciences
Committee Co-Chairperson



Date

10-23-20

Dr. Richard Niles, Department of Biomedical Sciences
Committee Member

Date

Dr. Gary Rankin, Department of Biomedical Sciences
Committee Member



Date

10/27/20

Dr. Monica Valentovic, Department of Biomedical Sciences
Committee Member



Date

10-27-20

© 2020
Melinda L. Asbury
ALL RIGHTS RESERVED

DEDICATION

The author wishes to dedicate this work to her family and friends. Without their support and belief, this dissertation would not have been possible. The beginning of my doctoral work to its 100% completion was a very convoluted, difficult, and challenging nine years of work balanced with difficult, almost impossible life circumstances. During that time, it often appeared and seemed as though the actualization of this work was not going to be possible. Through my family's and friends' unwavering belief in me, however, I made it.

I would like to thank the following individuals for their everlasting encouragement. First and foremost, I would like to thank my “Mammow,” Reva Snodgrass, who always told me, “You can do it, I know you can!” She has always been my biggest cheerleader and I will forever be grateful for her and the enormous impact she has had, and continues to have, on my life. I would like to thank my parents, Tammie and Big Ed Asbury, for their support, belief, patience, encouragement, and financial backing for those unforeseen circumstances that often plague MD/PhD, non-combined students. They have consistently served as a source of inspiration and have always given me a feeling of security that no matter what they have my back and are in my corner. I would like to thank my brother, Mike Asbury, for his much needed and perfectly-timed comic relief intermixed with an overt element of pride and belief in me as his sister. What an encouraging combination—pride and belief—that resonated through me when I needed it most. Finally, I would like to thank my loving canine companions, Harley and Henry Asbury. Even after countless late nights, missed walks, and forgotten trips to the park, these two never wavered in their loyalty, love, and companionship. For all of the late nights spent sitting by my side, both crammed in the same chair closest to my desk, I thank you for your everlasting unconditional love and solidarity.

ACKNOWLEDGMENTS

The author of this work would like to thank the Graduate College of Marshall University, Marshall University School of Medicine, and the Graduate Program in Biomedical Sciences for working together, in a combined effort, to navigate the challenges of completing a non-combined, but joint MD/PhD degree program. Also deserving of many thanks are my committee members, Drs. Richard Niles, Gary Rankin, and Monica Valentovic for their time, advisement, and much needed collaboration throughout this project. A special thank you goes to my committee co-chairpersons, Drs. Kelley Kiningham and Richard Egleton. Dr. Kiningham believed in the idea of this novel research and as such provided unparalleled assistance and support ranging from financial to the times she was in the laboratory running experiments with me late at night and on weekends. Her commitment to this project was inspiring and served as a source from which I found myself drawing strength and belief. Dr. Egleton “stepped up” in a big way with the sudden departure of Dr. Kiningham, and as such provided invaluable support during the most critical portion of my doctoral candidacy. His selfless willingness to “adopt” this project has made its completion possible, and I will forever be grateful for his mentorship. I would also like to thank the entire faculty, staff, and other candidates of the Biomedical Sciences Graduate Program, because without all those individuals, then none of this research would have been possible.

TABLE OF CONTENTS

List of Tables	x
List of Figures	xi
Abstract	xiv
Chapter 1	1
Literature Review.....	1
(Meth)amphetamine Abuse, Pharmacology, and Long-Term Consequences	1
Regional Neurotoxicity of Methamphetamine in the Striatum: Implications for Dopamine and the Dopamine D ₁ Receptor	4
Methamphetamine-Induced Dopamine Release and (Nitro)oxidative Stress	7
Key Enzymes in Methamphetamine Neurotoxicity: Friend or Foe?	9
Nitric Oxide Synthase	9
Superoxide Dismutase	10
Aim of Present Study	11
Chapter 2.....	13
Dopamine Stimulation Results in (Nitro)oxidative Protein Changes, Mitochondrial- Mediated Apoptosis, MnSOD Nitration, and Activation of MAPK and AP-1 Signaling Pathways in an <i>in vitro</i> Model of Methamphetamine Neurotoxicity.....	13
Introduction.....	13
Materials and Methods.....	18
Cell culture and treatment paradigm.....	18
Protein preparation and immunoblot analysis.....	18
Transient Transfections and Luciferase Assay	20
(Mn)SOD Activity Assay	21

Evaluation of MnSOD Nitration.....	21
Data analysis	21
Results.....	22
Markers of (nitro)oxidative stress are increased following dopamine exposure ..	22
Acute dopamine treatment resulted in mitochondrial-mediated cellular apoptosis	24
Treatment with dopamine enhanced expression of the i- and n-NOS isozymes ..	26
Dopamine-mediated MnSOD nitration results in enzyme inactivation despite an increase in enzyme levels.....	27
Supplementation with PEG-SOD attenuated markers of dopamine-induced cell death.....	29
Dopamine increased AP-1, but not NFκB, reporter activity in the SK-N-MC cell line.....	31
Dopamine increased MAPK p38 and ERK1/2 phosphorylation	33
Discussion.....	34
Chapter 3.....	47
The Mechanism by which Dopamine Induces MAPK p38 Serves as a “Molecular Switch” between Cellular Protection and Apoptosis in a Model of Methamphetamine Neurotoxicity	47
Introduction.....	47
Materials and Methods.....	50
Cell culture and treatment paradigm.....	50
Protein preparation and immunoblot analysis.....	51

Transient transfection and reporter assay	52
Data analysis	53
Results.....	53
D ₁ receptor stimulation <i>via</i> SKF-38393 exacerbates PARP cleavage in a manner independent of CASP3.....	53
D ₁ receptor antagonist SCH-23390 has no significant effect on CASP3 cleavage, but attenuates DA-induced PARP fragmentation	56
Dopamine or SKF-38393 treatment results in MAPK p38 phosphorylation	59
Inhibition of MAPK p38 with SB203580 attenuates toxicity in 25 μ M DA treated cells, but enhances toxicity with 50 μ M DA or SKF-38393 treatment	60
Antagonism of D ₁ coupled with MAPK p38 inhibition completely abolishes DA-induced toxicity.....	68
D ₁ receptor stimulation enhances HSP27 expression in a manner attenuated by MAPK p38 inactivation.....	70
Dopamine induces AP-1 transcriptional activity through a MAPK p38- dependent, D ₁ -independent mechanism.....	71
Dopamine-stimulated AP-1 transcription occurs through a cFos-containing complex and is a mediator of DA-induced apoptosis	74
Discussion	76
Chapter 4.....	92
Global Discussion and Future Direction.....	92

Global Discussion	92
Future Direction	95
References.....	100
Appendix A: Approval Letter.....	132
Appendix B: Abbreviations.....	135

LIST OF TABLES

Table 1: The Direction of Change in Markers of Apoptosis in Response to Dopamine is Influenced by the Mechanism Through Which p38 is Activated	82
Table 2: Difference in Dopamine Concentration Influences Whether p38 Phosphorylation Provides a Protective or Deleterious Response	83
Table 3: p38 Phosphorylation Mediates Either an Adaptive or Apoptotic Response Which is Determined by the Presence or Absence of D ₁ Receptor Stimulation.....	84

LIST OF FIGURES

Figure 1: The Structures of Methamphetamine (top) and Amphetamine (bottom).....	3
Figure 2: The Oxidation of Dopamine.....	9
Figure 3: Western Analysis of Dopamine-Induced 3-Nitrotyrosine (3-NT) Formation.....	23
Figure 4: Western Analysis of Dopamine-Mediated Adducted Proteins (4-HNE)	23
Figure 5: Western Analysis of Protein Carbonyl Formation After Dopamine Treatment.....	24
Figure 6: Immunoblot Analysis of Apoptotic Markers Following Dopamine Treatment	26
Figure 7: Time- and Concentration-Dependent Protein Expression of iNOS Following Dopamine Administration.....	27
Figure 8: Immunoblot Analysis and Protein Activity of MnSOD in Response to Dopamine.....	28
Figure 9: Western Analysis of MnSOD Enzyme following Immunoprecipitation of 3- Nitrotyrosine in Control versus Dopamine-Treated Samples	29
Figure 10: Photographic Demonstration of Dopamine Toxicity and the Protective Effects of Superoxide Dismutase in SK-N-MC Cells	30
Figure 11: Parallel Western Analysis of Cleaved Poly(ADP-ribose) Polymerase Expression with and without Dopamine and/or Superoxide Dismutase.....	31
Figure 12: Luciferase Activity in NFκB-Transfected SK-N-MC Cells Treated with Dopamine or Positive Control	32
Figure 13: Luciferase Activity in Activator Protein-1-Transfected SK-N-MC Cells Treated with Dopamine or Positive Control	33
Figure 14: Western Blot Analysis of Phosphorylated Protein Kinases p38 and ERK 1/2 with Variable Dopamine Treatment Time and Concentration.....	34

Figure 15: Qualitative and Quantitative Protein Analysis of Caspase 3 Cleavage in Dopamine or SKF-38393 Treated SK-N-MC.....	55
Figure 16: Qualitative and Quantitative Protein Expression of Full-Length and Cleaved Poly(ADP-ribose) Polymerase Following Dopamine or SKF-38393 Treatment	56
Figure 17: Qualitative and Quantitative Protein Expression of Cleaved Caspase 3 following Dopamine Treatment with and without Blockade of the D ₁ receptor with SCH-23390	58
Figure 18: Pre-Treatment with D ₁ Antagonist Attenuates Dopamine-Mediated PARP Cleavage	59
Figure 19: Both Dopamine and D ₁ Agonist Increase p38 Phosphorylation	60
Figure 20: Qualitative and Quantitative Protein Expression of Caspase 3 Cleavage following Inhibition of p38 Phosphorylation in Samples Treated with D ₁ Agonist or Dopamine	62
Figure 21: Qualitative and Quantitative Protein Expression of Full-Length PARP following Inhibition of p38 Phosphorylation in Samples Treated with D ₁ Agonist or Dopamine.....	64
Figure 22 A-J: Parallel Examination of SK-N-MC to Assess Morphological Changes Consistent with Toxicity Following Dopamine or D ₁ Agonist Treatment with and without Inhibition of p38 Phosphorylation	67
Figure 23: Co-Incubation with p38 Inhibitor and D ₁ Antagonist Prior to Dopamine Demonstrates Decreased Caspase 3 Cleavage Compared to Dopamine Alone.....	69
Figure 24: Co-Incubation with p38 Inhibitor and D ₁ Antagonist Prior to Dopamine Demonstrates Decreased Caspase 3 Cleavage Compared to Dopamine Alone.....	70
Figure 25: Enhanced Phosphorylation of Heat Shock Protein 70 Following Dopamine or D ₁ Agonist Appears Dependent Upon p38 Activation	71
Figure 26: Dopamine-Induced AP-1 Activity Appears to be Mediated Through p38	72

Figure 27 A, B: AP-1 Reporter Activity is Enhanced by D₁ Antagonism but Not D₁ Agonist... 74

Figure 28 A, B: Co-Transfection with a Dominant Negative to cFos, A-Fos, Precludes
Dopamine-Induced PARP Cleavage..... 76

Figure 29: The p38-Mediated Molecular Switch..... 91

Figure 30: Dopamine Increases Heme Oxygenase 1 Expression in a Time-Dependent Manner 95

Figure 31: Proposed Mechanism of Action of Methamphetamine Neurotoxicity..... 98

ABSTRACT

Methamphetamine (MA) neurotoxicity is particularly evident in the striatum where it causes extensive dopamine (DA) release and results in neurodegeneration. To identify specific signaling pathways and macromolecules involved in postsynaptic DA-induced striatal toxicity we used a SK-N-MC cell model that mimics postsynaptic D₁ receptor-expressing striatal neurons. The cells were treated for 6-24 h with 0-50 μ M DA. The concentration was chosen to impart physiological relevance to the study as it mirrors [DA] found within the striatum following MA exposure. We show that 25-50 μ M DA resulted in protein changes consistent with nitro(oxidative) stress as well as enhanced cleavage of caspase (CASP) 9, CASP 3, and poly (ADP-ribose) polymerase (PARP). Despite elevated MnSOD protein there was not increased enzymatic activity. Examination revealed that MnSOD was nitrated following DA treatment. Exogenous pretreatment with polyethylene glycol superoxide dismutase, an antioxidant, prevented PARP cleavage. These results suggest a detrimental role for DA-induced reactive oxygen/nitrogen species (RO/NS). To differentiate the D₁-mediated from D₁-independent effects of DA-stimulated signaling and toxicity, the cells were treated with 0-50 μ M SKF-38393, a D₁ agonist; or pretreated with 10 μ M SCH23390, a D₁ antagonist. Both treatments resulted in significant PARP cleavage versus control, although D₁ blockade was protective when compared to DA alone. Despite significant PARP fragmentation, treatment with the D₁ agonist did not result in significant CASP3 cleavage suggesting D₁ stimulation led to apoptosis in a manner independent of CASP3 activation. The MAP Kinase p38 was phosphorylated following D₁ stimulation as well as D₁-independent DA treatment. Inhibition of p38 with 2 μ M SB203580 exacerbated CASP3 cleavage following D₁ activation, but attenuated CASP3 and PARP fragmentation after D₁ blockade. The contradictory results of p38 phosphorylation on CASP3

suggest that its mechanism of activation alters its downstream signaling from CASP3 stabilization to CASP3 fragmentation; thus, we have named p38 the “molecular switch” in this system. We assessed AP-1 reporter activity as it is a downstream target of p38 and a regulator of cell-life and –death. AP-1 transfected cells pretreated with a D₁ antagonist had similar luciferase activity as DA, while stimulation of the D₁ receptor did not enhance the reporter. Pretreatment with a p38 inhibitor reduced AP-1 activity, and AFos-, a cFos dominant negative, transfected cells eradicated PARP cleavage. The findings indicate that DA-induced AP-1 is a D₁-independent, p38-mediated, cFos-dependent apoptotic pathway. We hypothesize that DA increases RO/NS and alters redox-sensitive signaling mechanisms which result in apoptosis; and by 1) blocking D₁- together with p38-activation, 2) inactivating AP-1, or 3) providing antioxidants we can prevent DA-mediated apoptosis that is stereotypical of MA-induced neurodegeneration.

CHAPTER 1

LITERATURE REVIEW

(Meth)amphetamine Abuse, Pharmacology, and Long-Term Consequences

The use of amphetamine-type stimulants (ATS) has been one of the most severe world-wide drug problems for the past 20 years. The recent upsurge in the abuse of prescription stimulants such as amphetamine salts, dextroamphetamine, and methylphenidate—known as “smarty drugs”; and cathinone derivatives such as mephadrone, methylone, and methedrone—known as “bath salts,” have only compounded the problematic issue in the United States (The United Nations Office on Drugs and Crime, 2012). Amphetamine type stimulants cause an initial release of DA in cultured cells (Sulzer et al., 1995), rodents (Cass et al., 1989; Heikkila et al., 1975; Schmidt et al., 1985), non-human primates (Finnegan et al., 1982; Preston et al., 1985), and humans (Drevets et al., 2001; Laruelle et al., 1995). The elevation of DA leads to feelings of euphoria, motivation, and alertness that initially drive the desire to consume ATS. The brain’s limbic system is responsible for these so-called “reward” feelings, and the main anatomical structures involved lie within the striatum of the brain, in particular a portion of the ventral striatum known as the nucleus accumbens. Dopaminergic neurons, both those that release DA and those that express DA receptors, exist in high concentration within the striatum. It is here that, in addition to feelings of reward, ATS-induced neurodegeneration is prevalent (reviewed in Volkow et al., 2004).

A variety of *in vitro* and *in vivo* models show that all ATS are neurotoxic due, at least in part, to their resultant DA surge (Harvey et al., 2000; Preston et al., 1985; Volkow et al., 2004). The pharmacokinetics of methamphetamine (MA; see Figure 1) causes ultra-supraphysiologic concentrations of striatal DA that far exceed those of other ATS, and this lends MA markedly

more neurotoxic than any stimulant (Derlet et al., 1990; Fowler et al., 2008; Volkow et al., 2010). Indeed, neither MA itself nor its metabolites are the cause of its neurotoxicity, but MA's ability to cause such a substantial rise in DA concentration is (reviewed in Krasnova & Cadet, 2009). Methamphetamine, as the name suggests, shares the same structural backbone as amphetamine (AMPH) with the addition of an amino methyl group (see Figures 1 and 2). Methylation of AMPH's amino group provides enhanced lipid solubility and basicity ($pK_a \sim 10.4$) and facilitates greater diffusion of MA across the blood brain barrier when compared to AMPH or other ATS (Albertson et al., 1999; Barr et al., 2006). Additionally, MA has a longer elimination half-life once in the brain than other stimulants. For example, cocaine has a CNS half-life of 1-3 h vs 8-30 h for that of MA (the half-life of MA largely varies based on urine pH; Derlet et al., 1990; Fowler et al., 2008; Volkow et al., 2010). When the lingering and potent effects of acute MA are exposed to the striatum, DA concentration within the synaptic cleft is drastically increased through the following mechanisms: 1) inhibition of DA re-uptake by blockade of dopamine transporters (DAT), 2) reverse transport of cytosolic DA into the synaptic cleft, 3) impaired monoamine oxidase-dependent metabolism of DA, 4) hampered activity of vesicular monoamine transporters, and 5) upregulation of tyrosine hydroxylase—the rate-limiting enzyme in DA synthesis (reviewed in Barr et al., 2006).

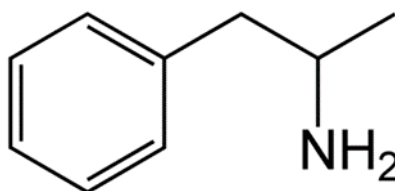
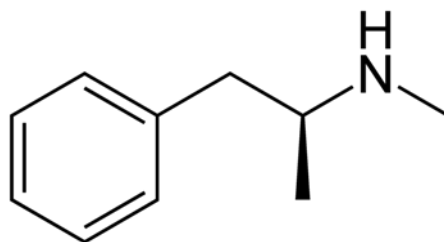


Figure 1: The Structures of Methamphetamine (top) and Amphetamine (bottom)

A comparison of the structural similarities and differences between methamphetamine (MA) and amphetamine (AMPH). The terminal methyl amine group within MA affords the compound higher lipid solubility and basicity than AMPH. These biophysical properties make MA more favorable for both diffusion across the blood brain barrier and entry into neurons than AMPH.

The neurotoxic effects of MA use have been well documented in human and rodent models. Moderate methamphetamine abuse has been shown by functional magnetic resonance imaging to cause regional gray matter neurodegeneration that is equal to that seen in early dementia and greater than that caused by schizophrenia in human subjects (Thompson et al., 2004). There is also a significant decrease in DA transporters (Wilson et al., 1996; Volkow et al., 2001a) and D₂ receptors (Volkow et al., 2001c) following human exposure to MA. Diminished striatal concentrations of DA (Finnegan, et al., 1982; Villemagne et al., 1998) and serotonin (Woolverton et al., 1989) as well as decreased tyrosine hydroxylase activity (Harvey et al., 2000; Preston et al.; 1985) also occur in non-human primates after chronic MA

administration. Prolonged abstinence from MA in primates (Fischman & Schuster, 1974; Seiden et al., 1976) and humans (McCann et al., 1998; 2008; Volkow et al., 2001a) for up to 6 months and 3 years, respectively, does not significantly reverse striatal DA depletion or DAT loss.

These findings indicate that MA-induced structural neurotoxicity is not reversible, even after three years of abstinence. Additionally, performance scores on neuropsychological and psychomotor assessments, executive functioning, and short-term memory are not significantly improved following 12-17 months of MA abstinence, suggesting compromised functional-cognitive sequelae of MA neurotoxicity (Chang et al., 2002; McCann et al., 2008; Volkow et al., 2001a, b). There are behavioral alterations, such as deficient attentional control and abnormal conflict adaptation in abstinent MA users' brains. These alterations are linked to neurochemical brain changes in MA users that are not seen in control groups (Salo et al., 2005; 2007).

Possessing attentional control and conflict adaptation skills are pivotal in decision-making and impulse control, thus their absence in MA users leads to cognitive impairment that is associated with, and may even predict, drug-seeking behavior and relapse (Vanderschuren et al., 1999). It is of paramount importance, therefore, to: 1) identify potential causes of MA-induced neurodegeneration and -toxicity, and 2) aim to combat the structural and functional damage sustained by the brain following MA use that would provide addicts with a better chance of recovery and abstinence.

Regional Neurotoxicity of Methamphetamine in the Striatum: Implications for Dopamine and the Dopamine D₁ Receptor

Various regions of the brain are targets of MA toxicity. A few of those areas are particularly susceptible to MA-induced damage, especially the striatum, which is located within the basal ganglia. This area has an abundance of pre- and postsynaptic dopaminergic neurons.

Acute administration of MA causes DA release that stimulates DA receptors, undergoes autoxidation, forms reactive oxygen/nitrogen species (RO/NS), and initiates a myriad of signaling events that all result in dopaminergic neurotoxicity (reviewed in Chan et al., 2007; Krasnova & Cadet, 2009). Chronic use of MA ultimately causes degeneration of pre-synaptic terminals that result in striatal DA depletion and reduction of tyrosine hydroxylase activity (Ares-Santos et al., 2013). Unlike idiopathic Parkinson's disease where only the dopaminergic cell bodies are damaged, MA-induced neurodegeneration occurs at presynaptic nerve terminals and postsynaptic cell bodies where the increase in DA concentration is most abundant (Mirecki et al., 2004).

Five known G protein-coupled receptors compose the subgroup of DA receptors. The five subtypes are further sorted into a family of receptor-type depending if the G protein associated with the DA receptor is a stimulator or inhibitor of adenylyl cyclase activity when exposed to DA. The prototype stimulatory DA receptor is the D₁ receptor. The D₅ receptor also belongs to the D₁ family as it too is stimulatory when activated by DA. The prototype inhibitory DA receptor is the D₂ receptor. Dopamine receptors D₃ and D₄ belong to the D₂ family. The DA D₁ receptor is the most widespread and most expressed receptor in the brain. The DA D₁ receptor is heavily expressed in the striatum, nucleus accumbens, and other areas of the basal ganglia. The DA D₂ receptor is also found in the striatum and nucleus accumbens, but is rarely co-localized with D₁ receptors (Missale et al., 1998). Historically, landmark studies involving substance addiction and neurotoxicity focused primarily on DA D₂ receptors and their receptor-expressing neurons. The availability of [¹¹C]raclopride and other radioactive DA D₂ ligands made positron emission tomography studies of DA D₂ receptors popular in the examination of addiction pathology and neurotoxicity (McCann et al., 1998; Morgan et al., 2002; Volkow et al.,

2001a; b; c; reviewed in 2004). More recently, the DA D₁ receptor has become a focus of addiction research (Albertson et al., 1999; Ares-Santos et al. 2012; Chen et al., 2004; Moussa et al., 2006; Vanderschuren et al., 1999).

The D₁ receptors contribute to MA withdrawal, craving, relapse, and neurotoxicity. Acute and chronic MA use selectively increases DA D₁ receptors in the striatum (Worsley et al., 2000) without altering the activity of basal adenylyl cyclase (Tong et al., 2003) or the concentration of stimulatory striatal G protein (McLeman et al., 2008) when compared to age-matched controls in post mortem analyses. Despite these findings, striatal DA D₁ receptor-stimulated adenylyl cyclase activity is decreased in acute and chronic MA users (Tong et al., 2003). It is postulated that this effect is due to impaired coupling of D₁ receptors with stimulatory G proteins that then leads to a functional down-regulation in D₁-stimulated adenylyl cyclase activity and subsequent desensitization of striatal D₁ receptors. This sequence of MA-mediated events may be responsible for the symptoms of physiologic withdrawal and consequential craving and relapse (Roberts-Lewis et al., 1986; Tong et al., 2003).

Pre-treatment with SCH-23390, a selective DA D₁ antagonist, reduces mortality following acute MA administration (Bronstein & Hong, 1995), and preserves both tyrosine hydroxylase activity and [DA] in the striatum following chronic MA treatment in rats (Sonsalla et al, 1986). These studies were among the first to attribute MA neurotoxicity, at least in part, to DA D₁ receptors. Methamphetamine-treated homozygous DA D₁ receptor knockout mice have diminished mortality and dopaminergic cell body loss within the basal ganglia as well as preserved levels of tyrosine hydroxylase and DAT when compared to DA D₁ receptor expressing mice (Ares-Santos et al., 2012; Ito et al., 2008). Furthermore, DA D₁ receptor knockout mice offer more neuroprotection than their DA D₂ receptor knockout counterparts (reviewed in Ares-

Santos et al., 2013). Microscopic evaluation shows that DNA fragmentation and chromatin condensation occur in immortalized CSM 14.1 neural cells and resembles an “apoptotic-like process” following MA treatment (Cadet et al., 1997). Mechanistic studies *in vitro* and *in vivo* indicate that MA-mediated postsynaptic apoptosis culminates from endoplasmic reticulum- and mitochondria-dependent cascades (Jayanthi et al., 2004; Krasnova & Cadet, 2009) mediated, in part, by D₁ activation (Jayanthi et al., 2009).

These properties have made DA and activation of its receptors, specifically D₁, the focus of many studies aimed at understanding stimulant-induced neurotoxicity and diminishing the phenomenon of withdrawal, craving, and relapse in humans (Karila et al., 2010; Tong et al., 2003) and animal models (Shuto et al., 2006; Vanderschuren et al., 1999).

Methamphetamine-Induced Dopamine Release and (Nitro)oxidative Stress

Methamphetamine is one of the most potent psychostimulants as its half-life is 18-times longer than and causes 3-times the amount of DA release as cocaine (Barr et al., 2006; Derlet et al., 1990; Feldman et al., 1997;). In addition to DA receptor stimulation, the abundant release of DA within the striatum is thought to be neurotoxic due in part to the generation of ROS (De Vito & Wagner, 1989; O’Dell et al., 1991; Seiden et al., 1984). Dopamine has a greater ability to form ROS and reactive metabolites than other catecholamines due to its higher rate of oxidation and slower rate of cyclization. In both *in vitro* and *in vivo* models, DA is more cytotoxic when directly injected into neuronal cells than other catecholamines (Graham, 1978; Rosenberg, 1988). The ROS and subsequent toxicity are thought to result from DA autoxidation leading to the hydroxyl radical (Giovanni et al., 1995), formation of dopaquinone (LaVoie & Hastings, 1999), and, through redox-cycling of dopaquinone, the generation of the reactive superoxide radical (O₂^{-•}; Stokes et al., 1999; see Figure 3).

These neuropharmacological properties of MA-induced DA release may be the reason that acute and chronic MA administration induces neuronal apoptosis, in contrast to cocaine that does not initiate apoptotic pathways in the rat brain. It has been theorized that the antioxidant capacity of the cell is sufficient to protect against cocaine-induced DA release, whereas the magnitude of MA-induced DA release overwhelms the cellular defense mechanisms (Dietrich et al., 2005; Mirecki et al., 2004). Methamphetamine neurotoxicity can be attenuated by antioxidant supplementation (DeVito & Wagner, 1989; Wagner et al., 1985). It took several years, however, before evidence of MA-induced intracellular pro-oxidant change was documented. Yamamoto and Zhu (1998) were the first to show definitive evidence of pro-oxidant changes within the striatum by measuring malonyldialdehyde, a lipid peroxidation product, in rats treated with MA (Yamamoto & Zhu, 1998). Since their initial report, additional studies provide definitive evidence of pro-(nitro)oxidant protein changes in the striatum of rodents consistent with increased RO/NS following MA administration (Gluck et al., 2001; Imam et al., 2001). Subsequent research has been directed toward understanding and preventing the sequelae of RO/NS-mediated neurotoxicity following MA treatment (Chen et al., 2004; Wu et al., 2007).

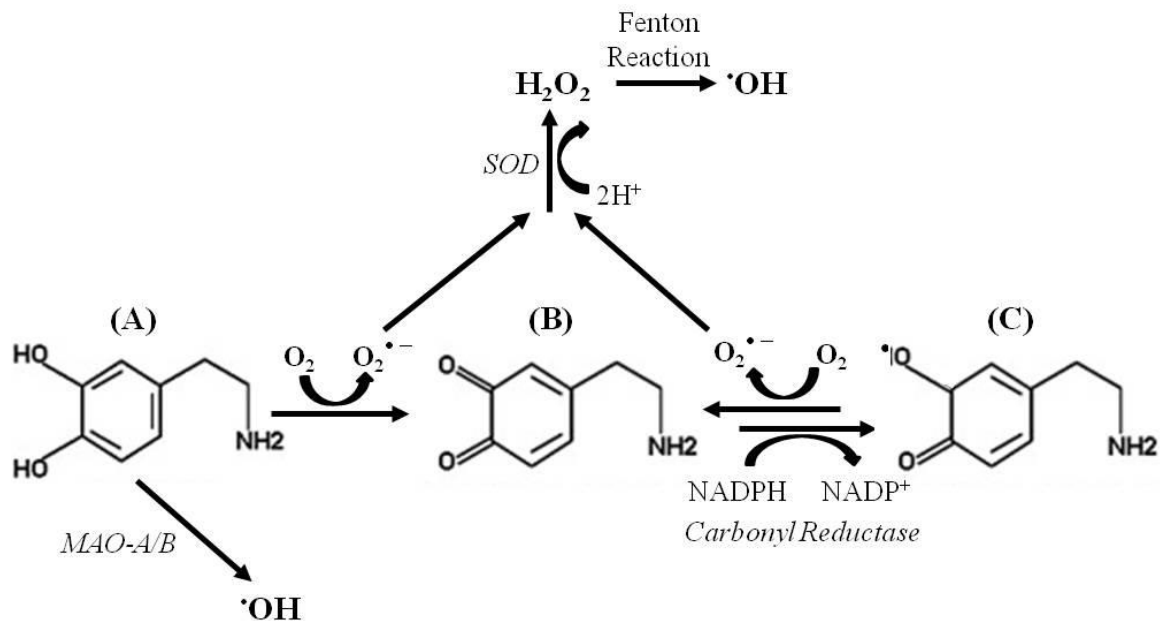


Figure 2: The Oxidation of Dopamine

In the initial step, dopamine (DA; **A**) can either be oxidized enzymatically by monoamine oxidase A or B (MAO-A/B) or non-enzymatically by molecular oxygen (O_2). In the former process, enzymatic metabolism of DA produces the reactive hydroxyl radical ($\cdot\text{OH}$) as a natural by-product. In the latter mechanism, DA autoxidation results in production of the superoxide radical ($\text{O}_2^{\cdot-}$) and dopa-*o*-quinone (**B**). Dopa-*o*-quinone is then converted to a semi-quinone (**C**) in the presence of NADPH. The quinone and semi-quinone, in the presence of O_2 and NADPH, redox-cycle between the reactive intermediates that generate a large quantity of $\text{O}_2^{\cdot-}$. Superoxide dismutase (SOD) converts $\text{O}_2^{\cdot-}$ to hydrogen peroxide (H_2O_2) in the presence of two hydrogen ions (H^+). Through the Fenton reaction, the H_2O_2 is converted to $\cdot\text{OH}$. As shown, the oxidation of DA is responsible for generation of great sums of highly reactive species.

Key Enzymes in Methamphetamine Neurotoxicity: Friend or Foe?

In addition to D_1 receptor stimulation and ROS generation, the nitric oxide synthase and superoxide dismutase isozymes (NOS, SOD) also play a key role in MA-induced apoptosis.

Nitric Oxide Synthase

There are three NOS isozymes generally referred to as neuronal (nNOS), endothelial (eNOS), or inducible (iNOS). Both n- and eNOS are constitutively expressed and their activity is Ca^{2+} -sensitive, whereas iNOS expression must be induced and is Ca^{2+} -insensitive. The Ca^{2+} -insensitive nature of iNOS is attributed to the tight coupling of calmodulin to iNOS at basal Ca^{2+}

levels, while n- and eNOS require elevated levels of Ca^{2+} in order to bind and activate the enzyme. The NOS isozymes catalyze the conversion of L-arginine, O_2 , and NADPH to NO^* , L- or D/L-citrulline, and NADP. Inducible NOS operates as a high-output enzyme that continuously produces NO^* until it is degraded while n- and eNOS have variable, low-output activity (Alderton et al., 2001). Several studies have reported a causative role for n- and iNOS overstimulation in MA-induced neurotoxicity (Cadet et al., 2001; Di Monte et al., 1996; Imam et al., 2001; Itzhak et al., 1996; 1998; 1999; Kita et al., 2003). Methamphetamine-induced striatal toxicity is attenuated in mice that are co-administered 7-nitroindazole, a nNOS inhibitor (Di Monte et al., 1996; Itzhak et al., 1996), or that lack the nNOS gene (Imam et al., 2001; Itzhak et al., 1998). Methamphetamine administered to iNOS deficient mice also results in significantly smaller depletions in striatal DA (Itzhak et al., 1999). A comparison of striatal DA concentration in nNOS(-/-) mice and iNOS (-/-) mice following MA administration shows that both have significantly less DA depletion, with nNOS(-/-) offering more protection (Itzhak et al., 2000). Although studies clearly demonstrate protection from MA-induced neurotoxicity in animals with diminished i- or nNOS expression and activity, there have been conflicting results regarding which isozyme is the most neurotoxic; therefore, it has been difficult to identify the primary target of intervention.

Superoxide Dismutase

Copper/zinc and manganese SOD are antioxidant enzymes found in the cytoplasm and mitochondria, respectively, of cells (Cu/ZnSOD; MnSOD). These enzymes catalyze the conversion of $\text{O}_2^{\cdot-}$, a reactive oxidant and a byproduct of DA autoxidation, to the less reactive hydrogen peroxide and O_2 (St. Clair et al., 2002). Compromised SOD activity leads to an increase in $\text{O}_2^{\cdot-}$ that can instantaneously react with NO^* to produce peroxynitrite (ONOO^-), a

powerful RNS whose presence has been associated with tyrosine nitration, mitochondrial dysfunction, and mitochondrial-mediated apoptosis (Squadrito & Pryor, 1998). Several studies have reported the involvement of ONOO⁻ in MA-induced apoptosis (Imam, et al., 2001). Methamphetamine-treated mice overexpressing Cu/ZnSOD have reductions in the following: striatal DA depletion (Cadet et al., 1994), ONOO⁻ formation (Imam et al., 2001), and apoptosis (Deng & Cadet, 2000). Likewise, MA treatment of transgenic mice that overexpress MnSOD results in a significant decrease in striatal DA depletion, protein oxidation, and apoptosis (Maragos et al., 2000). Studies using a known MnSOD inducer, deprenyl, demonstrated reduced MA-induced neurotoxic effects in rats and SH-SY5Y neuroblastoma cells (Davidson et al, 2007). However, some effects of deprenyl in these studies may be partially attributed to its inhibition of monoamine oxidase, an enzyme that metabolizes DA. Although these studies implicate a neuroprotective role for SOD isozymes in dopaminergic pathologies, no information is available about their DA-mediated intracellular expression and activity.

AIM OF PRESENT STUDY

The goal of this work was to discover and identify intracellular processes that may be responsible for the structural changes within the brain, such as regional gray matter neurodegeneration (Thompson et al., 2004), striatal DA depletion, and DAT loss (Volkow et al., 2001a); as well as functional impairments such as inattention and abnormal conflict adaptation (Salo et al., 2007) that have been associated with MA abuse. We and others hypothesize these losses are attributed to the cytotoxic effects of MA-induced DA release. If we can identify the macromolecular changes and associated signaling pathways that are responsible for DA-induced apoptosis, then appropriate interventions can be made to prevent further neurotoxicity. Since there are no known effective treatments for MA-induced neurotoxicity or the long-term cognitive

damage associated with MA use (Barr et al., 2006; Brackins et al., 2011), our goal was to discover ways to attenuate MA-induced neuronal damage during the cycle of addiction. By interfering with MA-mediated, DA-induced neurotoxicity we predict this will lessen the long-term behavioral and psychological consequences that foster further drug-seeking behavior and relapse.

Notably the relevance of DA-specific postsynaptic RO/NS production, apoptosis, enzyme expression, and signaling is not limited to MA neurotoxicity. The applicability of our findings and this model also extends to other drugs of abuse and pathologies such as schizophrenia, Parkinson's Disease and Huntington's disease, wherein DA toxicity is also fundamental to the pathophysiology of those disease processes.

CHAPTER 2

DOPAMINE STIMULATION RESULTS IN (NITRO)OXIDATIVE PROTEIN CHANGES, MITOCHONDRIAL-MEDIATED APOPTOSIS, MNSOD NITRATION, AND ACTIVATION OF MAPK AND AP-1 SIGNALING PATHWAYS IN AN *IN VITRO* MODEL OF METHAMPHETAMINE NEUROTOXICITY

Introduction

Reactive oxygen and nitrogen species have long been implicated as mediators in MA-induced neurotoxicity (Cadet et al., 1997; DeVito & Wagner, 1989; O'Dell et al., 1991; Seiden and Vosmer, 1984). Multiple studies have reported evidence of RO/NS in postsynaptic-models of DA-induced neurotoxicity such as elevated nitrate levels and protection by antioxidant supplementation with N-acetylcysteine or sodium metabisulfite (Chan et al., 2007; Chen et al., 2003; 2004; Moussa et al., 2006); but these studies did not show if there were macromolecular changes consequential to the (nitro)oxidative stress. It is necessary to determine if DA causes pro-(nitro)oxidant protein alterations. Damaged membrane integrity by lipid peroxidation, altered protein function by carbonyl formation, and diminished enzymatic activity by 3-nitrotyrosine (3-NT) conjugation are all sequelae of oxidative and nitrosative stress that can result in compromised cellular function. Identification of DA-mediated pro-(nitro)oxidant changes, which is an aim of this study, will offer insight on the intracellular ramifications of the previously reported spike in DA-induced RO/NS.

Given the RO/NS-plagued and neurotoxic nature of MA exposure, it is not surprising that studies have reported MA administration triggers postsynaptic apoptosis (Cadet et al., 1997; Cadet et al., 2001; Chang et al., 2007; Jayanthi et al., 2004; Krasnova & Cadet, 2009). To differentiate the neurotoxicity imparted by MA-induced DA release from that attributed to MA,

several studies examined SK-N-MC cell viability following a range of 0-200 μ M DA treatment for 16-48 h. Reports showed decreased cell viability by the trypan blue exclusion test or 3-(4,5-dimethylthiazol-2-yl)-2,5-dephenyl tetrazolium bromide (MTT) assay, but the studies did not demonstrate whether this was an apoptotic or necrotic process (Chen et al., 2003; 2004; Moussa et al., 2006). One study reported cleavage of effector caspase 3 (CASP3) and poly(ADP-ribose) polymerase (PARP) after 48 h of 50 μ M DA treatment (Chan et al., 2007). Although cleavage of these proteins suggest an apoptotic process, the markers are not specific for identifying mitochondrial, endoplasmic, or receptor-mediated mechanisms (Li et al., 1997); and the time of DA treatment far exceeded that used in most models (Chen et al., 2003; 2004; Junn & Mouradian, 2001; Moussa et al., 2006; Zafar et al., 2006; Zhen et al., 1998). Since DA-induced RO/NS is implicated in decreased cell viability and a majority of RO/NS are known to originate in the mitochondria (Holley et al., 2010), we examined markers specific for mitochondrial-mediated apoptosis following 0-50 μ M DA for 24 h in the SK-N-MC cell line. Our research has identified mechanisms through which DA-induced postsynaptic apoptosis occurs. This information may be used to target susceptible subcellular organelles for intervention to prevent or attenuate MA-mediated DA neurotoxicity.

Repeatedly, nitric oxide synthase isozymes have been reported as modulators of MA-induced neurotoxicity (Di Monte et al., 1996; Imam et al., 2001; Itzhak & Ali., 1996; Itzhak et al., 1998; 1999). There are conflicting results as to which isozyme, when overexpressed, is the most neurotoxic; therefore, it is difficult to identify a primary target of intervention. SK-N-MC cells and primary rat striatal neurons had 150% greater iNOS expression and 200% increase in iNOS activity than n- and e- NOS combined when treated with DA (Chen et al., 2003). This data suggests a critical role for iNOS overexpression in DA-mediated neurotoxicity, but this

study has not been replicated nor has the mechanism of DA-induced iNOS upregulation been investigated in this model. It is hypothesized that glutamate-mediated NMDA calcium influx is responsible for the activation of n- and e-NOS subsequent to MA exposure. In contrast, iNOS is not calcium-sensitive nor is it constitutively expressed. Thus, little is known about its mechanism of induction in MA/DA neurotoxicity. Given that 1) iNOS has the highest and longest NO[•] output of the NOS isozymes, and 2) RO/NS such as NO[•] have been implicated in MA/DA neurotoxicity, then it is critical to investigate the involvement and regulation of iNOS following DA stimulation. This was a major goal in this study and reported in this chapter.

Overexpression of copper/zinc or manganese superoxide dismutase (Cu/ZnSOD, MnSOD) isozymes attenuates pre- and postsynaptic MA-induced neurodegeneration in rodents (Cadet et al., 1994; Maragos et al., 2000). Evidence suggests that overexpression of Cu/Zn- or MnSOD prevents the cellular system from becoming overwhelmed with RO/NS species. It is not known, however, if the cells attempt to mount an inherent, but insufficient, adaptive response through upregulation of Cu/Zn or MnSOD following the MA-induced increase in DA autoxidation and signaling. It is important to determine whether Cu/Zn- and/or MnSOD undergo protein upregulation with a concurrent enhancement in enzymatic activity. This differentiation is particularly important in MnSOD as this isozyme, unlike its cytoplasmic counterpart Cu/ZnSOD, is essential for life and is susceptible to nitration by peroxynitrite with subsequent inactivation (Li et al., 1995). If DA-stimulation does not induce SOD expression, then intervention of DA neurotoxicity can be aimed at gene amplification. On the other hand, if MnSOD expression, but not activity, is enhanced then the integrity of the enzyme must be investigated. If DA treatment results in MnSOD nitration, then supplementation with general antioxidants may shift the intracellular redox-balance in a manner that would permit the endogenous upregulation of

MnSOD to exert its intended neuroprotective effect. In this study we assessed DA-mediated MnSOD expression, activity, and nitration with a goal of understanding these processes and directing our findings towards a protective intervention.

Despite the knowledge that NOS and SOD isozymes are associated with MA/DA neurotoxicity, little is known about their signaling and regulation. We investigated two transcription factors, Activator Protein-1 (AP-1) and Nuclear Factor kappa B (NF κ B), which have promoter sequences within human iNOS and MnSOD genes, are redox-sensitive, and whose activation is induced by ROS-derived neuronal injury (Alderton et al., 2001; Flora et al., 2002; Kinningham et al., 1997; 2001; Krasnova & Cadet, 2009; Pautz et al., 2010; St. Clair et al., 2002). Methamphetamine injections enhance expression of transcription factors from the AP-1 family in mouse brain (Cadet et al., 2001; Krasnova & Cadet, 2009) and increase AP-1 DNA binding in mouse striatum (Flora et al., 2002), but these studies did not investigate whether AP-1 activation is due to increased DA or another aspect of MA-mediated signaling. Similar to the lack of data on AP-1 signaling, there are no studies in this model to investigate the possible involvement of DA in NF κ B activation either.

The members of the mitogen-activated protein kinase (MAPK) family, in particular jun-N-terminal kinase (JNK), have been cited as participants in MA-mediated signaling within the striatum of rodents (reviewed in Krasnova & Cadet, 2009). Studies in postsynaptic dopaminergic models yield conflicting results as to the identification of the MAPKs that are specific to DA-stimulated signaling (Chen et al., 2004; Zhen et al., 1998). It is important to differentiate which MAPKs are involved in DA-mediated signaling since each member of the family has stereotyped modulatory functions such as those pertaining to cellular proliferation and apoptosis, as well as upstream participants in AP-1 and NF κ B activation. Identification of DA-

stimulated signaling pathways would offer much insight into potential therapeutic targets, such as modulation of: 1) enzyme expression, 2) apoptosis, and 3) adaptation.

In order to study the neurotoxic mechanisms of DA on postsynaptic neurons, we treated human SK-N-MC neuroepithelioma cells with 0-50 μ M DA and assessed for macromolecular evidence of pro-(nitro)oxidative changes, markers of apoptosis, enzyme expression of SOD and NOS isozymes, cellular adaptation, and activation of relevant cell signaling pathways including JNK, MAPK p38, extracellular signal related kinases 1 and 2 (ERK1/2), AP-1, and NF κ B. We chose human SK-N-MC cells as our model for several reasons. The cells endogenously express DA D₁ receptors, and lack DAT as well as tyrosine hydroxylase activity (Chen et al., 2003; Sidhu & Fishman, 1990). These properties are stereotypical of postsynaptic neurons and distinguish them from their presynaptic counterparts. Unlike presynaptic neurons that undergo terminal degeneration after MA exposure, postsynaptic neurons are susceptible to apoptosis (Jayanthi et al., 2004; Zhu et al., 2006), which was a major focus of our study. The presence of D₁ receptors also enabled the study of DA-mediated signaling, while the absence of DAT and tyrosine hydroxylase ensured that all pathophysiologic effects observed in this study were due to an exogenous source of DA. The DA concentrations that were used mirror those found within the human striatum after exposure to MA, and thus imparted physiological relevance to the study (Feldman et al., 1997).

Our findings in this work provide information relevant to possible therapeutic options, such as identification of specific enzymes that contribute to MA toxicity or, conversely, enzymes with a protective function. By identifying these enzymes and understanding their regulation, it is possible to either inhibit or upregulate their expression with the goal of averting MA-mediated, DA-induced neurotoxicity.

Materials and Methods

Cell culture and treatment paradigm

The human SK-N-MC neuroepithelioma cell line was obtained from the American Type Culture Collection (Manassas, VA). These cells were maintained in RPMI 1640 medium without phenol red and supplemented with 1% (v/v) nonessential amino acids, 1% antibiotics (penicillin/streptomycin/neomycin; Invitrogen Corp.; Carlsbad, CA), 10% Nu-Serum (BD Biosciences; San Jose, CA) and 1 mM sodium pyruvate and incubated at 37°C in a humidified atmosphere with 5% CO₂. All treatments were administered following 24 h pyruvate- and serum-starvation, shielded from light, and accompanied by untreated or vehicle-treated control samples (medium alone). Dopamine treatments were with 25 or 50 μM dopamine hydrochloride (Sigma-Aldrich; St. Louis, MO) dissolved in medium. Although the concentration range of DA used in these studies is higher than the normal human levels of 1-10 μM in the striatum, DA content in pathological systems has been reported to reach as high as 50 μM (Chen et al., 2003; Feldman et al., 1997). In the studies with polyethylene glycol superoxide dismutase (PEG-SOD; Calbiochem; La Jolla, CA), the cells were pre-treated with 100 U PEG-SOD in transfection-grade water for 30 min before administration of DA or control (medium alone). The cells were microscopically visualized using a Nikon Diaphot Inverted phase microscope (Frank E. Fryer Co., Cincinnati, OH) and photographed with a Nikon N2000 camera immediately prior to collection.

Protein preparation and immunoblot analysis

For immunoblot analysis, SK-N-MC cells were plated at a density of 3×10^6 /150 mm dish then serum- and pyruvate-starved once cells were ~85% confluent. Following 24 h treatment, mitochondrial fractions (for MnSOD nitration; Anantharaman et al., 2006)

cytoplasmic samples (for CASP3 and CASP9), and whole-cell lysates (for all other samples) were collected with the inclusion of protease inhibitors (pepstatin, leupeptin, aprotinin) at 1 $\mu\text{g}/\text{ml}$ as previously described (Humphrey et al., 2005;). Protein concentrations were determined by a colorimetric assay (Bio-Rad Laboratories; Richmond, CA) using bovine serum albumin as a standard. Homogenate protein samples (100 $\mu\text{g}/\text{lane}$) were separated on 10, 12.5, or 15% SDS-PAGE according to the method of Laemmli (1970) and transferred to a PVDF (3-NT) or nitrocellulose membrane (all others). Transfer efficiency was assessed by staining with 0.1% (w/v) Ponceau S. The membranes were washed with distilled water to remove excess stain and then the nonspecific binding sites were blocked at room temperature for 1 h with Blotto (5% [w/v] dried milk in tris-buffered saline with Tween-20 [TBS-T; 50 mM NaCl, 10 mM Tris-HCl (pH 8.0), 0.05% (v/v) Tween-20]). The membranes were then incubated overnight at 4°C with gentle shaking in Blotto and purified immunoglobulin for the protein of interest at 4°C with gentle shaking. After three washes with TBST, the membranes were incubated with secondary HRP-conjugated anti-rabbit or -mouse in Blotto for 1.5 h at room temperature with gentle shaking. Following three washes with TBST and one with TBS the protein bands of interest were visualized using the enhanced chemiluminescence detection system (Amersham Biosciences; Little Chalfont, U.K.). To confirm equal protein loading, all blots except for i- and nNOS were reprobbed with a rabbit polyclonal anti- glyceraldehyde-3-phosphate dehydrogenase (GAPDH) antibody. Due to their high molecular weight, iNOS and nNOS blots were reprobbed and normalized with heat shock protein 70 antibody. Preliminary studies in our laboratory determined there was no change in heat shock protein 70 expression upon treatment with 0-50 μM DA for 24 h. The dilutions and sources of each antibody used are as follows: n-, i-, and eNOS (1:2500, 1:10,000, 1:1000; BD Transduction Laboratories; San Diego, CA); GAPDH

(1:7500; Trevigen; Gaithersburg, MD), 4-hydroxy-2-nonenal (4-HNE; 1:1500; Alexis; San Diego, CA); 3-NT (0.5 µg/mL; Upstate; Charlottesville, VA); CASP9 (1:1000), CASP3 (1:2500), cleaved CASP3 (1:1000), PARP (1:5000), MnSOD (1:4000), phosphorylated MAPK p38 (1:750), phosphorylated ERK1/2 (1:3000), phosphorylated JNK (1:1000), heat shock protein 70 (hsp70; 1:3000; Cell signaling Technology; Beverly, MA), anti-rabbit and anti-mouse secondary antibodies (1:3000; Santa Cruz Biotechnology; Santa Cruz, CA).

Transient Transfections and Luciferase Assay

Cells were plated at a density of 6.7×10^6 /p100 plate and grown for 48 h. Using the calcium phosphate method, the cells were transfected in Minimal Essential Medium (supplemented with 10% heat inactivated fetal bovine serum, 1% nonessential amino acids, 1% antibiotics [penicillin/streptomycin/neomycin], and 1 mM sodium pyruvate) with 6 µM of pGL2 vector (Promega; Madison, WI) with or without an AP-1 construct containing four known consensus sequences (gift from Dr. Richard Niles, Marshall University), or pGL3 vector with or without a NFκB construct (Panomics; Fremont, CA). After 7 h, the cells were washed twice with PBS (137 mM NaCl, 3 mM KCl, 1 mM potassium phosphate, and 10 mM sodium phosphate) and the medium was replaced with supplemented RPMI 1640 without phenol red. The acclimated cells were plated in 24-well plates at a density of 3×10^5 cells/well and allowed to acclimate for 24 h. The next day the cells underwent 24 h serum and pyruvate starvation, and then were treated with 0-100 µM DA, 100 nM tumor necrosis factor (TNF), or 100 nM 12-O-tetradecanoylphorbol-13-acetate (TPA; a phorbol ester) in serum- and pyruvate-free medium. One, four, or six hours later the cells were lysed in 200 µL of reporter passive lysis buffer (Promega) and frozen at -20°C overnight. Transcriptional activity was assessed using the luciferase assay system (Promega) in a TD 20/20 luminometer (Turner Designs).

(Mn)SOD Activity Assay

Superoxide dismutase activity was measured by the nitro blue tetrazolium-reduction method as described (Anantharaman et al., 2006; and with the generous assistance of Dr. Douglas Spitz, University of Iowa). Potassium cyanide (5 mM) was added to inhibit Cu/ZnSOD. One unit of SOD activity was defined as the amount of SOD protein that caused a 50% reduction in the background nitro blue tetrazolium-reduction rate. The change in MnSOD activity was reported relative to the change in MnSOD protein expression for the same treatment.

Evaluation of MnSOD Nitration

The immunoprecipitation of 3-NT residues was performed as previously described (Anantharaman et al., 2006). Briefly, isolated mitochondrial protein (200 μ g) was resuspended in 200 μ L RIPA buffer. Anti-3-NT antibody (2 μ g/mL) was added and incubated overnight at 4°C. Protein A/G agarose (20 μ L) was then added to the mixture and incubated for 24 h. Immunocomplexes were collected by centrifugation at 1000 x *g* for 5 min followed by 4 washes with RIPA buffer. Immunoprecipitated samples were assessed for MnSOD protein expression by western analysis as described above.

Data analysis

All experiments were replicated at least twice, and representative findings are shown. Final statistical analyses were performed using Student's *t*-test or three-way analyses of data and variance (ANOVA) for multiple samples. *Post hoc* tests were examined with Tukey's method on SigmaStat software (SPSS Inc., Chicago, IL). A *p* value of <0.05 was considered statistically significant.

RESULTS

Markers of (nitro)oxidative stress are increased following dopamine exposure

Reports have indicated a role for RO/NS in DA-induced striatal cytotoxicity (O'Dell et al., 1991; LaVoie & Hastings, 1999), and tyrosine nitration is a known finding in cellular systems exposed to peroxynitrite-generated RO/NS species (Squadrito & Pryor, 1998). A western blot analysis (Figure 4) shows increased 3-NT residues in 25-50 μ M DA-treated cells. Furthermore, the amount of DA-mediated 3-NT appeared to be concentration-dependent. Protein adducts, specifically 4-HNE adducts, have long been used as a marker of lipid peroxidation (Spitz et al., 1990). To investigate the presence or absence of lipid peroxidation in response to DA in our system, we treated SK-N-MC cells with 0-50 μ M DA and evaluated 4-HNE adducts through western analysis. Figure 5 shows 4-HNE adducted proteins in the 50 μ M DA samples at approximately 20-30 kDa that are not present in the control and 25 μ M treatments. Protein carbonyl formation is found in several disease states associated with oxidative stress and is also used as a marker for ROS-induced protein alteration (Berlett & Stadtman, 1997). We probed for protein carbonyl formation in samples treated with 0 or 50 μ M DA and found an elevation in the samples treated with DA compared to control (Figure 6). The integrated findings from Figures 4-6 strongly suggest the presence of active RO/NS species caused protein modifications typical of (nitro)oxidative stress following administration of DA. Interestingly, the only modification noted at 25 μ M DA was 3-NT, while all parameters investigated showed alterations in 50 μ M DA treated samples.

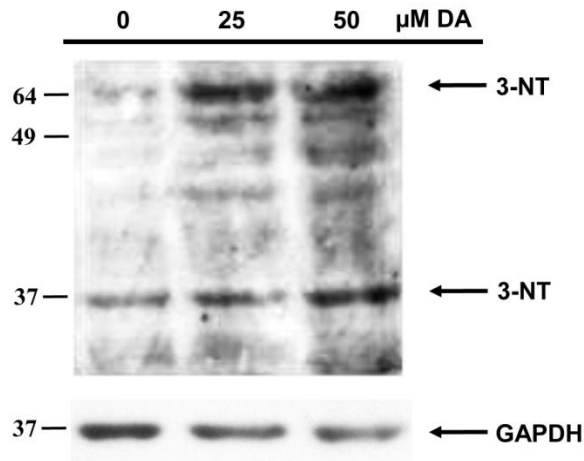


Figure 3: Western Analysis of Dopamine-Induced 3-Nitrotyrosine (3-NT) Formation

Western analysis following 24-hour treatment with 0-50 μ M DA. All bands to the left of the blot represent molecular weight in kilodaltons. Treatment with 25-50 μ M DA resulted in concentration-dependent increase in 3-NT formation. Figure is representative of findings repeated at least twice.

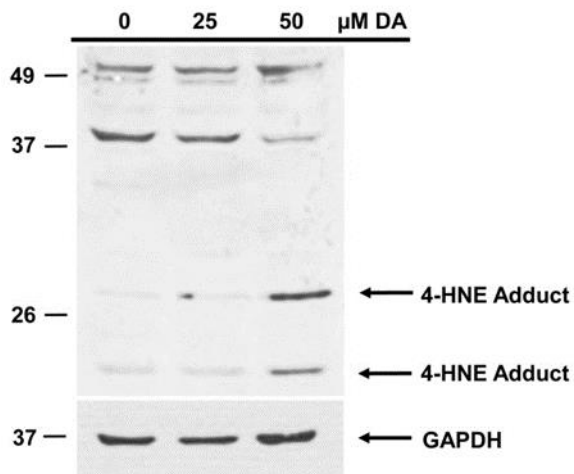


Figure 4: Western Analysis of Dopamine-Mediated Adducted Proteins (4-HNE)

Western analysis following 24-hour treatment with 0-50 μ M DA. All bands to the left of the blot represent molecular weight in kilodaltons. Adducted proteins (4-HNE) were noted at 20-30 kDa following treatment with 50, but not 25 μ M DA. Figure is representative of findings repeated at least twice.

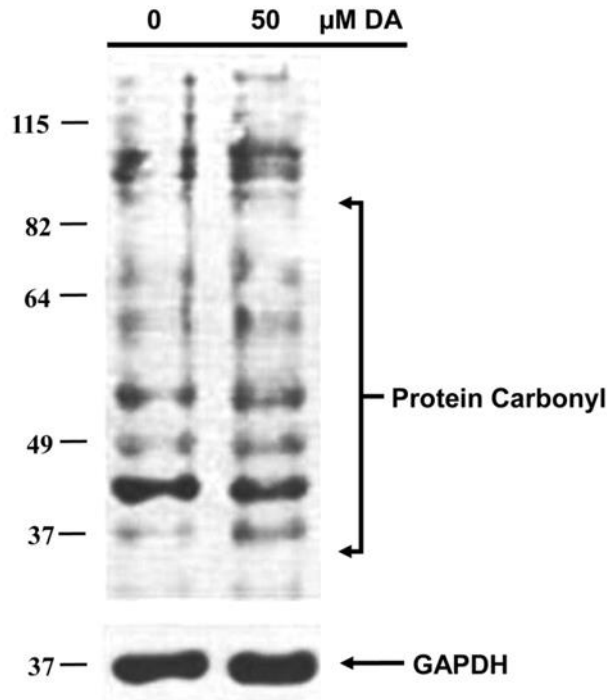


Figure 5: Western Analysis of Protein Carbonyl Formation After Dopamine Treatment

Western analysis following 24-hour treatment with 0-50 μM DA. All bands to the left of the blot represent molecular weight in kilodaltons. Formation of protein carbonyl was observed following treatment with 50 μM DA. Figure is representative of findings repeated at least twice.

Acute dopamine treatment resulted in mitochondrial-mediated cellular apoptosis

To determine if the observed DA-induced (nitro)oxidative stress resulted in activation of an apoptotic pathway, SK-N-MC cells were treated with increasing concentrations of DA (0-50 μM) for 24 h and then assayed *via* western blot analysis for the presence of apoptotic markers. Cleavage and thus activation of caspase 9 (CASP9) occurs specifically in mitochondrial-mediated apoptosis immediately following apoptosome formation (Li et al., 1997). Examination of the cleavage pattern of CASP9 in our model revealed a concentration-dependent decrease in CASP9 proform following DA treatment with a parallel increase in its cleavage fragments (Figure 7). Analysis of a downstream target of activated CASP9, effector CASP3, had the same cleavage pattern as CASP9 following DA treatment with an increase in p17 and p19 CASP3

cleavage products for 25-50 μ M DA versus control (Figure 7). The nuclear enzyme PARP, which functions in part to preserve DNA integrity and is thus considered an end-point for apoptotic activation, is a substrate for cleavage by activated CASP3 (Oliver et al., 1998). Figure 7 shows concentration-dependent degradation in PARP at 116 kDa with a concurrent increase in the 85 kDa PARP fragment following 25-50 μ M DA treatment. The DA-induced cleavages of CASP9, CASP3, and PARP suggest that cell death is occurring through activation of apoptotic pathways that are, at least in part, mitochondrial-mediated.

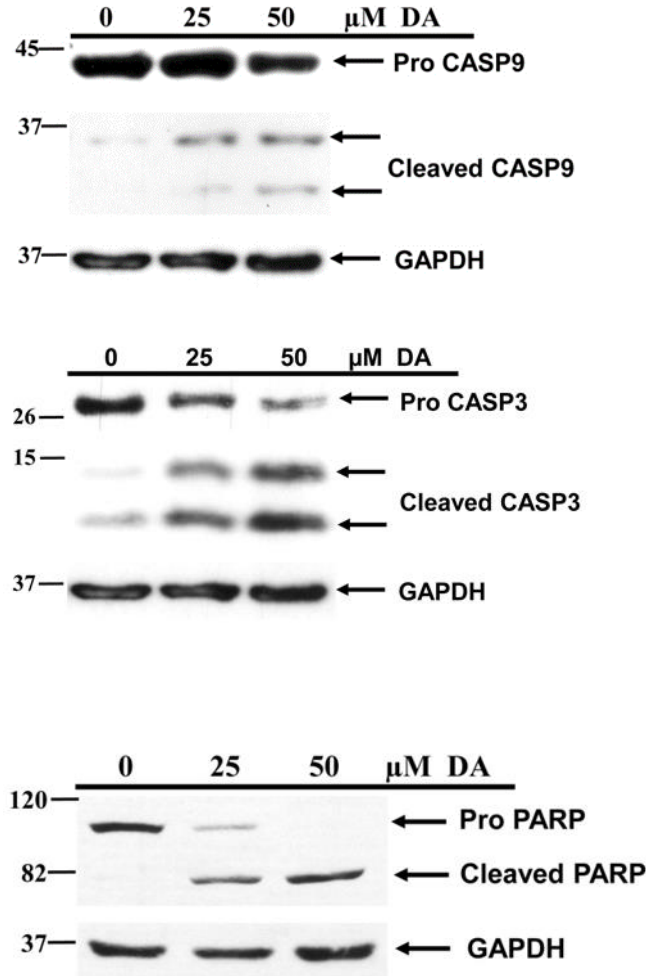


Figure 6: Immunoblot Analysis of Apoptotic Markers Following Dopamine Treatment

There is an increase in several apoptotic markers following 24 hours of treatment with 25 or 50 μM dopamine. Cleavage patterns of caspase 9 (CASP9, top figure), caspase 3 (CASP3, middle figure) and poly(ADP-ribose) polymerase (PARP), bottom figure) suggest apoptosis occurred after treatment with dopamine in a concentration-dependent manner. All bands to the left of the blot represent weight in kilodaltons. All figure representations were repeated at least thrice.

Treatment with dopamine enhanced expression of the i- and n-NOS isozymes

Previous reports suggest that upregulation of the NOS isozymes may play a role in the generation of RO/NS seen following treatment with DA (Chen et al., 2003). We examined the expression of iNOS protein following 1, 6, 12, 16, and 24 h treatment with 0-50 μM DA. Figure 8 displays a time- and concentration-dependent increase in iNOS enzyme expression upon DA

administration. Inducible NOS enzyme was not present at 1, 6, or 12 h (data not shown), but its expression was noted at 16 and 24 h in cells treated with 25-50 μ M DA (Figure 8). We also investigated the n- and e-NOS isozymes for dopamine-enhanced expression. Although there was a slight increase in nNOS expression after 25-50 μ M DA at 24 h, it did not appear as marked as the effect seen with iNOS (data not shown). We did not detect expression of eNOS in our model at any time or DA concentration examined (data not shown).

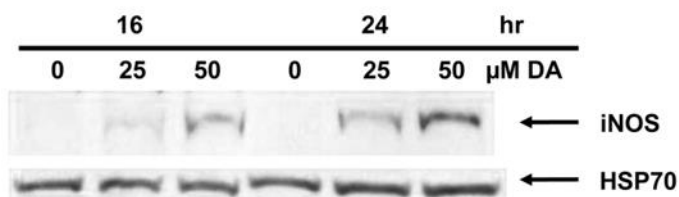


Figure 7: Time- and Concentration-Dependent Protein Expression of iNOS Following Dopamine Administration

Treatment with 25-50 μ M DA resulted in a concentration- and time-dependent increase in iNOS protein expression (below 140 kDa band, not shown) and normalized to heat shock protein 70 (HSP 70; at 70 kDa band, not shown). Figure is representative of findings repeated at least twice.

Dopamine-mediated MnSOD nitration results in enzyme inactivation despite an increase in enzyme levels

To determine if SK-N-MC cells underwent an adaptive response following the generation of RO/NS, we measured MnSOD protein expression *via* western analysis following administration of 0-50 μ M DA. Figure 9 demonstrates a significant increase in MnSOD expression for 50 μ M treated samples vs. control (181%, $p < 0.0001$) that is not seen with 25 μ M DA treatment. Despite the increase in MnSOD protein expression, there was not a concurrent enhancement of enzymatic activity with DA administration (Figure 9). The discordant finding of MnSOD protein versus activity suggests inactivation of the enzyme subsequent to its upregulation.

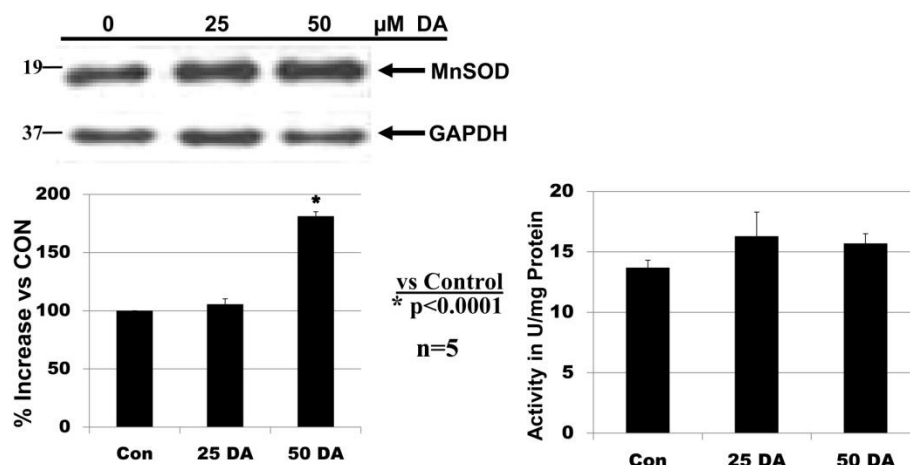


Figure 8: Immunoblot Analysis and Protein Activity of MnSOD in Response to Dopamine Protein expression of MnSOD was significantly increased following 24 hours of dopamine treatment at 50 μ M (left figure), while MnSOD activity (right figure) was not concomitantly elevated suggesting protein inactivation following upregulation. The data was normalized to protein content and is expressed as mean \pm S.E.M. of 5 independent experiments using Student's *t*-test. * $p < 0.0001$ vs. control.

Since MnSOD is known to be inactivated by nitration of key tyrosine residues (Spitz et al., 1990) and we have shown nitrotyrosine formation upon dopamine exposure (Figure 4), we assessed the presence of MnSOD nitration in response to elevated RO/NS. Following overnight immunoprecipitation of isolated mitochondria with 3-NT affinity sorbent, we detected elevated levels of MnSOD by immunohistochemistry in the samples treated with 50 μ M DA as shown in Figure 10. Incorporating the data from Figures 9 and 10 suggests that inactivation of MnSOD, secondary to nitration, negates a MnSOD-modulated adaptive response to the altered redox-state.

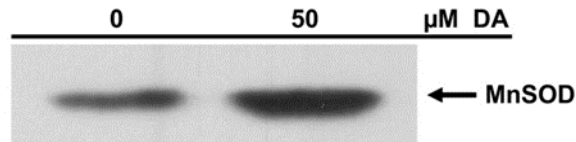


Figure 9: Western Analysis of MnSOD Enzyme following Immunoprecipitation of 3-Nitrotyrosine in Control versus Dopamine-Treated Samples

Following 24 h treatment with 0 or 50 μM DA, isolated mitochondria were immunoprecipitated with 3-nitrotyrosine affinity sorbent followed by western analysis of MnSOD (immediately below 19 kDa molecular weight marker). Dopamine treatment resulted in greater MnSOD nitration than control. Figure is representative of findings repeated twice.

Supplementation with PEG-SOD attenuated markers of dopamine-induced cell death

In order to challenge the hindered activity of MnSOD post-DA exposure, we pre-treated SK-N-MC cells for 1 h with 100 U PEG-SOD then treated with 0-50 μM DA. Treatment with DA showed microscopic morphological changes such as membrane alterations as well as cellular detachment and shrinkage that are consistent with toxicity (Figure 11C) and not visualized in control treated cells (Figure 11A, vehicle only; Figure 11B, 100 U PEG-SOD only). Pre-treatment with PEG-SOD followed by DA, however, yielded morphological characteristics more consistent with control treated cells than DA only treated cells (Figure 11D); and thus appeared protective against an apoptotic process. Parallel western analysis of DA-treated cells pre-treated with PEG-SOD demonstrated a drastic decrease in PARP cleavage products as compared to DA-only treated cells (Figure 12) confirming the protective effect of PEG-SOD pre-treatment.

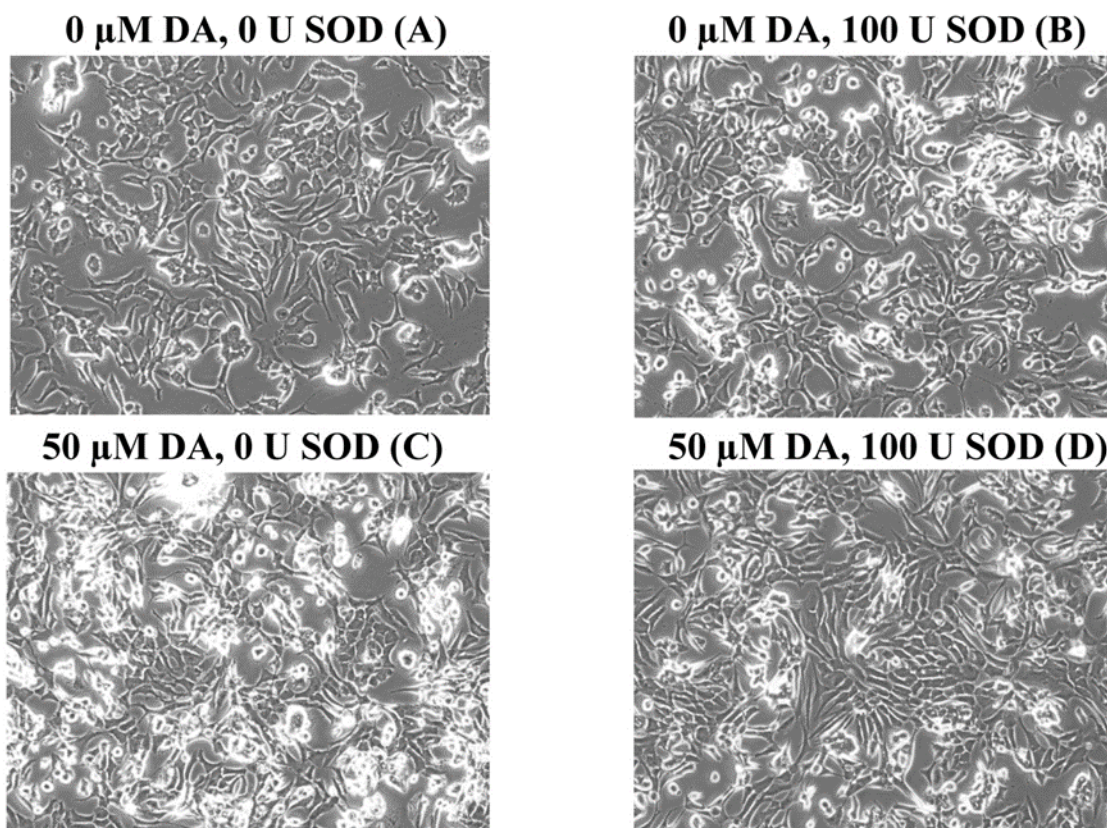


Figure 10: Photographic Demonstration of Dopamine Toxicity and the Protective Effects of Superoxide Dismutase in SK-N-MC Cells
 SK-N-MC cells were pretreated for 30 min with vehicle (**A, C**) or 100 Units of pegylated superoxide dismutase (SOD; **B, D**). The cells were then treated for 24 h with control (**A, B**) or 50 μ M DA (**C, D**). Morphological analysis of the cells demonstrates cellular shrinkage and detachment following dopamine treatment (**C**) that was precluded with superoxide pretreatment (**D**).

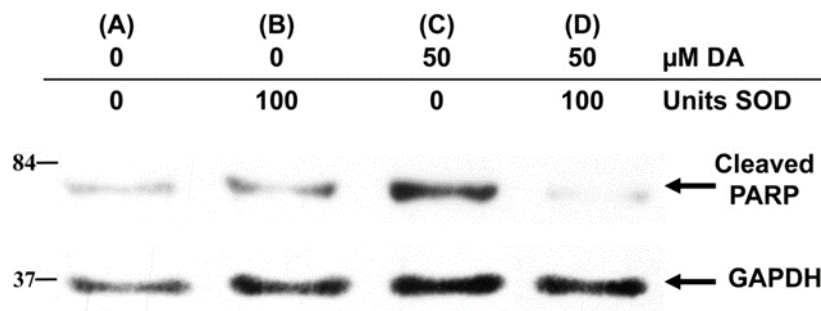


Figure 11: Parallel Western Analysis of Cleaved Poly(ADP-ribose) Polymerase Expression with and without Dopamine and/or Superoxide Dismutase

Samples shown in Figure 11 were analyzed for Poly(ADP-ribose) Polymerase expression. In the 50 μM DA treated samples (C, D), pre-treatment with pegylated superoxide dismutase (SOD, D) abolished dopamine-mediated PARP cleavage seen without SOD pretreatment (C). The results indicate a protective role for exogenous antioxidants in this system of DA-induced toxicity. Molecular weight markers on left of blot are in kDa and figure is representative of findings repeated at least twice.

Dopamine increased AP-1, but not NF κ B, reporter activity in the SK-N-MC cell line

To evaluate the potential role for DA-stimulated NF κ B or AP-1 regulation, we transiently transfected the cells with an NF κ B, AP-1, or empty construct and examined luciferase activity. Luciferase reporter activity in control or DA treated cells transfected with either an empty vector or NF κ B is shown in Figure 13. Although the positive control (100 nM TNF) significantly increased reporter activity ($p < 0.005$), treatment with as much as 100 μM DA failed to induce NF κ B transcription. Reporter activity for DA treated cells transfected with AP-1, however, showed a significant increase in activity compared to control or DA-treated cells containing an empty vector ($P < 0.005$; Figure 14). Although a concentration-dependent significance of DA-induced AP-1 reporter activity was not reached, a trend was noted wherein higher [DA] resulted in enhanced AP-1 luciferase activity.

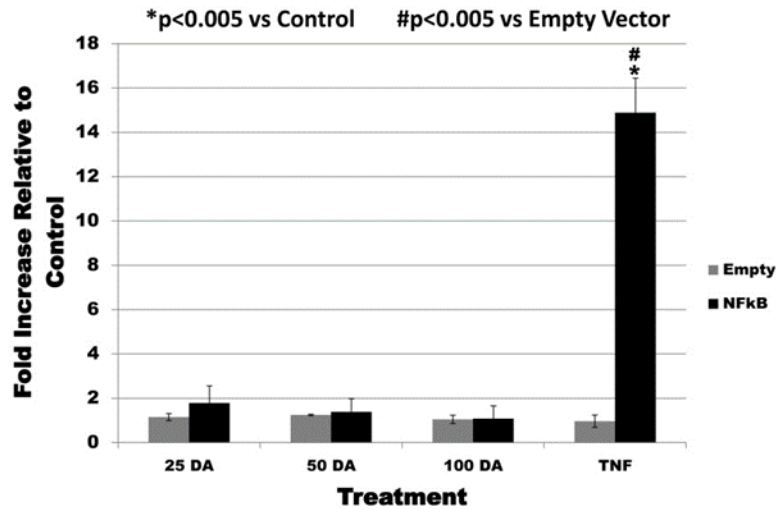


Figure 12: Luciferase Activity in NFκB-Transfected SK-N-MC Cells Treated with Dopamine or Positive Control

Treatment with 100 nM tumor necrosis factor (TNF) yielded a significant increase in luciferase signal indicating successful transfection of the NFκB construct. Dopamine administration, however, did not enhance NFκB reporter activity suggesting that dopamine signaling does not occur through the NFκB pathway in SK-N-MC cells. The data is expressed as mean ± S.E.M. of 5 independent experiments. * $p < 0.005$ vs. control; # $p < 0.005$ vs. empty vector.

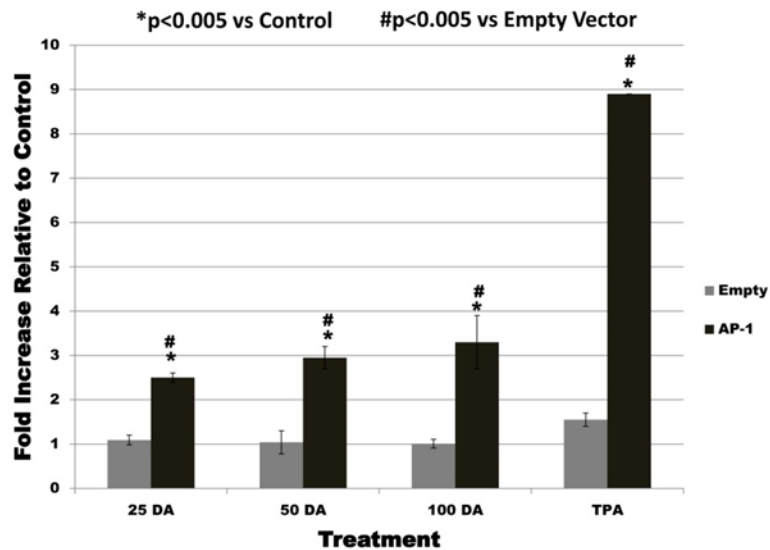


Figure 13: Luciferase Activity in Activator Protein-1-Transfected SK-N-MC Cells Treated with Dopamine or Positive Control

Dopamine stimulation significantly increased AP-1 reporter activity compared to control and dopamine-treated empty construct. There was no statistical difference in AP-1 transfected luciferase activity among 25, 50, or 100 μ M DA samples, and as such dopamine-stimulated AP-1 activity appears to be concentration independent. Treatment with 100 nM tissue plasminogen activator (TPA) was used as a positive control. The data is expressed as mean \pm S.E.M. of 5 independent experiments. * $p < 0.005$ vs. control; # $p < 0.005$ vs. empty vector.

Dopamine increased MAPK p38 and ERK1/2 phosphorylation

We evaluated the effect of DA on several pathways of MAPK phosphorylation. The following MAPKs were examined after treatment with 0-50 μ M DA for 1, 4, and 6 h: p38, extracellular ERK1/2, and JNK. Phosphorylation of p38 (P-p38) was noted after 1 h treatment with 50 μ M DA. After 4 and 6 h, P-p38 was present within the 25 and 50 μ M DA treated samples with a notable time- and concentration-dependence. Phosphorylation of ERK1/2 (P-ERK1/2) was noted in control samples after 4 and 6 h and after 6 h treatment with 50 μ M DA. Unlike the other two MAPKs examined, phosphorylation of JNK was not observed at any of concentration or time studied (data not shown). The findings implicate that phosphorylation of

p38 and ERK1/2 follow DA stimulation; however, it is unlikely that JNK is involved in DA-induced signaling events.

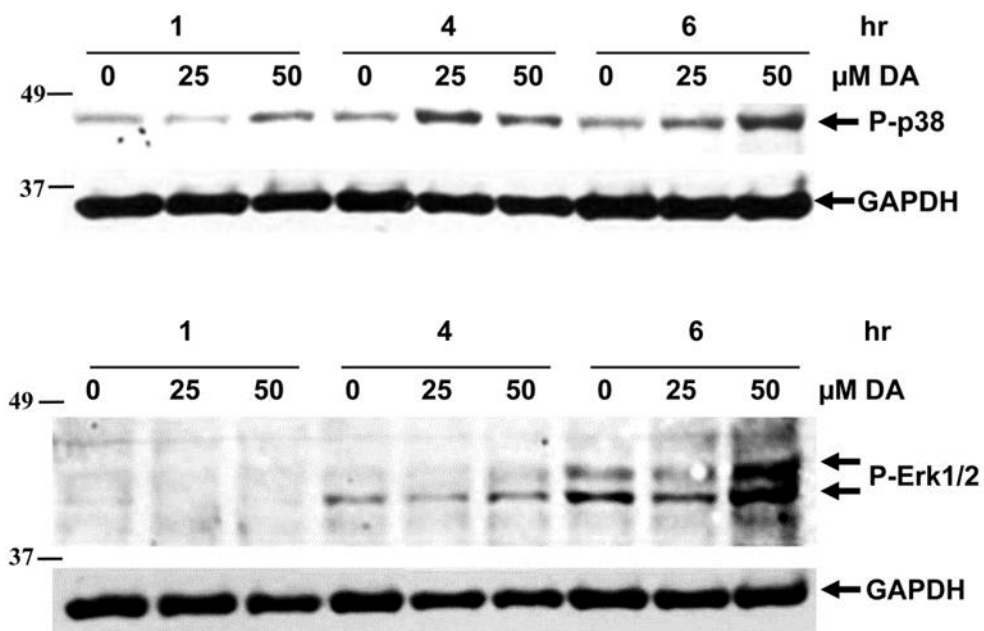


Figure 14: Western Blot Analysis of Phosphorylated Protein Kinases p38 and ERK 1/2 with Variable Dopamine Treatment Time and Concentration

SK-N-MC cells were treated with 0, 25, 50 μM dopamine for 1, 4, or 6 hours then collected for Western analysis. The top blot shows that phosphorylation of p38 is increased in a time- and concentration-dependent manner following dopamine treatment. The bottom blot demonstrates phosphorylation of ERK1/2 in all samples including control beginning at 4 hours, and markedly increased after 6 h treatment with 50 μM dopamine. Molecular weight markers to the left of the blot are in kDa and figures are representative of findings repeated at least twice.

DISCUSSION

The aim of this research was to study the effects of acute DA stimulation in concentrations (25-50 μM) that mirror those found within the human striatum after exposure to MA (Feldman et al., 1997). The properties of the SK-N-MC cell line make it an appropriate model to study DA-induced postsynaptic striatal neurotoxicity and apoptosis, as opposed to presynaptic terminal degeneration on which most studies have been previously focused.

Our results show that acute DA-stimulation in the SK-N-MC cell line resulted in increased nitrosative and oxidative stress with activation of the mitochondrial-mediated apoptotic pathway. Although RO/NS have long been implicated as mediators in DA-induced neurotoxicity (O'Dell et al., 1991; LaVoie & Hastings, 1999), we are the first to report DA-induced pro-oxidative/nitroxidative protein changes in the SK-N-MC model. We found concentration-dependent DA-induced 3-NT formation in response to 25 or 50 μ M DA treatments (Figure 4). Nitrotyrosine formation is seen in cellular systems exposed to RNS, in particular peroxynitrite-generated nitroxidative stress (Squadrito & Pryor, 1998). Previous studies have demonstrated elevated levels of nitrite, a stable marker of NO^{*}, following a 16 h treatment with 25-200 μ M DA in this cell line (Chen et al., 2003). This finding was replicated in two independent studies (Chen et al., 2004; Moussa et al., 2006), and both of these studies proposed the presence of RNS following DA treatment in SK-N-MC cells. Our results extend these findings by showing structural changes in proteins that are consistent with (nitro)oxidative damage. Further, our studies show evidence of RNS using lower physiological doses of DA, and not the toxicological doses (≥ 100 μ M DA) required to measure NO^{*} in the Chen studies (Chen et al., 2003, 2004). The studies by Moussa et al. reported a significant ~2.75 fold increase in nitrite levels compared to control after 16 h treatment with 50 μ M DA in SK-N-MC cells, which is contiguous with 3-NT formation we reported at 24 h (Moussa et al., 2006). Although neither the Chen nor the Moussa study assessed nitrite levels following 25 μ M DA treatment, we suspect, based on our findings, that nitrite levels are elevated.

Attenuation of DA-induced cytotoxicity by antioxidant supplementation or enzyme overexpression has led many reports to infer a causal role for ROS and oxidative stress in mediating cellular toxicity in SK-N-MC cells (Chan et al., 2007; Chen et al., 2003; Zafar et al.,

2006). These studies suggested, but did not conclusively show, macromolecular evidence of oxidative stress following DA stimulation. In our study, we are the first to show evidence of extracellular DA-induced, pro-oxidant change. Four-hydroxy-nonenal adducted proteins were observed following treatment with 50 μ M DA in our system indicating the presence of lipid peroxidation (Figure 5; Spitz et al., 1990). Adducts were noted at molecular weights of ~ 29 and 20 kDA. Similarly, 50 μ M DA stimulation resulted in protein carbonyl formation and revealed that DA-mediated protein oxidation had also occurred (Figure 6; Berlett & Stadtman, 1997). It is interesting to note that in contrast to 3-NT formation which occurred at 25 and 50 μ M DA (Figure 4), 4-HNE and protein carbonyl formation (Figures 5 and 6) were only seen following treatment with 50 μ M DA under our experimental conditions. This finding suggests that RNS are more prominent at lower DA concentrations than are ROS in this system. Another explanation may rest on the ability of Cu/ZnSOD, MnSOD, glutathione peroxidase, and/or catalase to effectively alleviate the ROS produced oxidative stress at 25 μ M DA, while these antioxidant systems may become overwhelmed at 50 μ M DA. Given that: 1) elevated 3-NT is seen at 25 μ M DA and is suggestive of RNS, and 2) NO^{*}, a RNS, is known to terminate propagation of lipid peroxidation, then it is plausible that the NO^{*} produced by 25 μ M DA stimulation diminished the extent of membrane damage sustained by lipid peroxidation and thus 4-HNE adducts were not observed. The ramp-up in RNS production might be an attempted adaptive response in SK-N-MC cells exposed to DA. The expression of apoptotic markers following 25-50 μ M DA, however, does not support this theory.

We observed increases in CASP3, CASP9, and PARP cleavage following 24 h 25-50 μ M DA treatments (Figure 7). We are the first to report DA-mediated CASP9 cleavage in SK-N-MC and thus show the apoptotic pathway is activated, at least in part, through the mitochondria (Li et

al., 1997). A previous study with SK-N-MC reported 50 μ M DA-induced CASP3 cleavage and PARP fragmentation; however, the cells were treated for 48 h before they were collected and assessed for CASP3 and PARP. The authors concluded that a minimum of 36 h treatment was needed in order to observe diminished cell viability and elicit apoptotic signaling, even though their data showed a significant decrease in MTT absorbance at 8, 12, and 24 h upon 50 μ M DA administration compared to control (Chan et al., 2007). The authors did not state if they evaluated CASP3 and PARP cleavage at time-points prior to 48 h, therefore these changes cannot be ruled out in this study.

Our results definitively demonstrated CASP-3, -9, and PARP cleavage at 24 h; therefore, we propose pro-apoptotic signaling does occur within this time-frame of DA administration. Consistent with our 24 h apoptotic findings, previous studies in SK-N-MC cells reported 16 h treatment with 50 μ M DA resulted in decreased cell viability (Chen et al., 2003; 2004; Moussa et al., 2006). Although the loss of cell viability could be attributed to DA-induced necrosis, findings such as mitochondrial cytochrome *c* release led the authors to suggest the mechanism of cellular death was through an apoptotic pathway (Moussa et al., 2006). A study by Junn and Mouradain in 2001, with SH-SY5Y cells, reported 15 h treatment with 200 μ M DA resulted in decreased cell viability by MTT assay, release of cytochrome *c*, and cleavage of CASP3, CASP9, and PARP. In support of our findings, the report concluded DA treatment activated pro-apoptotic pathways. The concentration of DA used in their study, however, was four-fold greater than the highest amount used in our study which questions the physiological relevance of the findings. Furthermore, the presence of DAT in SH-SY5Y allows for DA uptake into the cytoplasm of the cell and renders the cell susceptible to intracellular oxidative damage by DA. The SK-N-MC cell line lacks DAT, thus only the effects of extracellular DA are observed. In

addition, possession of DAT also renders the SH-SY5Y cell system a more appropriate model for investigating pre-synaptic toxicity as opposed to post-synaptic toxicity toward which our study is aimed.

Our report of DA-stimulated mitochondrial-mediated apoptosis is the first in this cell-line. These findings offer insight into the mechanism by which DA-induces postsynaptic cell death within the striatum. Mitochondrial- and endoplasmic reticulum-mediated postsynaptic apoptotic-processes occur upon acute MA administration (Cadet et al., 1997; Jayanthi, et al., 2005; Krasnova & Cadet, 2009). Our data suggests that the pathology of MA-induced apoptosis may be the result of DA-activation of the mitochondrial pathway. Future studies in this model should be aimed at the potential involvement of DA-activation of the endoplasmic reticulum pathway, which would impart significance not only to MA neurotoxicity, but also that of Parkinson's and Huntington's diseases, schizophrenia, and drugs of abuse other than MA.

In light of DA-induced RNS and subsequent apoptosis in our model, we evaluated the presence of NOS isozymes and found a time- and concentration-dependent increase in iNOS (Figure 8). There is a causative role of n- and iNOS overstimulation in MA-induced neurotoxicity, but with much debate as to overexpression of which NOS isozyme is more toxic (Cadet et al., 2001; Di Monte et al., 1996; Imam et al., 2001; Itzhak & Ali, 1996; Itzhak et al., 1998; 1999; 2000; Kita et al., 2003). Our data is consistent with those that implicate the inducible isozyme as the neurotoxic culprit *in vivo* (Itzhak et al., 1999) and in SK-N-MC cells (Chen et al., 2003). One notable difference between our study and that of Chen et al. is the time-dependence of DA-mediated iNOS expression. In the 2003 study, the authors show iNOS protein expression after 1 h DA treatment whereas we did not observe iNOS until 16 h of treatment. Without knowledge of the authors' exact DA preparation protocol, it is hard to

speculate why there is a large time difference in iNOS expression. One possibility is that the DA used in their study was prepared with ascorbic acid or sodium metabisulfite, which is commonly used in DA preparations to prevent DA oxidation. Preventing DA oxidation might render more DA available for D₁ receptor activation leading to quicker iNOS upregulation, since iNOS is known to be predominately mediated through D₁ in this system (Chen et al., 2003). Despite differences in time until expression, both studies implicated iNOS as the principal expressed isozyme following DA administration. The DA-stimulated overexpression of iNOS coupled with its known high output of NO[•] suggests that iNOS is a mediator of DA-induced RNS, 3-NT formation, and apoptosis in this model of postsynaptic neurotoxicity. Inducible NOS, therefore, should be considered a target for neuroprotective intervention. Furthermore, iNOS has also been named an important mediator of MA neurotoxicity in studies of MA-induced microglial activation and microgliosis in animal models (LaVoie et al., 2004; Thomas et al., 2004) and humans (Sekine et al., 2008). Understanding and modulating its overexpression in microglial cells might prove neuroprotective and should be investigated in future studies.

We found an upregulation of the antioxidant enzyme MnSOD and demonstrated that SK-N-MC cells attempted to mount an adaptive response to 50 μM DA (Figure 9). The absence of MnSOD upregulation following 25 μM DA may be due to diminished ROS at that DA concentration. Although there was 4-HNE and protein carbonyl formation in cells treated with 50 μM DA, there were no markers of ROS following treatment with 25 μM DA. Since oxidative stress and ROS, namely O₂^{•-} and H₂O₂, are known to induce MnSOD expression (St. Clair, 2002); then it is plausible that the absence of ROS after 25 μM treatment precluded the upregulation of MnSOD. Despite the significant enhancement of MnSOD protein upon 50 μM DA treated cells, there was not a concomitant increase in enzyme activity (Figure 9). The

discordant finding between protein vs activity points to alterations in MnSOD's functional integrity. Work by MacMillan-Crow et al. revealed that MnSOD was susceptible to tyrosine nitration and dityrosine formation by peroxynitrite-mediated protein modifications. These modifications resulted in MnSOD inactivation (MacMillan-Crow et al., 1998).

Tyrosine nitration and dityrosine formation are amino acid alterations that occur as a consequence of nitroxidative and oxidative stress, respectively, and we have shown the presence of both of these stressors in our DA treated cells. The 3-NT immunoprecipitants from 50 μ M DA treated cells contained a marked increase in MnSOD protein relative to control (Figure 10), thus demonstrating that MnSOD was indeed nitrated by peroxynitrite in our system. We hypothesize that DA-induced overexpression of iNOS markedly elevated NO^{*} production, and the NO^{*} then instantaneously reacted with O₂^{•-} from the oxidation of DA to form peroxynitrite. The peroxynitrite-compromised MnSOD function lead to even more O₂^{•-}, which then increased peroxynitrite production and furthered the inactivation of MnSOD. We speculate that the continued production of peroxynitrite was responsible for the 50 μ M DA-induced MnSOD nitration (Figure 10) and lipid peroxidation (Figure 5) discovered in this system. Given that MnSOD activity following 50 μ M DA treatment was not reduced below that of control, however, suggests that the enzyme maintained at least a basal level of activity (Figure 9). It is unlikely that this finding is due to nitration of MnSOD protein away from the enzyme's active site as tyrosine modification of mutant MnSOD (Y34F; tyrosine → phenylalanine substitution of the active site tyrosine residue most susceptible to nitration) by peroxynitrite still significantly decreases MnSOD activity (MacMillan-Crow & Thompson, 1999). Peroxynitrite is required for complete inhibition of MnSOD activity (MacMillan-Crow et al., 1998), thus it is expected that

the 50 μ M DA treated samples would have diminished the enzyme to zero activity. This discrepancy in findings will be further investigated in future studies.

We hypothesized that the DA-mediated nitration and inactivation of MnSOD in this system is of central importance based on findings from previous studies. Keller et al. and Kinningham et al. reported overexpression of MnSOD protects against peroxynitrite production, lipid peroxidation, PARP cleavage, and mitochondrial-mediated apoptosis in systems subject to oxidative stress (Keller et al., 1998; Kinningham et al., 1999). Additionally, Maragos et al. reported a reduction in MA-induced protein oxidation and striatal dopamine depletion in transgenic mice that overexpress human MnSOD (Maragos et al., 2000). These studies suggest that the DA-mediated inactivation of MnSOD in our system may be at least partly responsible for the observed apoptosis.

To determine whether augmentation of SOD activity attenuated or even prevented DA-mediated apoptosis in our cell system, we treated with 100 units PEG-SOD 30 min prior to 50 μ M DA treatment. Our theory of inadequate SOD activity in SK-N-MC was substantiated by the abolishment of DA-induced PARP fragmentation upon addition of PEG-SOD (Figure 12). The microscopic morphological appearance of the SK-N-MC cells also suggests a protective effect for PEG-SOD in the DA treated samples (Figure 11A-D). The presence of the polyethylene glycol substituent of PEG-SOD permits SOD to diffuse inside of cells and act as an intracellular antioxidant as opposed to solely an extracellular antioxidant that would be the case if the SOD was not PEGylated. This distinction is important in examining the findings from Zafar et al. in which pre-treatment with 1 mg/mL of SOD did not offer protection against DA-induced cell death in SK-N-MC (Zafar et al., 2006). These results, however, can only be attributed to extracellular actions of SOD on DA administration since the SOD was not PEGylated.

Furthermore, the Zafar study used [DA] of 500 μ M that far exceeds concentrations within the striatum following MA use (Feldman et al., 1997). It is not surprising then that the supra-toxic concentration of DA overwhelmed the antioxidant capacity of SOD.

Superoxide dismutase can also have differing levels of activity per mg of enzyme rendering it imperative to standardize the use of an SOD mimetic by activity rather than amount by weight (Squadrito & Pryor, 1998). The study by Zafar et al. used SOD measured in mg/mL instead of units of activity; therefore, it is difficult to speculate the amount of active SOD that was actually employed in that study. We standardized the amount of SOD activity in our studies to 100 units and found it to be protective. Overall, the absence of 1) DA-triggered PARP cleavage, and 2) morphologic changes consistent with cellular toxicity following pre-treatment with PEG-SOD indicate that by improving the antioxidant capacity of the cellular system we can prevent DA-stimulated apoptosis that is stereotypical of MA-induced neurotoxicity. The importance of this finding is underscored by research that has reported the antioxidant capacity of neural cells is sufficient to protect against cocaine-induced dopaminergic toxicity, whereas the magnitude of DA release following MA (which is approximately four-fold higher) overwhelms the cellular antioxidant defense mechanisms and thus leads to regional neurotoxicity (Dietrich et al., 2005; Mirecki et al., 2004). Therefore, the antioxidant properties of MnSOD and its susceptibility to inactivation *via* nitration make it a notable target for the prevention of MA-triggered DA neurotoxicity.

As stated earlier, identification of iNOS and/or MnSOD protein regulation is of paramount importance to understand the modulation of MA-initiated DA neurotoxicity. To elucidate possible regulators of iNOS or MnSOD expression, we assessed for DA-stimulated reporter activity in SK-N-MC cells using NF κ B or AP-1 constructs. Both of the aforementioned

transcription factors: 1) are redox-sensitive, 2) have consensus sequences within the human iNOS and MnSOD genes, 3) are upregulated following ROS-derived neuronal injury, and 4) their regulation is responsive to MA treatment (Flora et al., 2002; Kiningham et al., 1997; Krasnova & Cadet, 2009; Maragos et al., 2000).

We are the first to report that DA treatment of SK-N-MC does not enhance NF κ B reporter activity at 25, 50, or 100 μ M DA (Figure 13), which is a concentration above the EC₅₀ of 75 μ M DA for the D₁ receptor in this cell line (Moussa et al., 2006). In contrast, Chen et al. (2003) reported that incubation with SN50, an NF κ B inhibitor, significantly decreased nitrite production following 16 h 50 μ M DA treatment in SK-N-MC. Given the SN50-attenuated nitrite production along with previous reports of transcriptional regulation of iNOS by NF κ B, the authors concluded that DA-stimulated iNOS induction in SK-N-MC may occur in part through NF κ B regulation (Chen et al., 2003). Studies have questioned the selectivity of SN50 for NF κ B due to its inhibitory effects on several other transcription factors including AP-1, STAT (signal transducer and activator of transcription; D'Acquisto & Ianaro, 2006; Torgerson et al., 1998), and Nrf2 (nuclear factor E2-related factor; Theodore et al., 2008). Activator Protein-1 and STAT have transcriptional binding sites within the human iNOS promoter, and Nrf2 has also been shown to modulate iNOS expression (Rojo et al., 2010). The reported attenuation of nitrite production following co-treatment with SN50 and DA, therefore, might have resulted from non-selective inhibition of a variety of transcription factors that are known to regulate iNOS expression. A study by Flora et al. (2002) examined NF κ B activation following acute MA treatment. This study also reported an absence of MA-induced NF κ B DNA binding in mouse brain that was independent of exposure, time and brain region studied (Flora et al., 2002). Combining the findings from our study with that of the Flora study, it is highly unlikely that

MA-induced DA stimulation results in NF κ B activation. Additional studies should be conducted to solidify this data and perhaps remove NF κ B as a potential target to upregulate MnSOD or modulate iNOS overexpression in an attempt to prevent MA/DA-induced neurotoxicity.

We are the first to show dopamine-stimulated reporter activity in SK-N-MC cells transfected with an AP-1 construct (Figure 14). We demonstrated that reporter activity tends to increase proportionally with DA concentration. The findings in our model complements *in vivo* reports that MA injections result in enhanced expression of transcription factors from the AP-1 family in mouse brain (Cadet et al., 2001) and increased AP-1 DNA binding in mouse striatum (Flora et al., 2002). Additionally, given the non-selective nature of SN50, it is possible that the reduced DA-triggered nitrite production reported by Chen et al. (2003) was a result of SN50 inhibition of AP-1 transcription and subsequent iNOS expression (Chen et al., 2003). Although we have reported DA stimulation activates AP-1, we have not shown if its transcription modulates iNOS or MnSOD expression as both enzymes contain consensus sequences for AP-1 within their promoter region. We also did not study if AP-1 activation was protective or deleterious. Future studies will be aimed at employing transfection of dominant negative AP-1-containing plasmid then assessing iNOS and MnSOD protein expression as well as PARP fragmentation and cell viability. Once a definitive role for DA-stimulated AP-1 transcription is determined, its activity can be modulated in a way to maximize cell survival.

The MAPK family is a known upstream modulator of AP-1. Given that DA stimulated AP-1 activity in our model, we assessed the phosphorylation status of three members of the MAPK family following DA treatment. Dopamine-stimulated p38 phosphorylation occurred in a time- and concentration-dependent manner beginning at 4 h, while DA-stimulated ERK1/2 phosphorylation occurred after 6 h of treatment with 50 μ M DA (Figure 15), and

phosphorylation of JNK was not noted at any time or concentration of DA (data not shown). Phosphorylated ERK1/2 also appeared in control treated samples at 4 and 6 h which is not surprising as ERK1/2 activation is a well-documented response to serum-starvation within animal and human cell lines (Jung et al., 1999). These findings implicate P-p38 and P-ERK1/2 as participants in DA-mediated cell signaling in SK-N-MC. Both of these MAPK members mediate neuronal survival and death in response to various stimuli (Shaulian & Karin, 2001; 2002), thus their regulation in response to DA may be integral in modulating neurotoxicity or neuroprotection.

Two previous studies in SK-N-MC cells yielded conflicting reports of DA receptor-mediated MAPK activation. The first study demonstrated a time- and concentration-dependent increase in p38 and JNK phosphorylation following DA D₁ receptor stimulation with a D₁ selective agonist, SKF-38393. Phosphorylated p38 and P-JNK appeared with ~15 min with 1-500 μ M SKF-38393, while the presence of P-ERK1/2 was not detected after 120 min of incubation with a maximum concentration of 500 μ M SKF-38393 (Zhen et al., 1998). Interestingly, the second study reported D₁ stimulation with 200 μ M SKF-38393 for 1 h resulted in phosphorylation of ERK1/2 only, while 100 μ M DA increased phosphorylation of ERK1/2 and p38, but not JNK (Chen et al., 2004). Although some of the data from the three studies on MAPK activation in SK-N-MC are contradictory, there are findings that prove consistent. First, p38 activation was shown in all studies, including ours. Second, in the two studies utilizing DA as the stimulus, ERK1/2 was phosphorylated in both whereas the presence of P-JNK was slight at best. The most striking difference came in the two studies that used a D₁ agonist in which one reported the phosphorylation of ERK1/2 while the other did not. In the context of deducing the cause of MA-induced neurotoxicity, for which our study was designed, the MAPK regulation of

DA stimulation is more relevant than that of specific D₁ activation since DA, and not a non-oxidizable D₁ agonist, is the endogenous neurotransmitter released after MA exposure. Thus the roles of ERK1/2 and p38 should be further elucidated in DA-mediated pro-apoptotic vs protective signaling as well as their potential downstream affect on AP-1. Future studies will also investigate the role of the relatively new MAPK member, ERK5 (Zhou et al., 1995). Reports indicate a protective role for ERK5 in cortical neurons (Liu et al., 2003) and in dopaminergic cells exposed to 6-hydroxydopamine, an oxidative metabolite of DA (Cavanaugh et al., 2006). Preliminary studies in our laboratory have shown phosphorylation of ERK5 in response to DA treatment (data not shown), but its regulatory role in SK-N-MC has not yet been investigated.

Taken together we have shown DA treatment resulted in protein modifications that are consistent with (nitro)oxidative stress. We hypothesize that a central source of nitroxidative stress is due to DA-triggered iNOS upregulation. The observed mitochondrial-mediated apoptosis, we believe, resulted from nitration of and thus a failure to mount an adaptive response by the key mitochondrial antioxidant enzyme, MnSOD. Dopamine did not stimulate NFκB reporter activity but did significantly increase AP-1 luciferase signal. Furthermore, we identified P-p38 and P-ERK1/2 as possible upstream modulators of DA-induced AP-1 activation. These findings may be extended to not only MA neurotoxicity, but also several other pathologic settings such as schizophrenia, Parkinson's disease, Huntington's disease, and various drugs of abuse wherein dopaminergic neurotoxicity is fundamental. Interventions to augment antioxidant capacity; up- or down-regulate MnSOD or iNOS, respectively; and target AP-1 activity and its upstream modulation could prove to be neuroprotective in any of those disease processes.

CHAPTER 3

THE MECHANISM BY WHICH DOPAMINE INDUCES MAPK P38 SERVES AS A “MOLECULAR SWITCH” BETWEEN CELLULAR PROTECTION AND APOPTOSIS IN A MODEL OF METHAMPHETAMINE NEUROTOXICITY

Introduction

With the growing world-wide popularity of methamphetamine and other stimulants of abuse, much research has been dedicated to the study of their neurotoxic and addictive properties. Despite the volume of research there is still a multitude of unanswered questions, unexplored mechanisms, and a most unfortunate disconnect between basic and clinical research. The goals of this research were to investigate mechanisms responsible for the profound dopaminergic neurotoxicity associated with stimulant abuse and subsequently identify ways to prevent this toxicity from occurring. Another focus of this work was to provide information on a macromolecular and cellular level about potential neurotoxicity resulting from the use of dopamine D₁ receptor (D₁) agonists and antagonists that are currently used in behavior-modifying studies of stimulant addiction.

Central to the pathology of addiction is the cyclic nature of the disease within the mesolimbic and mesocortical pathways. The majority of acute neurotoxicity and initiation of the addictive process occurs within the mesolimbic system, in particular the ventral and dorsal striata (Chang et al., 2007; Goldstein et al., 2002; Veeneman et al., 2011; Volkow et al., 2004). Dopamine has long been implicated as a mediator of this pathway by its ability to modulate feelings of reward, motivation, and craving (Robinson and Berridge, 1993). The striatal toxicity associated with stimulant abuse occurs as a result of the supra-physiologic DA concentration that is reached following drug administration (O'Dell et al., 1991; 1993). These properties have

made DA and activation of its receptors, specifically D₁, the focus of many studies aimed at understanding stimulant-induced neurotoxicity and diminishing the phenomenon of craving and subsequent relapse in humans (Karila et al., 2010) and animal models (Shuto et al., 2006; van Gaalen et al., 2006).

Many clinical and translational studies indicate a need for a mechanistic study of striatal dopaminergic synapses (Goldstein et al., 2002; Veeneman et al., 2011; Volkow et al., 2004;), especially the D₁ expressing postsynaptic neurons (Chang et al., 2007; Krasnova & Cadet, 2009; van Gaalen et al., 2006; Wang et al., 2012; Xu et al., 2005). The D₁ postsynaptic striatal neurons show sustained morphological changes as well as prolonged alterations in gene expression of the Fos family following exposure to and absence from methamphetamine in rodent and human striata (Badiani et al., 1999; Beauvais et al., 2010; Gross & Marshall, 2009; Robinson & Nestler, 2011). Their D₂-expressing counterparts, however, revert to their original morphology after cessation and only activate Fos in novel environments (Badiani et al., 1999; Lee et al., 2006). The observed DA-mediated neurotoxicity and alterations in D₁ postsynaptic striatal neurons are a key factor in the development of addiction (Chang et al., 2007; Larson et al., 2010; Lee et al., 2006; Robinson & Nestler, 2011). For these reasons, we studied and identified molecular mechanisms and signaling systems responsible for DA-induced neurotoxicity in an *in vitro* model of D₁ expressing postsynaptic striatal neurons.

The SK-N-MC cell line was used as a model because they endogenously express the D₁ receptor, are absent of dopamine transporters (DAT) and tyrosine hydroxylase and have a morphology that is similar to postsynaptic medium-spiny density neurons of the striatum (Chen et al., 2003; Sidhu & Fishman, 1990). To mimic dopaminergic neurotoxicity following stimulant abuse, namely MA, we treated cells with 0-50 μ M DA for 24 h to impart physiological relevance

(Chen et al., 2003; Feldman et al., 1997) and subsequently monitored for indicators of cellular toxicity. We also evaluated markers of apoptosis following treatment with a specific D₁ agonist, SKF-38393; and co-treatment with DA and a specific D₁ antagonist, SCH-23390. Western analysis of the cleavage products of caspase 3 (CASP3) and poly(ADP-ribose) polymerase (PARP), as well as morphological changes consistent with cellular toxicity were used as indicators of apoptosis (Cadet et al., 1997; Deng et al., 2002b; Lazebnik et al., 1994). In this chapter, we demonstrated the involvement of mitogen activated protein kinase p38 (MAPK; p38) and activator protein-1 (AP-1) following DA stimulation (Figures 13-15). In the current work, we examined the pivotal role of p38 as orchestrator of cellular adaptation versus apoptosis depending on D₁ receptor stimulation or blockade. Recent evidence suggests the Fos family of proteins function as modulators of stimulant-induced neurotoxicity, initiation of addiction, and sustained morphologic changes following prolonged abstinence (Beauvais et al., 2010; Gross & Marshall, 2009; Krasnova & Cadet, 2009; Larson et al., 2010; Martin et al., 2012; Robinson & Nestler, 2011). We, therefore, studied the participation of cFos in DA-induced apoptosis and AP-1 transcription.

In this study we describe multiple mechanisms of DA-induced cellular apoptosis in our model including specific D₁ activation as well as a D₁-independent pathway. We are also the first to report that MAPK p38 acts as a “molecular switch” between cellular adaptation and apoptosis depending on the specific way it is activated by DA i.e., through D₁ receptor stimulation or through a D₁-independent mechanism. Additionally, we show that cFos is a regulator of DA-mediated AP-1 transcription and is pro-apoptotic. Furthermore, we provide indirect evidence that DA-induced cFos activation occurs through a p38-dependent, D₁ receptor independent manner in our model of postsynaptic striatal neurons. Perhaps most compelling we

have identified two ways to ameliorate DA-induced PARP fragmentation in this system by: 1) co-inhibition of D₁ and p38, or 2) inactivation of AP-1 through use of a cFos dominant negative.

The findings from this research are important to understanding several aspects of dopaminergic neurotoxicity and addiction. This study offers mechanistic answers to clinical and translational findings regarding stimulant-induced D₁ postsynaptic striatal neurotoxicity, including the identification of pro-apoptotic signaling pathways. The findings also demonstrate a need for additional research to investigate potential neurotoxic side-effects in the use of D₁ agonists to modify human behavior and cravings. Lastly, we identified two signaling molecules, p38 and cFos, whose activation modulates the execution of DA-induced apoptosis and thereby serve as potential pharmacological targets to avert stimulant neurotoxicity.

Materials and Methods

Cell culture and treatment paradigm

The human SK-N-MC neuroepithelioma cell line was obtained from the American Type Culture Collection (Manassas, VA) and maintained in RPMI 1640 medium without phenol red and supplemented with 1% (v/v) nonessential amino acids, 1% antibiotics (penicillin/streptomycin/neomycin; Invitrogen Corp.; Carlsbad, CA), 10% Nu-Serum (BD Biosciences; San Jose, CA) and 1 mM sodium pyruvate. Cells were incubated at 37°C in a humidified atmosphere with 5% CO₂. All treatments were 6 or 24 h and were administered following 24 h pyruvate- and serum-starvation, shielded from light, and accompanied by untreated and/or vehicle-treated control samples. Dopamine treatments were with 25 or 50 μM dopamine hydrochloride (Sigma-Aldrich; St. Louis, MO) dissolved in cell culture medium. In D₁ dopamine receptor-specific studies, the cells were treated with 25 or 50 μM of the D₁ specific agonist, (R)-(+)-SKF-38393 (Sigma-Aldrich), in the absence of DA; or pretreated for 30 min

with 10 μ M of the D₁ specific antagonist, (R)-(+)-SCH-23390 (Sigma-Aldrich), followed by co-treatment with DA as previously described (Chen et al., 2003; 2004). Both the D₁ receptor agonist and antagonist were dissolved in sterile water. In MAPK p38 inhibition studies, 2 μ M of the p38 selective inhibitor SB203580 (Calbiochem; La Jolla, CA) was administered 30 min prior to treatment with SKF-38393, DA, or DA with SCH-23390. The concentration of SB 203580 was chosen based on the lowest concentration needed to return p38 phosphorylation found in control cells. The SB 203580 was dissolved in 0.07% (v/v) DMSO. The cells were microscopically visualized using a Nikon Diaphot instrument (Frank E. Fryer Co., Cincinnati, OH) and photographed with a Nikon N2000 camera immediately prior to collection.

Protein preparation and immunoblot analysis

For immunoblot analysis, SK-N-MC cells were plated at a density of 3×10^6 /150 mm dish then serum-starved once cells were ~85% confluent. Following 24 h treatment, whole-cell lysates were collected with the inclusion of protease inhibitors (pepstatin, leupeptin, aprotinin) at 1 μ g/ml. Protein concentrations were determined by a colorimetric assay (Bio-Rad Laboratories; Richmond, CA) using bovine serum albumin as a standard. Homogenate protein samples (100 μ g/lane) were run on 10, 12.5, or 15% SDS-PAGE according to the method of Laemmli (1970) and transferred to a nitrocellulose membrane. Transfer efficiency was assessed by staining with 0.1% (w/v) Ponceau S. The membranes were washed with distilled water to remove excess stain, then the nonspecific binding sites were blocked at room temperature for 1 h with Blotto (5% [w/v] dried milk in tris-buffered saline with Tween-20 [TBS-T; 50 mM NaCl, 10 mM Tris-HCl (pH 8.0), 0.05% (v/v) Tween-20]). The membranes were then incubated overnight at 4 $^{\circ}$ C with gentle shaking in Blotto with primary rabbit polyclonal antibodies directed against cleaved caspase-3 (1:1000), phosphorylated p38 MAPK (1:750), phosphorylated heat shock protein 27

(1:5000), or PARP (1:4500; Cell Signaling Technology, Inc; Beverly, MA.). After three washes with TBST, the membranes were incubated with secondary HRP-conjugated anti-rabbit IgG in Blotto (1:3000; Santa Cruz Biotechnology; Santa Cruz, CA) for 1.5 h at room temperature with gentle shaking. Following three washes with TBST and one with TBS, the protein bands of interest were visualized using the enhanced chemiluminescence detection system (Amersham Biosciences; Little Chalfont, U.K.). To confirm equal protein loading, all blots were reprobbed with a rabbit polyclonal anti-GAPDH antibody (1:50,000; Trevigen; Gaithersburg, MD).

Transient transfection and reporter assay

Cells were plated at a density of 4.2×10^6 /100 mm plate and grown for 48 h (~75% confluent). One hour prior to transfection, the cells were washed twice with phosphate-buffered saline (PBS; 137 mM sodium chloride, 3 mM potassium chloride, 1 mM potassium phosphate, 10 mM sodium phosphate) and then the medium was replaced with Minimal Essential Medium supplemented with 10% heat inactivated fetal bovine serum (Invitrogen Corp.), 1% nonessential amino acids, 1% antibiotics, and 1 mM sodium pyruvate. The cells were then transfected with 6 μ M of a pGL2 vector (Promega; Madison, WI) with or without the AP-1 construct (a generous gift from Dr. Richard Niles, Marshall University School of Medicine) via the calcium phosphate method (Graham & van der Eb, 1973). The AP-1 construct contains four consensus binding sequences inserted into a pGL2 vector. In the dominant negative assays, 0.75 μ g of CMV-500 vector with or without an A-Fos construct (a generous gift from Dr. Charles Vinson, National Institutes of Health) was co-transfected with an empty or AP-1 containing pGL2 vector. The A-Fos construct is a dominant negative to c-Fos and works by adding an amphipathic, acidic extension to the N-terminus of the Fos leucine zipper thereby inhibiting DNA binding of AP-1 in equimolar competition (Olive et al., 1997). After 7 h incubation in transfection medium, the

cells were washed twice with PBS and the transfection medium was replaced with the regular culture medium. The next day, the cells were trypsinized and plated in 24-well plates at a density of 3.0×10^5 cells/well for the reporter assay or at 4×10^6 cells/100 mm plate for immunoblot analysis and allowed to grow overnight. Following 24 h serum and pyruvate starvation, the cells were treated for 6 or 24 h for reporter or immunoblot analysis, respectively, with 0-50 μ M DA or 100 nM TPA; the latter compound is a strong inducer of AP-1 transcriptional activity and was used as a positive control. The cells were lysed in 200 μ L of reporter passive lysis buffer (Promega) then frozen at -20°C overnight. Transcriptional activity was assessed using the luciferase assay system (Promega) in a TD 20/20 luminometer (Turner Designs; Sunnyvale, CA).

Data analysis

All experiments were at least twice replicated (for $n \geq 3$) and representative findings are shown. Grubbs' Outlier Test was performed on all data, and significant data outliers were removed from further analysis. Final statistical analysis was conducted using three-way analyses of data and variance for multiple samples. Post hoc tests were examined with Student Newman-Keuls on SigmaStat software (SPSS Inc., Chicago, IL). A p value of <0.05 was considered statistically significant.

Results

D₁ receptor stimulation via SKF-38393 exacerbates PARP cleavage in a manner independent of CASP3

We have previously shown that acute DA treatment led to apoptosis in this cell model (Figure 7). To study the involvement of D₁ receptor stimulation in the activation of apoptotic pathways, we treated SK-N-MC cells with 0-50 μ M of DA or the specific D₁ agonist, SKF-

38393, for 24 h. We analyzed caspase 3 (CASP3) and poly (ADP-ribose) polymerase (PARP) cleavage products to serve as indicators of apoptosis. Effector CASP3 was cleaved following DA treatment (Figure 16) with a significant increase in the levels of p17 and p19 products in cells treated with 25 ($p<0.05$) and 50 ($p<0.01$) μM DA versus control. The dopamine-induced cleavage was concentration dependent. SKF-38393 did not significantly increase CASP3 cleavage compared to control suggesting that DA-mediated CASP3 cleavage occurs through a pathway independent of D_1 activation (Figure 16).

Figure 17 demonstrates that treatment with 25 or 50 μM DA significantly decreased native PARP levels in a concentration dependent manner ($p<0.001$ vs control). Treatment with 50 μM DA resulted in a ~36% greater loss of full-length PARP when compared to 25 μM DA ($p<0.05$). This change was accompanied by a significant elevation in PARP fragmentation in 25 and 50 μM DA treated cells when compared to control ($p<0.05$, $p<0.005$; Figure 17). Following treatment with 25 and 50 μM SKF-38393 there was a significant decrease in full-length PARP protein ($p<0.001$; Figure 17) with a concomitant significant increase in its fragmented products ($p<0.001$; Figure 17) vs control. Further analysis of 25 μM SKF-38393 treated cells demonstrated a significant increase of ~23% in PARP cleavage compared to 25 μM DA treatment ($p<0.05$) with the same trend observed between the 50 μM DA treated groups. The observed PARP fragmentation suggests that D_1 -mediated apoptosis occurred, albeit through a mechanism that circumvented CASP3 cleavage.

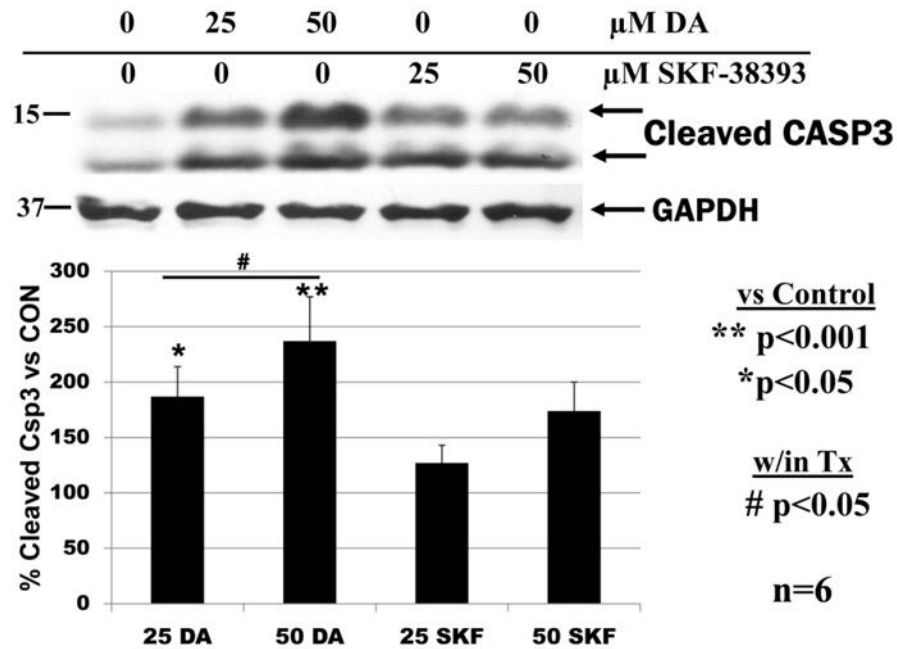


Figure 15: Qualitative and Quantitative Protein Analysis of Caspase 3 Cleavage in Dopamine or SKF-38393 Treated SK-N-MC

Treatment with dopamine for 24 hours resulted in concentration-dependent caspase 3 cleavage (CASP3) whereas D₁ stimulation with the D₁ agonist, SKF-38393, did not. The findings suggest that dopamine-induced caspase 3 cleavage occurs through a process that is independent of the D₁ receptor. The data was normalized to protein content and is expressed as mean ± S.E.M. of 6 independent experiments. **p*<0.05, ***p*<0.001 vs. control; # *p*<0.05 between concentrations of same treatment.

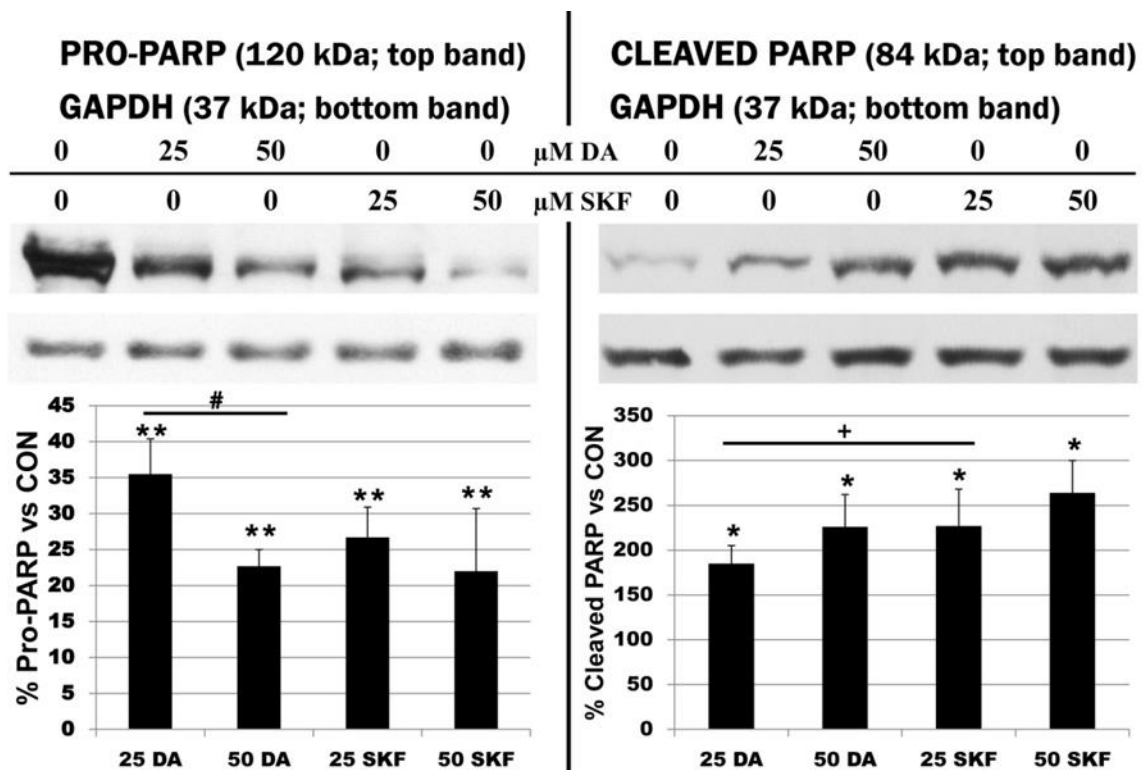


Figure 16: Qualitative and Quantitative Protein Expression of Full-Length and Cleaved Poly(ADP-ribose) Polymerase Following Dopamine or SKF-38393 Treatment

Treatment with 25-50 μM dopamine or the D_1 agonist, SKF-38393, for 24 hours resulted in a significant decrease in full-length PARP with a concurrent increase in PARP fragmentation. Dopamine treatment decreased the presence of full-length PARP in a concentration dependent manner, suggesting more toxicity at higher dopamine concentrations. Treatment with 25 μM SKF-38393 yielded more PARP cleavage than the same concentration of dopamine, while there was no difference between the 50 μM treated SKF-38393 or dopamine treated groups. The data was normalized to protein content and is expressed as mean \pm S.E.M. of 5 independent experiments. * $p < 0.05$, ** $p < 0.001$ vs. control; # $p < 0.05$ between concentrations of same treatment; + $p < 0.05$ between treatments of the same concentration.

D_1 receptor antagonist SCH-23390 has no significant effect on CASP3 cleavage, but attenuates DA-induced PARP fragmentation

Dopamine is known to rapidly autoxidize and, thus, it accordingly acts as a strong oxidizing agent that causes neuronal cytotoxicity (Chan et al., 2007; Krasnova & Cadet, 2009). In order to study the oxidative effects of DA on SK-N-MC cells and determine if the differences noted between 25 and 50 μM DA could be attributed to non- D_1 receptor mediated apoptotic

mechanisms, we pre-treated the cells with 10 μ M SCH-23390, a specific D₁ antagonist, then assayed CASP3 and PARP cleavage patterns following a 24 h treatment with 0-50 μ M DA. The data in Figure 18 illustrate that pre-treatment of the 25 μ M DA group with 10 μ M SCH-23390 attenuated the significant increase in CASP3 cleavage that was seen with DA treatment when compared to control. The effect of D₁ receptor blockade at 50 μ M DA revealed a different pattern of CASP3 cleavage where addition of SCH-23390 resulted in a significant increase in fragmentation when compared to control ($p < 0.001$) but not significantly different than DA alone. The results from Figure 18 suggest CASP3 cleavage occurred, at least in part, through a non-D₁-mediated mechanism.

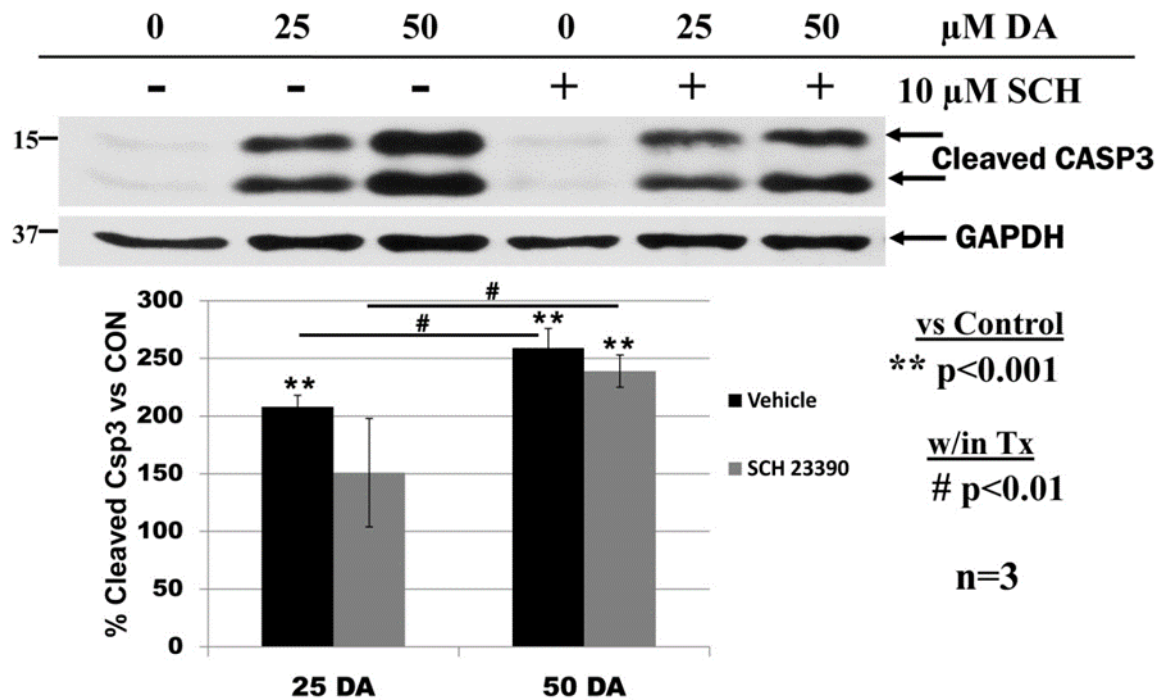


Figure 17: Qualitative and Quantitative Protein Expression of Cleaved Caspase 3 following Dopamine Treatment with and without Blockade of the D₁ receptor with SCH-23390

Pre-treatment with 10 μM SCH-23390, a D₁ antagonist, prior to 24 h treatment with 25-50 μM DA did not significantly attenuate CASP3 cleavage compared to DA vehicle (sterile water) treatment alone. The data was normalized to protein content and is expressed as mean ± S.E.M. of 3 independent experiments. **p<0.001 vs. control; # p<0.05 between concentrations of same treatment.

As shown in Figure 19, the PARP cleavage pattern of 25 μM DA samples were like those of CASP3 (Figure 18). Pre-treatment of 25 μM DA samples with SCH-23390 decreased PARP fragmentation by ~30% when compared to 25 μM DA but did not reach statistical significance. In contrast to cleaved CASP3, a significant decrease in PARP fragmentation was observed in the SCH 23390 pre-treated 50 μM DA group when compared to DA alone (~41% reduction; p<0.05) suggesting D₁ antagonism is protective against 50 μM DA-mediated PARP cleavage (Figure 19). Although SCH-23390 offered protection when compared to DA alone, D₁ antagonism did not prevent PARP fragmentation as there was a significant elevation in both DA groups when

compared to control ($p < 0.05$) suggesting that DA oxidation triggers the activation of pro-apoptotic pathways.

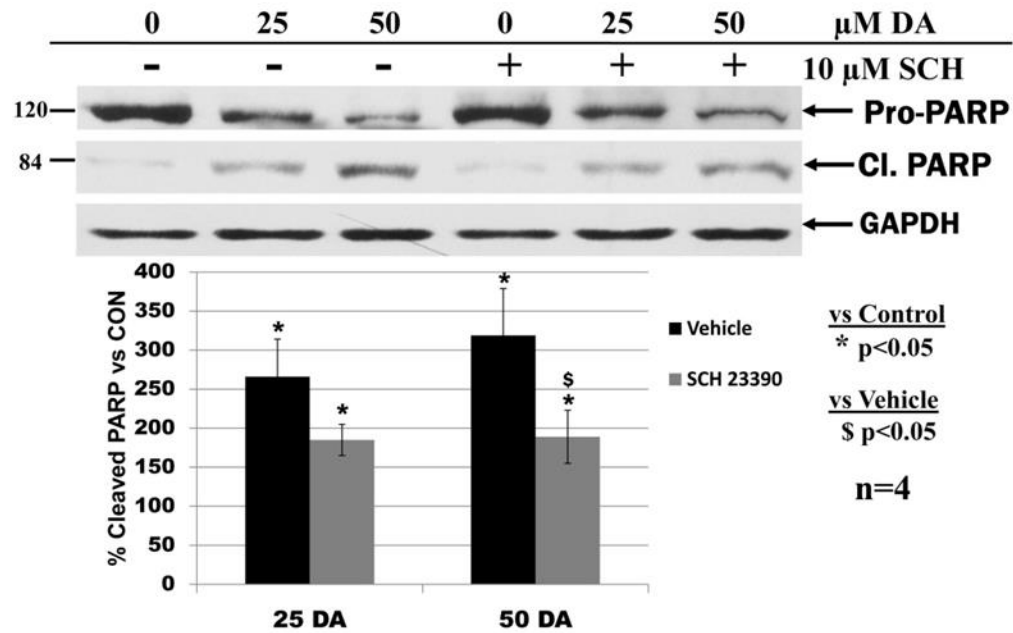


Figure 18: Pre-Treatment with D₁ Antagonist Attenuates Dopamine-Mediated PARP Cleavage

Pre-treatment with 10 μM SCH-23390, a D₁ antagonist, prior to 24 h treatment with 50 μM DA significantly attenuated PARP cleavage compared to DA vehicle treatment alone. SCH-23390 pre-treatment, however, did protect against significant PARP fragmentation when compared to control. The data was normalized to protein content and is expressed as mean ± S.E.M. of 4 independent experiments. * $p < 0.05$ vs. control; \$ $p < 0.05$ vs. vehicle (sterile water).

Dopamine or SKF-38393 treatment results in MAPK p38 phosphorylation

In order to ascertain if the intracellular signaling molecule mitogen activated protein kinase (MAPK) p38 was involved in either the DA-mediated, CASP3-dependent apoptotic pathway; or through the D₁-specific, CASP3-independent mechanism, we analyzed p38 phosphorylation after a 24 h treatment with 0-50 μM DA or SKF-38393. Figure 20 shows that all treatments significantly increased phosphorylation when compared to control indicating that p38 is activated in response to D₁ stimulation ($p < 0.001$ for 50 μM DA, $p < 0.01$ for 25-50 μM SKF, $p < 0.01$ for 25 μM SKF-38393). A concentration-dependent trend in phosphorylation was

observed in the DA and SKF-38393 groups. To ascertain if there was D₁-independent activation of MAPK; p38, the cells were pre-treated with 10 μM SCH-23390 followed by 25-50 μM DA. Receptor antagonism did not result in a significant change in p38 phosphorylation compared to DA alone (data not shown) suggesting MAPK p38 is also activated through a D₁-independent pathway.

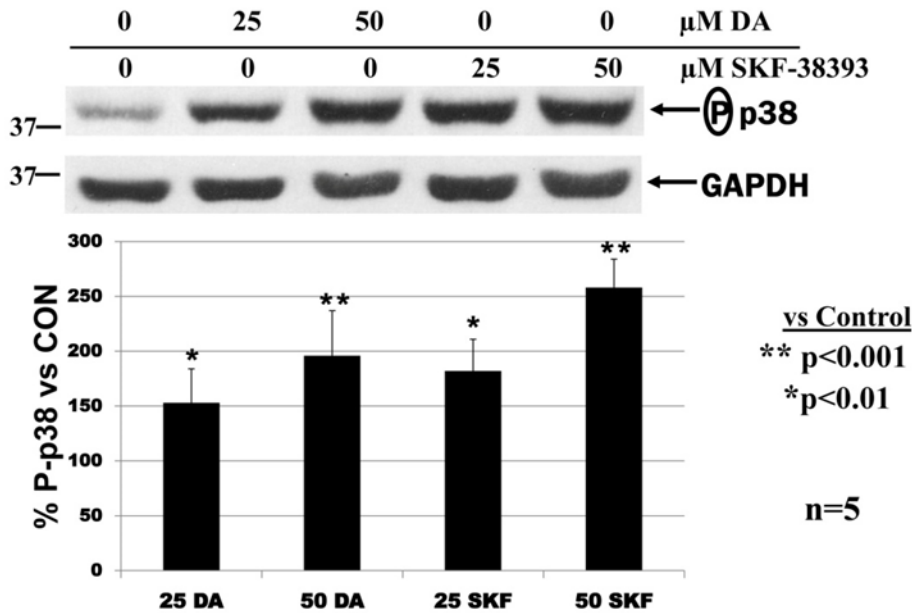


Figure 19: Both Dopamine and D₁ Agonist Increase p38 Phosphorylation

MAPK p38 phosphorylation (P-p38) was significantly increased 24 h after treatment with 25-50 μM DA or the D₁ agonist, SKF-38393 as measured by Western Blot analysis. The data was normalized to protein content and is expressed as mean ± S.E.M. of 4 independent experiments. * p<0.01, ** p<0.001 vs. control.

Inhibition of MAPK p38 with SB203580 attenuates toxicity in 25 μM DA treated cells, but enhances toxicity with 50 μM DA or SKF-38393 treatment

To decipher whether the observed p38 activation was protective or deleterious, we pre-treated cells with 2 μM of the cell-permeable p38 inhibitor, SB203580, then analyzed CASP3 and PARP cleavage. Preliminary studies were conducted using a range of SB203580 concentrations (0, 1, 1.5, 2, and 5 μM) prior to treatment with 50 μM DA then assessing MAPK

p38 phosphorylation via western analysis (data not shown). Pre-treatment with 2 μ M SB203580 was chosen for all subsequent experiments as that concentration provided \sim 63% (\pm 4%, n=3) reduction in phosphorylation following 50 μ M DA administration, and thus returned MAPK p38 phosphorylation status to that of control. Furthermore, p38 inhibition was verified via western analysis following each experiment that involved SB203580. Figure 21 shows that SB203580 pre-treatment resulted in a significant increase in CASP3 cleavage when compared to control for 50 μ M DA ($p < 0.05$), 25 μ M SKF-38393 ($p < 0.005$) or 50 μ M SKF-38393 ($p < 0.001$), but not 25 μ M DA. The inhibition of p38 phosphorylation significantly exacerbated CASP3 cleavage for both SKF-38393 treated samples when compared to samples in which p38 underwent phosphorylation ($p < 0.001$). In contrast, inhibition of p38 phosphorylation afforded significant protection against CASP3 cleavage in the 25 μ M DA group ($p < 0.05$). The inhibition of p38 phosphorylation also resulted in a concentration-dependent cleavage of CASP3 within the SKF-38393 treated groups, which was not present without the inhibitor ($p < 0.05$). Although concentration-dependence was seen within the DA treated samples without p38 inhibition, the dependence was enhanced following administration of SB203580 ($p < 0.001$). Unlike the results in Figure 18 where DA resulted in greater CASP3 cleavage than treatment with the D₁ agonist at the same concentration, the addition of SB203580 reversed this finding. Following p38 inhibition, treatment with the D₁ agonist resulted in greater cleavage than DA alone at the same concentration. A greater effect of inhibition of p38 phosphorylation was observed among with 25 μ M relative to 50 μ M DA although both were significant (2.8 vs 1.4-fold; $p < 0.001$ and $p < 0.005$). Results from Figure 21 suggest that inhibition of p38 phosphorylation augments CASP3 cleavage in a manner associated with increased D₁ receptor activation, as demonstrated by elevated cleavage following D₁ stimulation with SKF-38393 and 50 μ M DA. Conversely,

p38 inhibition stabilized CASP3 after 25 μ M DA concentration and thus presumably less D₁ activation occurred.

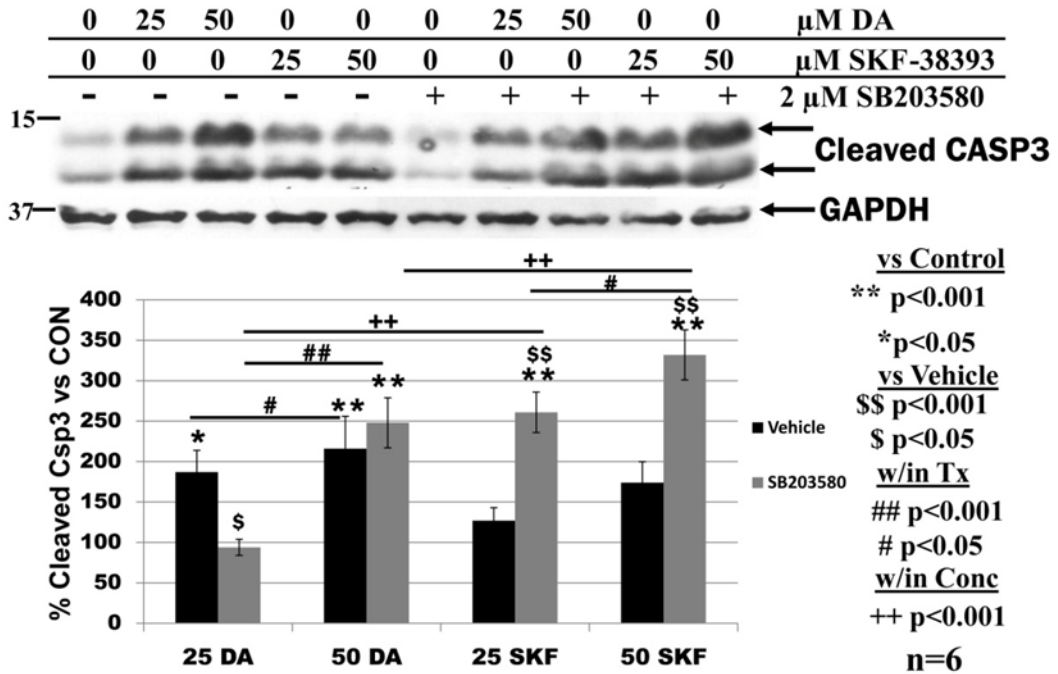


Figure 20: Qualitative and Quantitative Protein Expression of Caspase 3 Cleavage following Inhibition of p38 Phosphorylation in Samples Treated with D₁ Agonist or Dopamine

Inhibition of p38 phosphorylation with SB203580 significantly enhanced CASP3 cleavage in samples treated with the D₁ agonist, SKF-38393, when compared to SKF-38393 treatment alone. Conversely, p38 inhibition prior to 25 μ M DA treatment attenuated CASP3 cleavage compared to DA alone and returned the levels to that seen in control. The data was normalized to protein content and is expressed as mean \pm S.E.M. of 6 independent experiments. *p<0.05, **p<0.001 vs. control; \$ p<0.05, \$\$ p<0.001 vs. vehicle; # p<0.05, ## p<0.001 between concentrations of same treatment; ++ p<0.001 between treatments of same concentration.

Figure 22 shows inhibition of MAPK p38 phosphorylation resulted in a significant decrease in native PARP when compared to control for all groups indicating cellular toxicity was present (p<0.001). In the 25 μ M DA treated samples, however, inhibition of p38 phosphorylation resulted in a significant stabilization of native PARP when compared to 25 μ M DA without p38 inhibition (p<0.001). An opposite trend was observed in the 50 μ M DA and 25-

50 μ M SKF-38393 treated cellular samples whereupon p38 inhibition led to decreased levels of native PARP protein. The effect was significant in the 50 μ M SKF-38393 treatment group with a 70% reduction in full-length PARP following p38 inhibition compared to 50 μ M SKF-38393 alone ($p < 0.05$). As seen with Figure 21, the addition of SB203580 resulted in more toxicity as evidenced by less native PARP protein in samples treated with the D₁ agonist compared to DA of the same concentration. The effect was significant in the 25 μ M samples with an 80% more reduction in native PARP levels following SKF treatment compared to DA treated cells ($p < 0.01$). When the phosphorylation of p38 was inhibited, DA treated cells had a significant concentration-dependent loss of native PARP. The 50 μ M DA treatment resulted in 58% less native PARP than 25 μ M ($p < 0.001$). Investigating the DA- or SKF-38393-induced cleavage pattern of PARP following SB 203580 pre-treatment revealed complementary findings to those of native PARP where inhibition of p38 hampered PARP cleavage in 25 μ M DA while augmenting it in SKF-38393 and 50 μ M DA treated samples (data not shown).

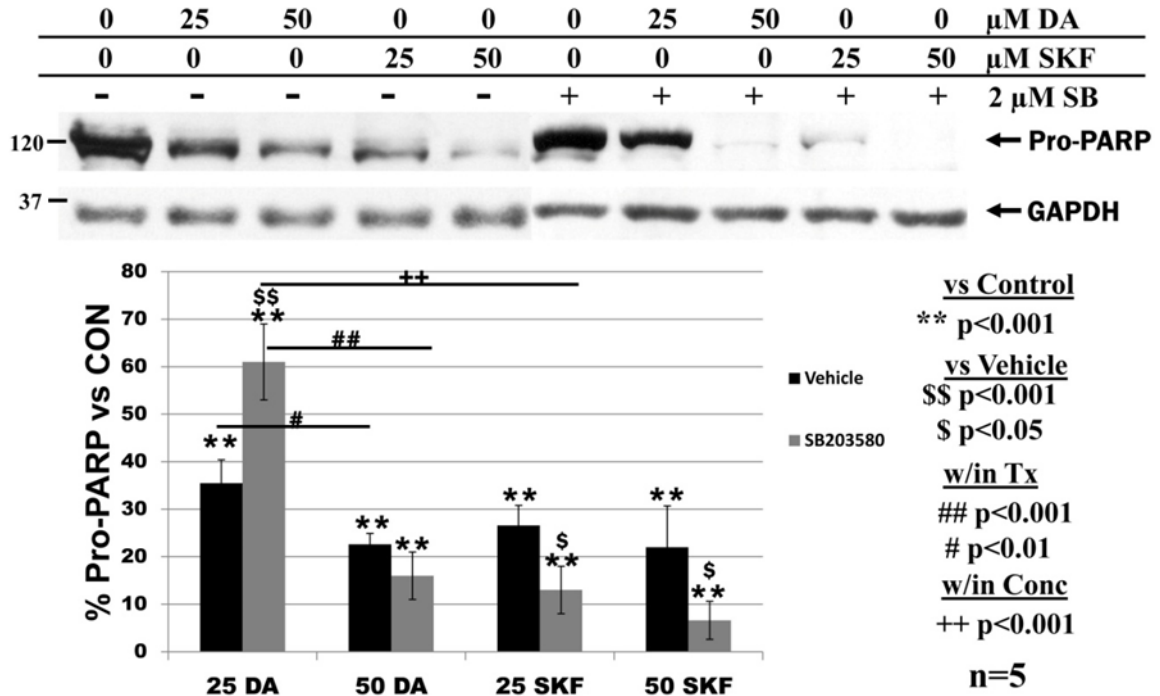


Figure 21: Qualitative and Quantitative Protein Expression of Full-Length PARP following Inhibition of p38 Phosphorylation in Samples Treated with D1 Agonist or Dopamine

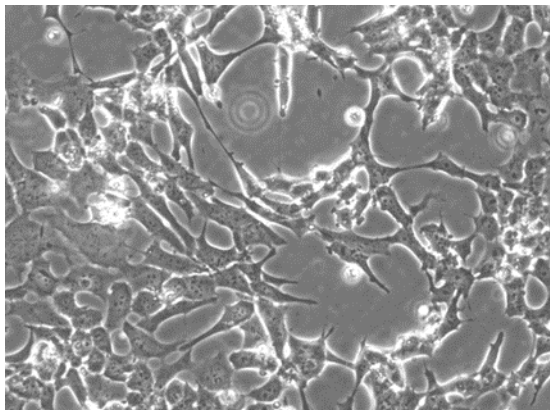
Inhibition of p38 phosphorylation with SB203580 led to significant decreases in full-length (Pro) PARP upon 24 h treatment with the D1 agonist, SKF-38393, suggesting a protective function of p38 in its phosphorylated form when stimulated by the D1 agonist. Significant stabilization of PARP was noted upon p38 inhibition in samples treated with 25 μM DA, suggesting a deleterious effect from p38 activation. The data was normalized to protein content and is expressed as mean ± S.E.M. of 5 independent experiments. **p<0.001 vs. control; \$ p<0.05, \$\$ p<0.001 vs. vehicle; # p<0.01, ## p<0.001 between concentrations of same treatment; ++ p<0.001 between treatments of same concentration.

The findings from Figures 21 and 22 suggest a critical role for p38 acting as a molecular buffer against the toxicity triggered by increased DA concentration and isolated receptor stimulation with SKF. At 25 μM DA, MAPK p38 seems to have a different role as a pro-apoptotic modulator.

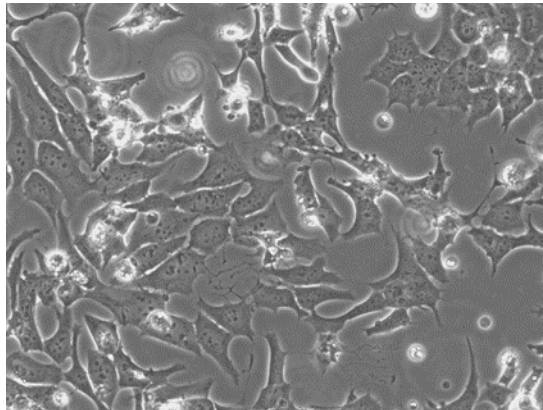
To confirm cytotoxicity and substantiate the findings in Figures 21 and 22, we administered the same treatment regime as above, then microscopically examined SK-N-MC cells to assess morphological changes consistent with toxicity as previously described (Herdman

et al., 2006; Figures 23F-J). Figure 23 shows control (A), 25 (B), and 50 (C) μM DA, as well as 25 (D) and 50 (E) μM SKF-38393 treated SK-N-MC cells. All treatments (Figure 23 B-E) displayed morphologies consistent with toxicity such as membrane alterations, cell shrinkage, and cell detachment when compared to control treated cells. The morphological changes following pre-treatment with SB 203580 are consistent with the data in Figures 21 and 22 in that p38 inhibition of 25 μM DA treated cells (Figure 23G) showed protection against cytotoxicity when compared to 25 μM DA alone (Figure 23B). Conversely, p38 inhibition prior to 50 μM DA (Figure 23H) and 25-50 μM SKF-38393 (Figures 23I-J) treatment displayed morphological characteristics consistent with exacerbated toxicity compared to 50 μM DA or SKF-38393 alone.

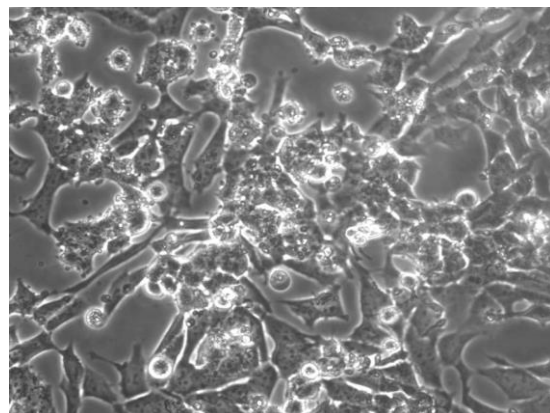
(A) Vehicle Control



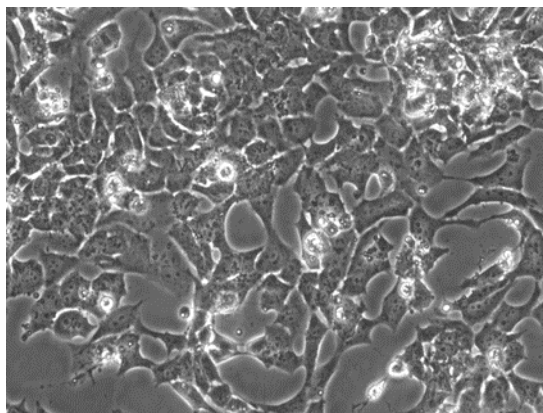
(F) 0 DA, + SB203580



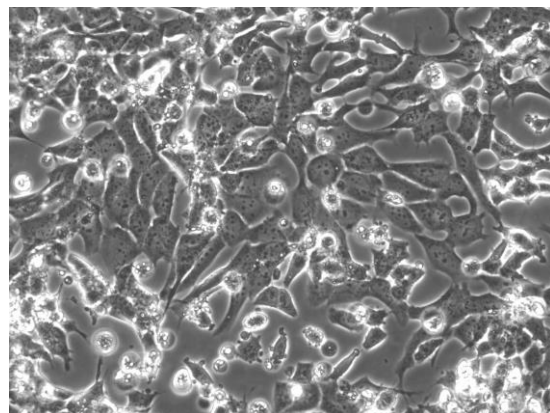
(B) 25 μ M DA



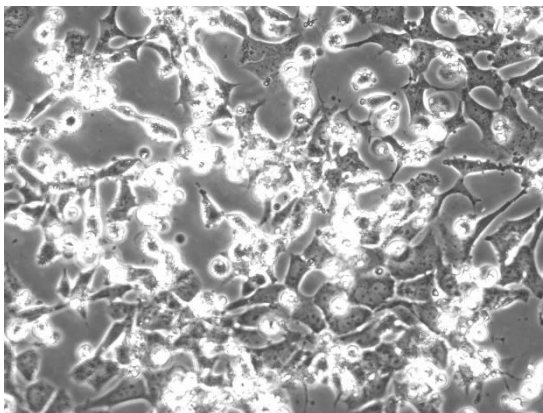
(G) 25 μ M DA, + SB203580



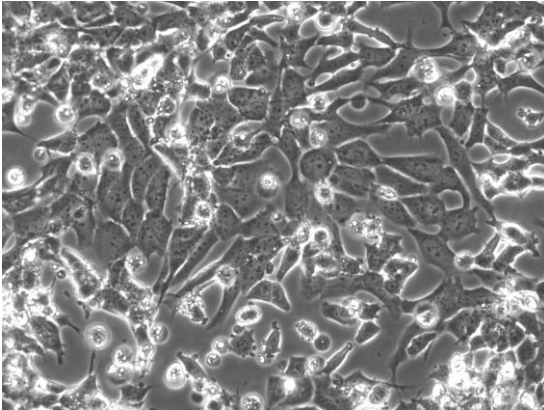
(C) 50 μ M DA



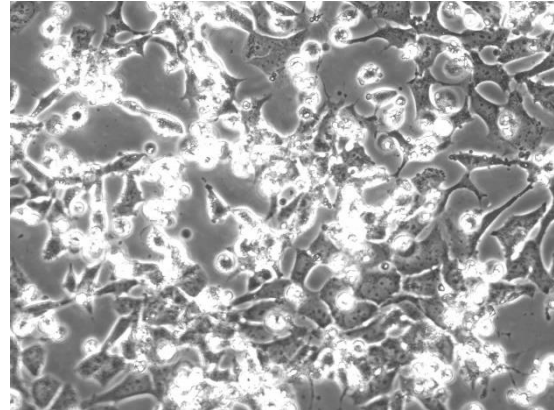
(H) 50 μ M DA, + SB204580



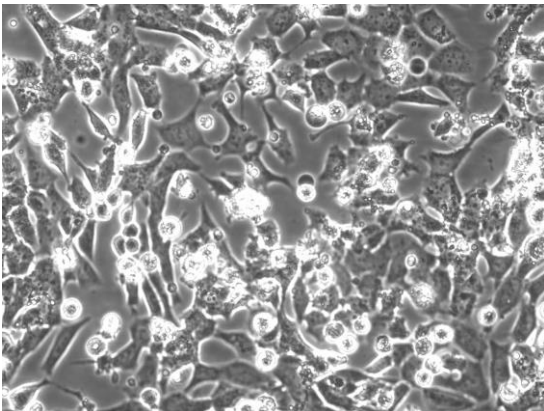
(D) 25 μ M SKF-38393



(I) 25 μ M SKF-38393, + SB203580



(E) 50 μ M SKF-38393



(J) 50 μ M SKF-38393, + SB203580

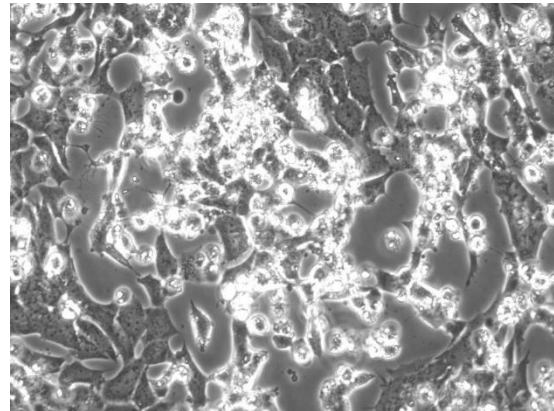


Figure 22 A-J: Parallel Examination of SK-N-MC to Assess Morphological Changes Consistent with Toxicity Following Dopamine or D₁ Agonist Treatment with and without Inhibition of p38 Phosphorylation

SK-N-MC cells were pretreated for 30 min with vehicle **A-E** or 2 μ M SB203580, a p38 inhibitor, **F-J**. The cells were then treated for 24 h with the following: **A** and **F**) control; **B** and **G**) 25 μ M DA; **C** and **H**) 50 μ M DA; **D** and **I**) 25 μ M SKF-38393; **E** and **J**) 50 μ M SKF-38393. Morphological analysis of the cells shows that pre-treatment with SB203580 is protective in 25 μ M DA treated samples (**B**, **G**); while it exacerbates toxicity in 25 (**D**, **I**) and 50 (**E**, **J**) μ M SKF treated samples. Interestingly, inhibition of p38 phosphorylation with SB203580 yielded little morphological change in cells treated with 50 μ M DA (**C**, **H**).

Antagonism of D₁ coupled with MAPK p38 inhibition completely abolishes DA-induced toxicity

Given that SCH-23390 and SB203580 each affected CASP3 stabilization when administered prior to 25 μ M DA, we co-incubated the cells with both the D₁ antagonist and the p38 inhibitor. This treatment regime was done to gauge if the CASP3 protection afforded by SCH-23390 or SB203580 was working through a similar or different mechanistic pathway. Co-incubation completely abrogated CASP3 cleavage in 25 μ M DA treated samples returning the levels of cleavage to that of control (Figure 24). The 25 μ M DA samples co-treated with SCH-23390 and SB 203580 were also significantly protected against cleavage when compared to SCH-23390 or SB203580 treatment alone ($p < 0.05$, $p < 0.01$).

Unlike the 25 μ M DA treated group, pre-treatment of 50 μ M DA samples with SCH-23390 resulted in a different CASP3 cleavage pattern than SB203580. D₁ antagonism provided slight protection against cleavage following 50 μ M DA treatment, while p38 inhibition significantly intensified fragmentation ($p < 0.01$). Co-incubation of 50 μ M DA treated cells with SCH-23390 and SB203580, however, prevented CASP3 cleavage that was seen following DA alone, returning the level of cleavage to that of control ($p < 0.001$; Figure 24). Examining the differences between co-incubation of 50 μ M DA samples and individual pre-treatment revealed significant decreases in cleavage when compared to either SCH-23390 or SB 203580 alone ($p < 0.001$).

As was seen with CASP3 cleavage, co-incubation with SCH-23390 and SB203580 effectively nullified PARP fragmentation in the 25 and 50 μ M DA samples when compared to DA treatment alone and returned levels to that of control (Figure 25; $p < 0.01$, $p < 0.001$). Correspondingly, samples co-treated with SCH-23390 and SB203580 significantly attenuated

PARP fragmentation when compared to either pre-treatment with SCH-23390 ($p < 0.05$) or SB 203580 alone ($p < 0.05$ for 25 μM DA, $p < 0.001$ for 50 μM DA). The results in Figure 25 indicate that D₁ antagonism attenuates, but does not prevent, PARP-mediated apoptosis thus indicating that D₁ stimulation and DA autoxidation are both mechanisms of toxicity in this cell line. When coupled with D₁ blockade, p38 inhibition abolishes PARP fragmentation revealing a deleterious role for MAPK p38 activation when activated through a D₁ independent mechanism.

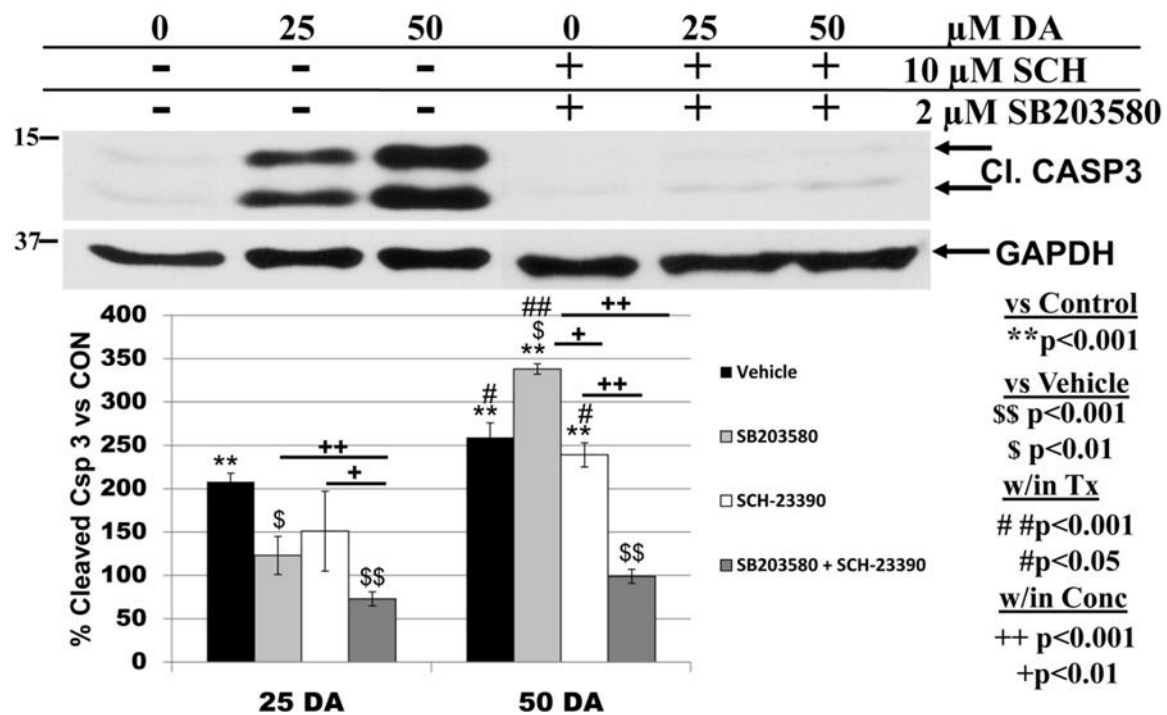


Figure 23: Co-Incubation with p38 Inhibitor and D₁ Antagonist Prior to Dopamine Demonstrates Decreased Caspase 3 Cleavage Compared to Dopamine Alone

Co-incubation (dark-gray bars) with a p38 inhibitor, SB203580 (light-gray bars), and D₁ antagonist, SCH-23390 (white bars) 30 min prior to 25-50 μM DA administration prevented CASP3 cleavage that was seen in DA alone (black bars). Likewise, co-incubation with SB203580 and SCH-23390 resulted in significantly less CASP3 cleavage than pre-treatment with SB203580 or SCH-23390 alone. The data was normalized to protein content and is expressed as mean \pm S.E.M. of 3 independent experiments. * $p < 0.05$, ** $p < 0.001$ vs. control; \$ $p < 0.01$, \$\$ $p < 0.001$ vs. vehicle; # $p < 0.05$, ## $p < 0.001$ between concentrations of same treatment; + $p < 0.05$; ++ $p < 0.001$ between treatments of same concentration.

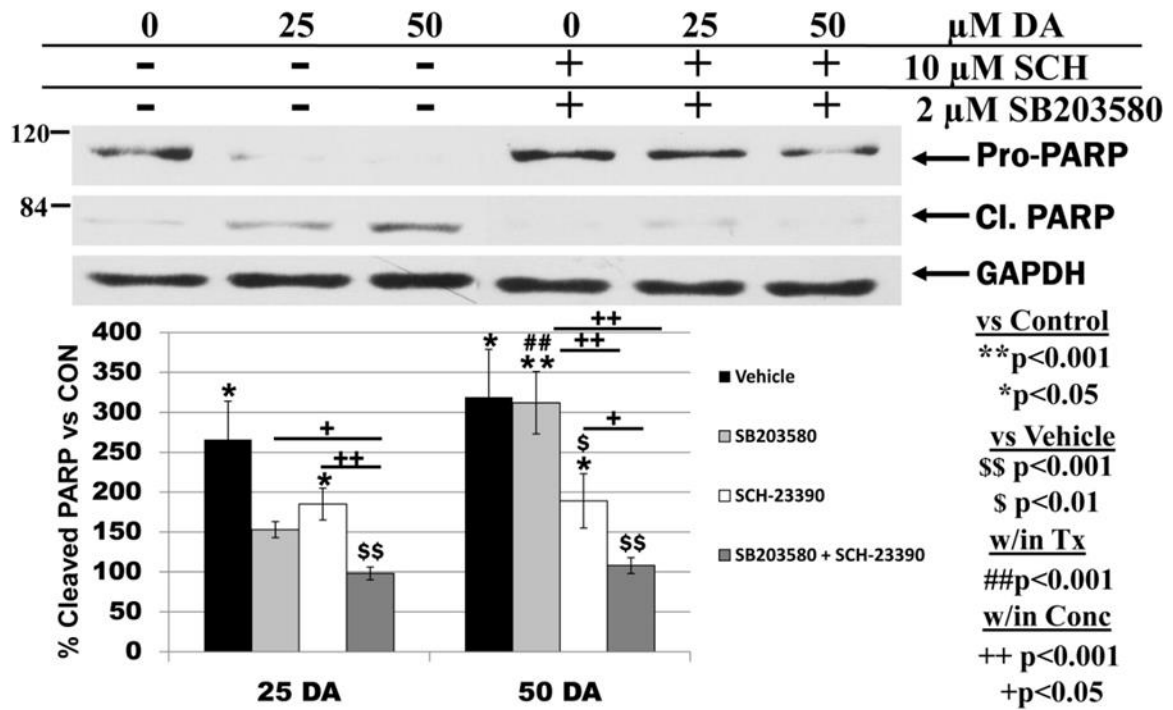


Figure 24: Co-Incubation with p38 Inhibitor and D₁ Antagonist Prior to Dopamine Demonstrates Decreased Caspase 3 Cleavage Compared to Dopamine Alone

Co-incubation (dark-gray bars) with a p38 inhibitor, SB203580 (light-gray bars), and D₁ antagonist, SCH-23390 (white bars) 30 min prior to 25-50 $\mu\text{M DA}$ administration prevented PARP fragmentation that was seen in DA alone (black bars). Likewise, co-incubation with SB203580 and SCH-23390 resulted in significantly less PARP fragmentation than pre-treatment with SB203580 or SCH-23390 alone. The data was normalized to protein content and is expressed as mean \pm S.E.M. of 3 independent experiments. *p<0.05, **p<0.001 vs. control; \$ p<0.01, \$\$ p<0.001 vs. vehicle; # p<0.05, ## p<0.001 between concentrations of same treatment; + p<0.05; ++ p<0.001 between treatments of same concentration.

D₁ receptor stimulation enhances HSP27 expression in a manner attenuated by MAPK p38 inactivation

To further study the mechanism of the D₁-mediated, MAPK p38-dependent anti-apoptotic pathway, as well as the D₁-independent, p38-dependent pro-apoptotic pathway, we investigated heat shock protein 27 (HSP27). This protein is a downstream target of p38 and has neuroprotective properties such as CASP3 stabilization when upregulated or phosphorylated (Bruey et al., 2000; Pandey et al., 2000). Treatment with 50 $\mu\text{M DA}$ or 25-50 $\mu\text{M SKF-38393}$

led to a significant increase in HSP27 protein compared to control (Figure 26; $p < 0.01$, $p < 0.05$, $p < 0.05$, respectively). A significant concentration-dependent elevation in HSP27 occurred between 25 and 50 μM DA ($p < 0.005$) that was nullified by pre-treatment with SB203580. Moreover, inhibition of p38 resulted in significantly reduced HSP27 protein in all samples with the largest decrease reported in the 50 μM SKF-38393 group (~80% ; $p < 0.05$ for 25 μM DA, $p < 0.001$ for 50 μM DA, $p < 0.01$ for 25 μM SKF-38393, $p < 0.001$ for 50 μM SKF-38393). The data suggests that HSP27 protein expression is positively associated with D₁ receptor stimulation and is dependent on p38 activation.

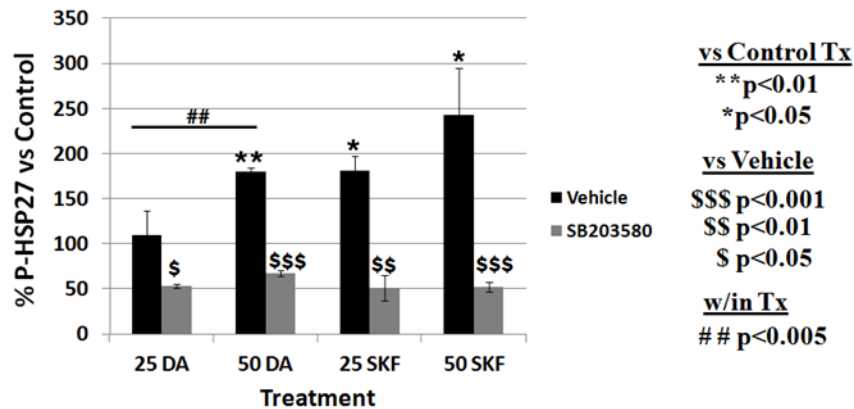


Figure 25: Enhanced Phosphorylation of Heat Shock Protein 70 Following Dopamine or D₁ Agonist Appears Dependent Upon p38 Activation

Phosphorylation of HSP27 was significantly elevated following 24 h treatment with 50 μM DA or 25-50 μM SKF-38393, a D₁ agonist. Inhibition of p38 with SB203580 significantly decreased HSP27 phosphorylation in all treatments. The results suggest HSP27 phosphorylation is p38-dependent. The data was normalized to protein content and is expressed as mean \pm S.E.M. of 3 independent experiments. * $p < 0.05$, ** $p < 0.01$ vs. control; \$ $p < 0.05$, \$\$ $p < 0.01$, \$\$\$ $p < 0.001$ vs. vehicle; ## $p < 0.005$ between concentrations of same treatment.

Dopamine induces AP-1 transcriptional activity through a MAPK p38-dependent, D₁-independent mechanism

To further study the dual role of dopamine-induced MAPK p38 activation, we investigated a known downstream target of p38-mediated signaling, Activator Protein-1 (AP-1).

This regulatory protein is a redox-sensitive transcription factor whose activation is known to have pro-apoptotic as well as proliferative properties (Sun and Oberley, 1996; Shaulian & Karin, 2002). Figure 27 shows that transient transfection with an AP-1 construct resulted in a significant increase in luciferase reporter activity following 6 h of 50 μ M DA treatment of the transfected cells when compared to control ($p < 0.001$) or 50 μ M DA-treated cells transfected with the empty pGL2 vector ($p < 0.05$). Pre-treatment of the transfected cells with 1.5 μ M SB203580 followed by 50 μ M DA significantly decreased reporter activity when compared to DA alone ($p < 0.05$), and did not significantly increase reporter activity when compared to control or DA treatment of cells containing the empty vector (Figure 27). This data indicates that AP-1 transcription is upregulated following DA treatment in the SK-N-MC cell line in a manner dependent upon activation of p38.

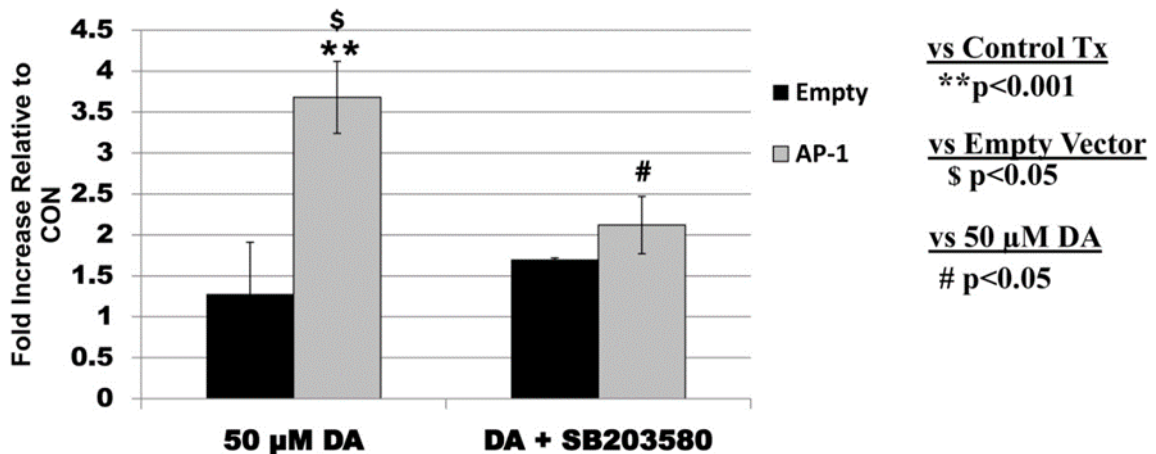


Figure 26: Dopamine-Induced AP-1 Activity Appears to be Mediated Through p38

AP-1 reporter activity (gray bars) was significantly increased 6 h after treatment with 50 μ M DA. Pre-treatment with 1.5 μ M SB203580 significantly decreased AP-1 luciferase activity. The results suggest DA-induced AP-1 activity is mediated through p38. The data is expressed as mean \pm S.E.M. of 3 independent experiments. ** $p < 0.001$ vs. control; \$ $p < 0.05$ vs. empty vector; # $p < 0.05$ vs. 50 μ M DA.

To decipher whether receptor stimulation or autoxidation was responsible for AP-1 activation, we treated AP-1 or PGL2 (empty vector) transfected cells with 0-100 μM of DA or SKF-38393, or pre-treated cells with 10 μM SCH-23390 followed by 50 μM DA. The cells were also treated with a phorbol ester (TPA, 100 nM) to serve as a positive control for AP-1 activation. Figure 28A illustrates that 25-100 μM DA-, but not in 25-100 μM SKF-38393-, induced significant increases in AP-1 reporter activity when compared to control or the empty vector ($p < 0.001$; $p < 0.001$). Furthermore, there was a significant increase in reporter activity among DA treated samples when compared to cells receiving the same concentration of SKF-38393 ($p < 0.005$) suggesting that AP-1 activity is not regulated through D_1 . Pre-treatment with the D_1 antagonist, SCH-23390, followed by 50 μM DA (Figure 28B) revealed a significant increase in AP-1 activity when compared to control or DA-treated empty vector ($p < 0.05$). SCH-23390 pretreatment did not hinder reporter activity when compared to 50 μM DA alone indicating that AP-1 activation is sensitive to DA stimulation through a non- D_1 -mediated mechanism. The results from Figures 28A and 28B suggest that AP-1 activation occurs in a D_1 -independent, perhaps redox-sensitive manner in SK-N-MC.

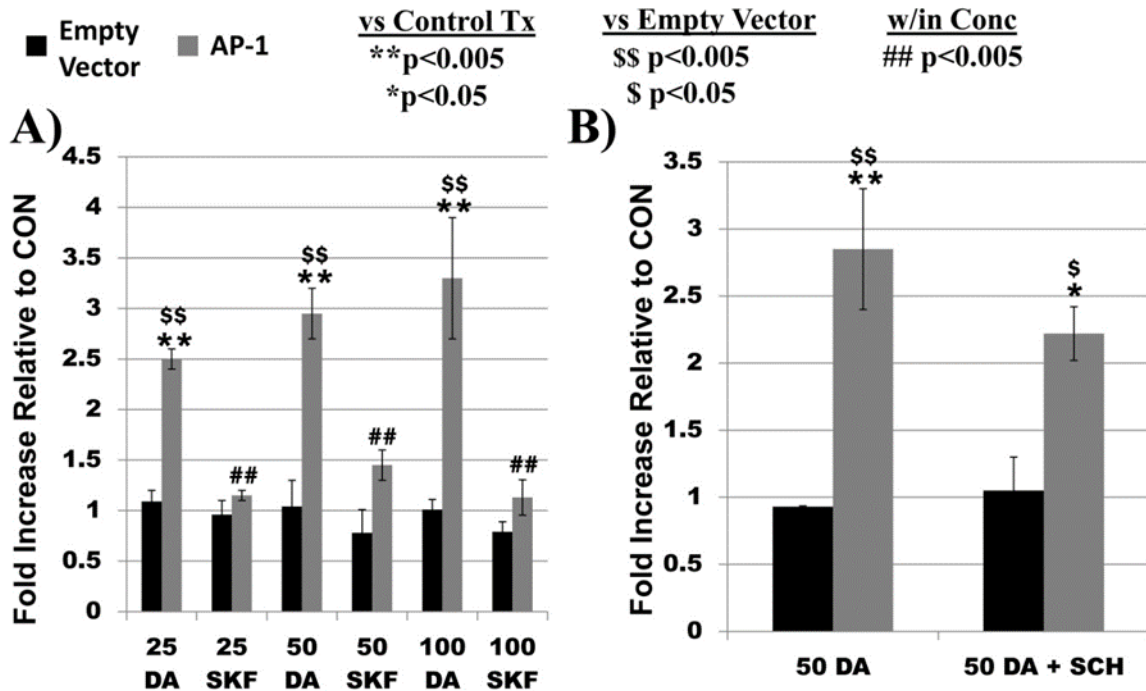


Figure 27 A, B: AP-1 Reporter Activity is Enhanced by D₁ Antagonism but Not D₁ Agonist (A) AP-1 reporter activity (gray bars) was significantly increased 6 h after treatment with 25-100 μ M DA compared to control or DA-treated empty vector, whereas treatment with 25-100 μ M SKF-38393, a D₁ agonist, did not enhance reporter activity in AP-1 transfected cells. (B) Pre-treatment with 10 μ M SCH-23390, a D₁ antagonist, did not significantly attenuate DA-induced AP-1 luciferase activity when compared to DA alone. The results suggest DA-induced AP-1 activity is mediated through a D₁-independent mechanism. The data is expressed as mean \pm S.E.M. of 4 independent experiments. *p<0.05, **p<0.005 vs. control; \$ p<0.05, \$\$ p<0.005 vs. empty vector; ## p<0.005 between treatments of the same concentration.

Dopamine-stimulated AP-1 transcription occurs through a cFos-containing complex and is a mediator of DA-induced apoptosis

The AP-1 complex exists as a homo- or hetero-dimer of proteins from the subfamilies of: Jun, Fos, Jun dimerization partners, activating transcription factors, and Maf. The most transcriptionally active and stable dimer is a cJun:cFos heterodimer, and cFos is a known substrate for MAPK p38 phosphorylation (Halazonetis et al., 1988; Shaulian & Karin, 2002). In order to determine if cFos was a constituent of the DA-sensitive AP-1 complex in SK-N-MC, we transiently co-transfected cells with an empty pGL2 or AP-1 vector and 0.75 μ g of an empty

CMV-500 vector or a vector containing a dominant negative to cFos, designated as A-Fos. We then treated with 0-50 μ M DA or 100 nM TPA and measured AP-1 reporter activity (Figure 29A). Treatment with 50 μ M DA in the AP-1, CMV-500 co-transfected cells potentiated reporter activity over 3-fold when compared to control or empty vector ($p < 0.001$). Dopamine-treated cells co-transfected with AP-1 and A-Fos had significantly reduced reporter activity (~45% reduction) when compared to AP-1 and CMV-500 co-transfected cells ($p < 0.001$) and did not yield a significant increase when compared to control or empty vector (Figure 29A). Treatment with TPA in the AP-1, A-Fos co-transfected cells significantly reduced reporter activity by ~66% when compared to AP-1 transfected cells ($p < 0.05$) and thereby confirmed effectiveness of the A-Fos dominant negative vector. The data in Figure 29A indicate that DA-induced AP-1 transcriptional activity occurs in part through activation of cFos.

Activator protein-1 stimulation is involved in the induction of both pro- and anti-apoptotic mechanisms in the nervous system (Krasnova & Cadet, 2009; Shaulian & Karin, 2002). To determine if DA-induced, c-Fos mediated AP-1 activation was protective or deleterious in our model, we transiently transfected the dominant negative A-Fos or empty vector into SK-N-MC cells then treated with 0-50 μ M DA. After 24 h DA treatment, we assessed PARP fragmentation via immunoblot analysis. A parallel co-transfection with AP-1, A-Fos or empty vectors was conducted to measure luciferase activity following 6 h DA treatment to ensure that AP-1 transcription was successfully attenuated by A-Fos at the DNA level. Figure 29B shows that transfection with A-Fos substantially diminished PARP cleavage when compared to control or empty vector. Our observation that A-Fos attenuated DA-induced PARP fragmentation is the first to report that c-Fos-dependent AP-1 activation is a mediator of apoptosis following DA treatment in the SK-N-MC cell line.

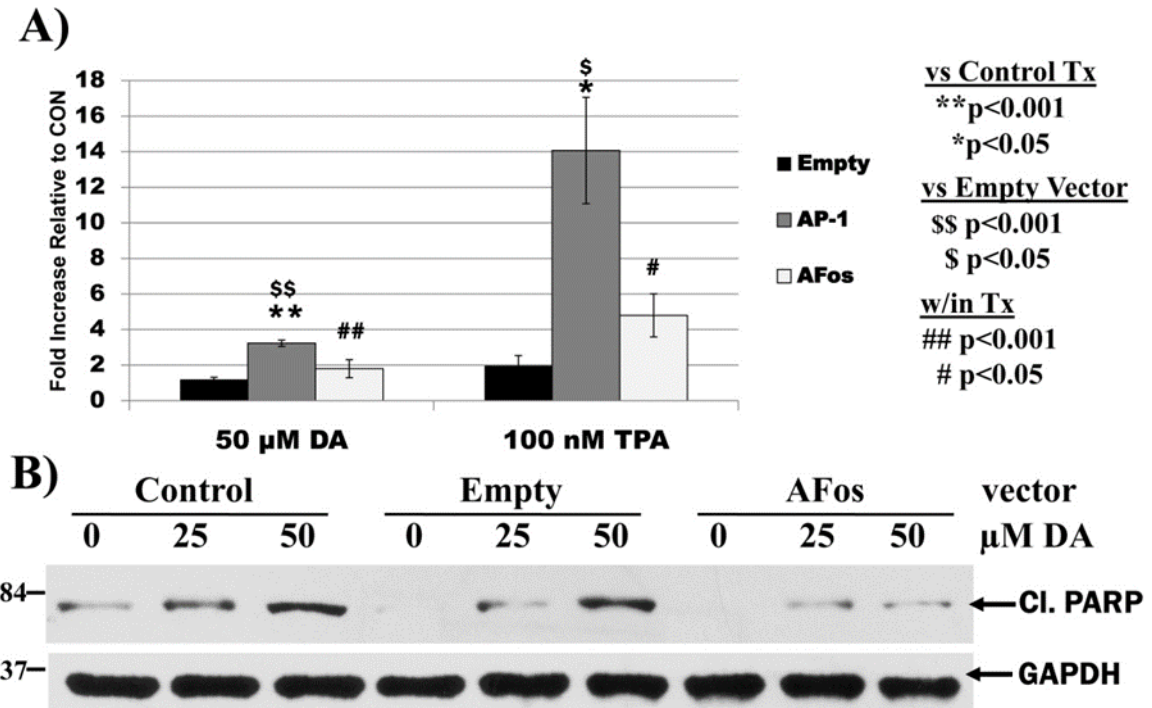


Figure 28 A, B: Co-Transfection with a Dominant Negative to cFos, A-Fos, Precludes Dopamine-Induced PARP Cleavage

(A) Dopamine-induced AP-1 reporter activity (gray bars) was significantly decreased when co-transfected with a dominant negative to cFos, A-Fos (white bars). Co-transfection with A-Fos significantly attenuated TPA-induced AP-1 activity 6 h after treatment thereby confirming efficacy of A-Fos. (B) Western analysis of A-Fos transfected cells showed attenuation of PARP fragmentation (Cl. PARP) following treatment with 25-50 μM DA for 24 h. The findings suggest that AP-1 is a mediator in dopamine-induced apoptosis through a mechanism involving PARP fragmentation. The data is expressed as mean ± S.E.M. of 3 independent experiments. *p<0.05, **p<0.001 vs. control; \$ p<0.05, \$\$ p<0.001 vs. empty vector; # p<0.05, ## p<0.001 between AP-1/CMV-500 transfected cells of the same treatment.

Discussion

In the present study we identified two mechanisms through which DA treatment stimulated apoptosis in a model of D₁-expressing postsynaptic striatal neurons. Elegant research from a multitude of clinical and translational studies has identified stimulant-induced cell death in D₁ expressing postsynaptic neurons (Chang et al., 2007; Krasnova & Cadet, 2009). Studies have detailed mechanisms responsible for stimulant- and DA-induced toxicity, but a majority of these studies have been aimed at striatal presynaptic terminal degeneration (Jayanthi et al., 2004;

Krasnova & Cadet, 2009). Limited knowledge on the mechanisms responsible for postsynaptic cell death, however, may create a potential barrier to further research on stimulant-induced neurotoxicity.

In addition to DA receptor stimulation, the structural properties of DA render a fraction of the neurotransmitter susceptible to oxidation prior to receptor interaction (Giovanni et al., 1995; Stokes et al., 1999). By employing the specific D₁-agonist SKF-38393 or -antagonist SCH-23390, we studied the toxicity of D₁ stimulation versus non-receptor mediated DA effects in our model of postsynaptic striatal neurons. Figure 17 demonstrates alterations in PARP consistent with apoptosis following treatment with 25-50 μ M SKF-38393. The data from Figure 17 indicated D₁ stimulation was sufficient to induce apoptosis. Poly (ADP-ribose) polymerase cleavage tended to be greater in samples treated with D₁ agonist than those receiving equivalent concentrations of DA (Figure 17). The immediate implications of this finding are clear in that 1) D₁ stimulation is a mechanism of DA toxicity by apoptosis, and 2) caution should be taken when using D₁ agonists to thwart craving and relapse in addiction research. Our results are congruent with previous studies in SK-N-MC that reported 16 h treatment with 50 μ M SKF-38393 resulted in decreased cell survival as measured by the trypan blue exclusion test (Chen et al., 2003) or MTT assay (Moussa et al., 2006). Although these studies reported decreased cell survival following D₁ stimulation, they did not demonstrate the mechanism by which this occurred nor identified the process as apoptotic or necrotic. The novelty in our findings comes from further investigation of the mechanism by which D₁ stimulation causes apoptosis in SK-N-MC. The cleavage of effector caspase 3 prior to PARP fragmentation is a prominent event of apoptosis (Herceg and Wang, 1999; Lazebnik et al., 1994). Caspase 3 cleavage occurs following activation of the Fas ligand/Fas death receptor as well as mitochondrial- and endoplasmic-

mediated apoptosis from a variety of stimuli (Breckenridge et al., 2003) including MA (Jayanthi et al., 2004; 2005). We are the first to report that in our model, however, D₁-mediated PARP cleavage occurred through a process that circumvented CASP3 cleavage (Figure 16). Apoptosis-inducing factor (AIF) is a caspase-independent facilitator of apoptosis that is released in response to mitochondrial membrane damage (Susin et al., 1999; 2000), and its presence has been documented in neuronal (Cregan et al., 2002) as well as SK-N-MC apoptotic processes (Komjáti et al., 2004). We hypothesize that D₁ stimulation with 25-50 μ M SKF-38393 resulted in mitochondrial damage that facilitated the release of AIF and subsequent apoptosis. We previously presented indirect evidence of mitochondrial stress in SK-N-MC following DA treatment, such as caspase 9 cleavage (Figure 7) as well as nitration and inactivation of MnSOD (Figures 9 and 10). There are limited and conflicting results about the involvement of stimulant-induced AIF in neuronal apoptosis. One study reported translocation of AIF from the mitochondria to cytoplasmic fractions in mouse striata \leq 7 days following a single treatment with 40 mg/kg MA (Jayanthi et al., 2004). A later study using primary rat neurons isolated from the frontal cortex reported no change in AIF location or amount following 24 h incubation with 1-2 mM amphetamine or 1-3 mM cocaine (Cunha-Oliveira et al., 2006). The discrepancies between the two studies could be attributed to disparity in the brain region from where the samples were acquired, or due to the difference in stimulants used in the study. Our study design more closely mimics that used by Jayanthi et al. wherein the authors concluded AIF was a participant in MA-induced striatal apoptosis (Jayanthi et al., 2004). Future work should be aimed at identifying the possible role of AIF following D₁ stimulation in SK-N-MC.

Pre-treatment with 10 μ M of the D₁ specific antagonist, SCH-23390, significantly decreased PARP cleavage when compared to 50 μ M DA treatment alone but did not afford

complete protection from PARP fragmentation (Figure 19). The findings in Figure 19 indicate that although D₁ receptor blockade attenuated DA-induced apoptosis, a non-D₁ mediated process also facilitated cell death following 25-50 μM DA treatment. Accordingly, two previous studies reported preserved cell viability upon pre-treatment of SK-N-MC with 10 μM SCH-23390 when compared to 16 h treatment with 50 μM DA alone; however, there was still a significant decrease in viability in cells pre-treated with SCH-23390 when compared to control treated cells. These studies concluded that DA cytotoxicity occurred through a D₁-dependent route as well as an oxidative pathway that was independent of D₁ stimulation (Chen et al., 2003; Moussa et al., 2006). Examination of CASP3 cleavage (Figure 18) following SCH-23390 pretreatment was equivalent to that seen in 50 μM DA alone thereby suggesting the apoptotic protection afforded by D₁ receptor blockade occurred through a process independent of CASP3 stabilization. Relating these findings to those in Figures 16 and 17 again implicate AIF as a possible participant specific to D₁ stimulation. It is plausible that D₁ blockade by SCH-23390 hinders AIF-mediated apoptosis and, thus, significant preservation of PARP is seen (Figure 19). Attenuation of MA-induced striatal neurotoxicity has also been reported in mice (Xu et al., 2005) and rats (Jayanthi et al., 2005) following pre-treatment with SCH-23390. Both studies demonstrated complete protection against MA-induced presynaptic toxicity with only partial attenuation of postsynaptic apoptosis, which the latter is congruent with our findings. Jayanthi et al. noted SCH-23390 pre-treatment blocked postsynaptic Fas expression but only partially suppressed CASP3 activation. The authors reported SCH-23390 inhibited MA-induced hyperthermia and suggested that this may explain the non-caspase 3 mediated protection from striatal apoptosis (Jayanthi et al., 2005). We observed the same finding in regards to CASP3 and apoptosis in our model; however, the system we employed removed the element of

hyperthermia-induced toxicity. We propose AIF and other intracellular signaling pathways may be responsible for D₁-dependent, CASP3-independent MA-induced striatal apoptosis. To our knowledge there is a lack of research in any model on D₁-mediated activation of AIF. Further studies should be aimed at identifying the plausible participation of AIF in D₁-mediated versus D₁-independent mechanisms of DA-induced apoptosis in this cell line.

In an effort to examine cell signaling involved in DA-mediated apoptosis, we studied the effects of D₁- vs. non-D₁-mediated activation of MAPK p38. This signaling molecule is known to regulate both apoptosis and adaptation in response to various stimuli (Shi et al., 2011). Additionally, we previously demonstrated that DA-induced p38 phosphorylation in SK-N-MC cells (Figure 15). Figure 20 shows p38 was phosphorylated following treatment with the D₁ agonist SKF-39393, while pre-treatment with the D₁ antagonist SCH-23390 did not significantly decrease p38 phosphorylation when compared to DA alone (results not shown). These results suggest p38 is phosphorylated by D₁-dependent and DA-mediated D₁-independent pathways. The latter mechanism may occur as a result of an alteration in intracellular redox status following DA autoxidation. Previous studies have incongruent findings regarding D₁-mediated p38 phosphorylation in SK-N-MC. One study revealed p38 phosphorylation following 5-120 minute treatment with 1-500 μ M SKF-38393 in a manner that was insensitive to pre-treatment with 10 μ M of the D₁ antagonist SCH-23390 (Zhen et al., 1998). Another study reported an absence of p38 phosphorylation upon treatment with 10-200 μ M SKF-38393 for 1 h despite significant p38 activation following treatment with 50-100 μ M DA (Chen et al., 2004). In the latter experiment, however, the absence of a loading control may explain the discrepant findings between the two studies. We are the first to report that p38 is phosphorylated through both D₁-dependent and DA-mediated non-D₁-dependent mechanisms in SK-N-MC.

The significance of p38 phosphorylation following D₁-dependent or D₁-independent DA stimulation became evident in our system after inhibition of the MAPK by pre-treatment with SB203580. As shown in Figure 22, p38 inactivation prior to D₁ stimulation with SKF-38393 significantly decreased parental PARP protein levels when compared to samples without p38 inhibition. This finding suggests an adaptive response was initiated following D₁-dependent p38 activation. Of interest, p38 inactivation was significantly protective at the level of parental PARP in samples treated with 25 μM DA, while SB203580 pre-treatment was inconsequential at the level of PARP in samples treated with 50 μM DA. Contrary to the protective role of p38 following isolated D₁ stimulation, p38 activation following treatment with 25 μM DA appeared to be pro-apoptotic. The discordant consequences of p38 phosphorylation suggest that its downstream targets and/or activity may differ depending on the original signaling stimuli.

The results from Figure 25 show that p38 inactivation is protective at the level of PARP fragmentation following 25-50 μM DA stimulation in a D₁-independent manner. The complete attenuation of PARP fragmentation following p38 inhibition suggests that p38 signaling is pro-apoptotic when activated through a D₁-independent manner. Interestingly, p38 inactivation had no effect on PARP following 50 μM DA stimulation; however, once the D₁ receptors were blocked with SCH-23390, then p38 appeared to play a pro-apoptotic role (see Tables 1 and 2).

	Cleaved CASP3		Cleaved PARP	
	vs. 25 μ M DA	vs. 50 μ M DA	vs. 25 μ M DA	vs. 50 μ M DA
SKF-38393	↔	↔	↑	↑
DA + SCH-23390	↓	↔	↓	↓*
DA + SB203580	↓*	↔	↓*	↔
SKF-38393 + SB203580	↑*	↑*	↑↑*	↑↑*
DA + SCH-23390 + SB203580	↓↓*	↓↓*	↓↓*	↓↓*

Table 1: The Direction of Change in Markers of Apoptosis in Response to Dopamine is Influenced by the Mechanism Through Which p38 is Activated

Given that caspase 3 cleavage (Cleaved CASP3) and PARP cleavage (Cleaved PARP) are increased following inhibition of p38 following dopamine receptor stimulation, then it is plausible that the phosphorylation of p38 serves a protective role when it is stimulated by the D₁ receptor. Conversely, given that caspase 3 cleavage (Cleaved CASP3) and PARP cleavage (Cleaved PARP) are increased following inhibition of p38 following blockade of the D₁ receptor, then it is plausible that the phosphorylation of p38 serves a deleterious role when it is activated by dopamine in a manner independent of the D₁ receptor. * *at least* $p < 0.05$ compared to dopamine; arrows without * indicate *trend* in change; DA (dopamine), SB203580 (P-p38 inhibitor), SCH-23390 (D₁ antagonist), SKF-23390 (D₁ agonist).

	vs. 25 μ M DA		vs. 50 μ M DA	
	Cl. CASP3	Cl. PARP	Cl. CASP3	Cl. PARP
SKF-38393	\leftrightarrow	\uparrow	\leftrightarrow	\uparrow
DA + SCH-23390	\downarrow	\downarrow	\leftrightarrow	\downarrow^*
DA + SB203580	\downarrow^*	\downarrow^*	\leftrightarrow	\leftrightarrow
SKF-23390 + SB203580	\uparrow^*	$\uparrow\uparrow^*$	\uparrow^*	$\uparrow\uparrow^*$
DA + SCH-23390 + SB203580	$\downarrow\downarrow^*$	$\downarrow\downarrow^*$	$\downarrow\downarrow^*$	$\downarrow\downarrow^*$

Table 2: Difference in Dopamine Concentration Influences Whether p38 Phosphorylation Provides a Protective or Deleterious Response

Integrating the above table helps to discern if p38 phosphorylation is protective or deleterious at different concentrations of dopamine. A concentration of 25 μ M DA has lower expression of apoptotic cleavage markers when p38 is inhibited, while concentrations of 50 μ M DA are unchanged. This pattern of apoptotic cleavage most closely mimics that seen in the dopamine receptor independent activation pathway; thus, it is plausible that lower concentration of 25 μ M DA operates mostly through receptor independent pathways. The opposite is observed for the higher concentration of 50 μ M DA which operates similarly to cleavage patterns seen in D₁ receptor stimulation.

	D₁ (SKF-38393)		Non-D₁ (DA + SCH-23390)	
	Cl. CASP3	Cl. PARP	Cl. CASP3	Cl. PARP
Active P-p38 (without SB203580)	↔	↑	↔	↓*
Non-Active P-p38 (with SB203580)	↑*	↑↑*	↓↓*	↓↓*

Table 3: p38 Phosphorylation Mediates Either an Adaptive or Apoptotic Response Which is Determined by the Presence or Absence of D₁ Receptor Stimulation

Inactivation of p38 exacerbated caspase 3 and PARP cleavage when the D₁ receptor was stimulated, but upon receptor blockade with SCH-23390 the inhibition of p38 led to protection against caspase 3 and PARP cleavage. * p <0.001 compared to dopamine; arrows without * indicate directional trend of change; Cl. CASP3 (cleaved caspase 3), Cl. PARP (cleaved PARP), DA (dopamine), SB203580 (P-p38 inhibitor), SCH-23390 (D₁ antagonist), SKF-23390 (D₁ agonist).

The findings in Figures 21 and 22 support a dichotomous role for p38 activation in SK-N-MC. We found a difference in CASP3 cleavage that was dependent upon D₁-mediated vs. non-D₁-mediated DA stimulation (Figures 16 and 18). Figures 21 and 24 demonstrate that p38 inhibition had an effect on CASP3 cleavage which mimicked that seen with PARP analysis (Figures 22 and 25) wherein p38 inactivation was deleterious following D₁ stimulation and protective after D₁ blockade. The findings from 50 μM DA samples were compelling in that p38 inactivation exacerbated CASP3 cleavage when the D₁ receptors were available for binding, but upon receptor blockade with SCH-23390, the role of p38 transposed and its inhibition led to complete protection against CASP3 cleavage (Figure 24; see Table 3). The findings clearly implicate p38 phosphorylation as a mediator of DA-induced cellular adaptation versus apoptosis depending on its upstream activation. We propose that the D₁-mediated increase in cell death following p38 inhibition occurred through recruitment of an additional apoptotic pathway i.e., activation and cleavage of CASP3. As shown, inhibition of p38 phosphorylation resulted in a

significant increase in CASP3- and PARP-cleavage following SKF-38393 treatment suggesting that p38 may serve a protective function when stimulated exclusively through D₁. Conversely, simultaneous inhibition of D₁ and p38 worked in a synergistic fashion to completely stabilize CASP3 from cleavage, thus suggesting that p38 activation through redox-sensitive mechanisms, such as DA autoxidation, may have a causal role in CASP3 cleavage. The disparity in results between 25 and 50 μM DA treatments may reside in the extent to which the D₁ receptor is activated. It is plausible that the reduced concentration of 25 μM DA does not confer sufficient D₁ agonistic capability, due to rapid DA oxidation, to elicit the protective effects of p38 seen at 50 μM concentration. The majority of p38 phosphorylation may be, therefore, in response to DA autoxidation resulting in activation of the pro-apoptotic p38 signaling cascade. Similarly, the pharmacodynamic properties of SKF-38393 offer ~1000 times greater affinity for D₁ than DA (Missale et al., 1998); consequently, the lower 25 μM concentration of SKF-38393 provides substantially more D₁ stimulation than does the same concentration of DA, and thus activates the p38-protective pathway (see Table 3).

Only a limited amount of research on the role of stimulant-induced p38 expression in neurons is available. One study examined rat primary cortical neurons following treatment with methamphetamine and found p38 inhibition with SB203580 exacerbated apoptosis and suggested p38 phosphorylation served an anti-apoptotic role in MA-induced neurotoxicity (Huang et al., 2009). Another study reported neuronal protection in nematodes with a genetic mutation of the p38 signaling pathway following treatment with the DA oxidation metabolite 6-hydroxydopamine (Schreiber & McIntire, 2011). The results from the latter study are comparable to our findings in Figure 25 whereby we demonstrate a pro-apoptotic role for p38 when activated by DA through a non-D₁ mediated manner, such as DA oxidation. We

hypothesize that a difference in stimuli results in activation of separate isoforms of p38. There are four isoforms of p38, and they may have dual-roles in cancer, ischemia-reperfusion, and other pathologies (Pramanik et al., 2003; Risco & Cuedna, 2012; Tanno et al., 2003). The antibody we used reacts with multiple p38 isoforms, thus future research should determine if DA activates alternate p38 isoforms depending on D₁ stimulated vs. non-D₁ mediated mechanisms.

In order to investigate potential downstream targets of p38 that may modulate CASP3 cleavage, we examined the phosphorylation status of heat shock protein 27 (HSP27) in SK-N-MC. Heat shock protein 27 is a known target of p38, and its activation inhibits components of apoptosis (Mearow et al., 2002; Shi et al., 2011). Activation of HSP27 attenuates apoptosis through stabilization of CASP3 (Pandey et al., 2000; Parcellier et al., 2003) and inhibition of cytochrome *c*-mediated activation of caspases (Bruey et al., 2000). Figure 26 shows a significant increase in HSP27 phosphorylation following treatment with 25-50 μ M of the D₁ agonist SKF-38393 as well as 50 μ M DA, but not 25 μ M DA. The increase in HSP27 phosphorylation was significantly attenuated by pre-treatment with the p38 inhibitor SB203580. The results show that HSP27 is phosphorylated following D₁ stimulation in a manner dependent on p38 activation. Integration of Figures 21 and 22 suggests that D₁-mediated p38 activation offers protection from CASP3 through recruitment of HSP27. Furthermore, HSP27-mediated protection does not occur through an inhibition of AIF release from the mitochondria (Bruey et al., 2000); thus our hypothesis that D₁-stimulated apoptosis occurred through AIF activation is plausible. Although research on stimulant-induced HSP27 is sparse, one study reported increased expression of *hspb1*, the gene that codes for HSP27 protein, in rat striatum following 2-4 h treatment with 20-40 mg/kg MA (Jayanthi et al., 2009). The authors speculated the increase in *hspb1* was a neuroprotective response to MA administration. Future studies should be aimed at further

understanding the role of HSP27 in DA toxicity, such as analyzing apoptotic markers following DA treatment in cells overexpressing HSP27.

In addition to HSP27, we examined another downstream target of p38, AP-1. This protein is a known modulator of cell survival and death (Shaulian & Karin, 2001; 2002), and MA injections enhance expression of transcription factors from the AP-1 family in mouse brain (Cadet et al., 2001; Krasnova & Cadet, 2009) as well as increase AP-1 DNA binding in mouse striatum (Flora et al., 2002). Additionally, we have shown enhanced AP-1 reporter activity following treatment with 25-50 μ M DA in our system (Figure 14). In order to determine the mechanisms responsible for AP-1 activation following DA treatment we evaluated the role of p38 in specific D₁ stimulation and DA-mediated D₁-independent effects on AP-1 reporter assays. Figure 27 shows that 50 μ M DA-induced AP-1 luciferase activity was significantly decreased following treatment with the p38 inhibitor SB203580. The results from Figure 27 suggest that DA-induced AP-1 is dependent upon p38 activation. We have evidence for two pathways by which p38 may be activated following treatment with DA. Figure 28A displays an absence of AP-1 activity following treatment with 0-100 μ M of the D₁ agonist SKF-38393 despite significant enhancement with the same concentrations of DA. Conversely, Figure 28B shows that a D₁-independent mechanism of DA treatment significantly increased AP-1 activity as evidenced by no significant change in AP-1 luciferase activity compared to DA following D₁ blockade with SCH-23390. The results from Figure 28A and B demonstrate that AP-1 is activated by DA in a manner independent of D₁ receptor stimulation, such as DA oxidation. Our findings from Figure 25 suggest that the D₁-independent activation of p38 enhances apoptosis in this system. Given that AP-1 is mediated through this pathway of p38 activation (Figure 27), we hypothesize that AP-1 activation is involved in DA-induced SK-N-MC cell death.

Activator Protein-1 exists as a dimer composed of members from the AP-1 family such as: c-Jun, c-Fos, ATF, junB, and junD (Shaulian & Karin, 2001; 2002). Since c-Fos has long been implicated as a precursor to neuronal apoptosis (Smeyne et al., 1993; Shaulian & Karin, 2001), we examined AP-1 activity after transiently transfecting a dominant negative to c-Fos called A-Fos (Olive et al., 1997) as shown in Figure 29A. The dominant negative protein significantly decreased AP-1 reporter activity thereby suggesting c-Fos is a component of DA-activated AP-1 in SK-N-MC. A parallel experiment examining DA-induced PARP cleavage after A-Fos transfection showed that the knock-down of AP-1 was sufficient to prevent PARP fragmentation (Figure 29B). These findings suggest that AP-1 is a c-Fos dependent mediator of DA-induced apoptosis in SK-N-MC, which fits with our hypothesis that the D₁-independent activation of p38 is a pro-apoptotic pathway. In opposition to our findings that AP-1 is pro-apoptotic in a model of MA-induced neurotoxicity, studies with c-Fos heterozygous mice showed an increase in MA-stimulated degeneration when compared to their wild type controls and led the authors to suggest a protective role for AP-1 transcription (Deng et al., 1999). The markers used in this study, however, were decreased DAT binding and reduced tyrosine hydroxylase activity, both of which are markers of presynaptic toxicity rather than postsynaptic neurotoxicity. In support of our work, a 2008 study reported inhibition of MA-induced JNK phosphorylation decreased cell death in SH-SY5Y cells. The authors of this study suggest that protection was through inhibition of JNK-mediated c-Jun activation; and therefore concluded that downstream AP-1 transcription may be detrimental to cell viability (Wang et al., 2008)—which is in accordance with our studies. Since SH-SY5Y cells contain DAT and do not possess DA receptors this model more appropriately served as a study for pre-synaptic terminal degeneration as opposed to postsynaptic apoptosis. Methamphetamine-induced terminal PARP

fragmentation (Jayanthi et al., 2004) and deoxynucleotidyl transferase-mediated dUTP nick-end labeling (TUNEL) staining (Zhu et al., 2006) have been used as markers for striatal postsynaptic apoptosis in mice. One study examined TUNEL staining and PARP fragmentation within the striatum of c-Jun heterozygous mice following 30 min to 3 days treatment with 40 mg/kg MA. The report showed that c-Jun heterozygotes were protected against MA-induced PARP fragmentation and had significantly less TUNEL-positive cells within the striatum (Deng et al., 2002b). The authors suggest that MA-induced striatal AP-1 activation is pro-apoptotic, a conclusion consistent with our findings.

We hypothesize that D₁-independent mechanisms of DA treatment, such as DA oxidation, are responsible for activation of AP-1 as its activation is sensitive to alteration in redox-status such as elevated reactive oxygen/nitrogen species (Flora et al., 2002; Krasnova & Cadet, 2009). We have also provided evidence that p38 and c-Fos are involved in DA-mediated activation of AP-1 in SK-N-MC. We are the first to show that DA stimulation activates AP-1 through a p38-dependent and D₁-independent manner in SK-N-MC. We are also the first to report that DA-induced AP-1 contains c-Fos and is pro-apoptotic in this system.

Figure 30 shows our hypotheses regarding mechanisms responsible for DA-induced apoptosis in SK-N-MC based on a consolidation of findings from the current research. We conclude that DA treatment leads to apoptosis through two distinct mechanisms. The first mechanism occurs through stimulation of the D₁ receptor. Dopamine D₁ stimulation leads to activation of AIF and subsequent PARP fragmentation in a caspase-independent manner. We propose that D₁-stimulated p38 activates HSP27, which then stabilizes CASP3 in an attempt to mount a protective response. The second mechanism of apoptosis involves D₁-independent effects of DA, such as DA oxidation. We speculate that p38 is activated through a change in

intracellular redox status from DA-mediated RO/NS generation. When p38 is activated through this pathway it serves as a pro-apoptotic mediator by activating AP-1 in a c-Fos dependent manner with resultant CASP3 and PARP cleavage. We are the first to report a dual-role for p38 in DA-induced neurotoxicity, and thus we deem MAPK p38 as the “molecular switch” between adaptation and apoptosis in this system. We used these findings to develop two separate ways to prevent DA-induced apoptosis in this model by: 1) co-inhibiting D₁ receptor stimulation and p38, or 2) employing a c-Fos dominant negative to block AP-1 activity.

The findings from our study offer mechanistic insight into clinical and translational data involving D₁ postsynaptic striatal apoptosis following stimulant exposure wherein we identified key participants of associated neurotoxic signaling pathways. The results also demonstrated potential neurotoxic side-effects in the use of D₁ agonists to combat craving and relapse. Toxicological studies should be conducted on such compounds before further research is continued. Our identification of two unique ways to prevent DA-induced apoptosis could serve as a starting point for the development of pharmacological intervention against the cycle of MA-induced neurotoxicity.

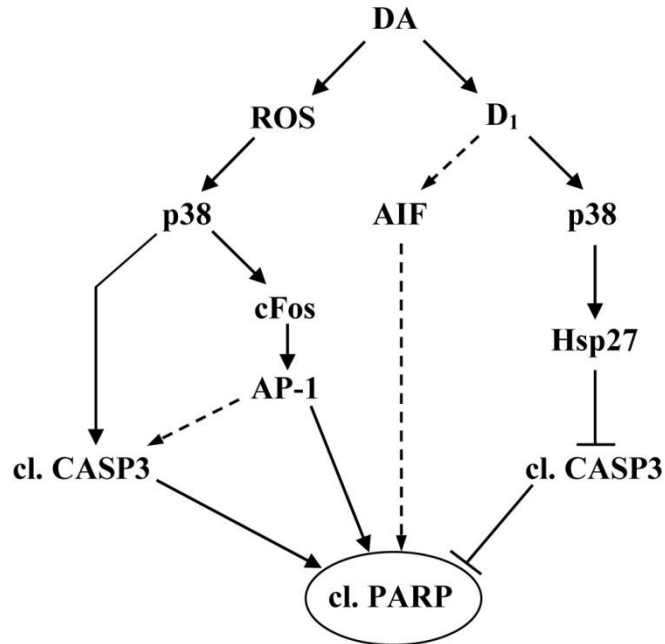


Figure 29: The p38-Mediated Molecular Switch

The initial route of p38 activation by dopamine (DA), either through generation of reactive oxygen species (ROS) or DA stimulation of the D₁ receptor (D₁) determines the downstream effect of p38. If it is activated by ROS, then p38 triggers both the cleavage of caspase 3 (cl. CASP3) and transcription of cFos-containing Activator Protein-1 (AP-1). These events culminate in cleavage of poly(ADP-ribose) polymerase (cl. PARP) and subsequent cellular apoptosis. If p38 is activated by D₁ stimulation, then CASP3 is stabilized by p38-modulated heat shock protein 27 (Hsp27) expression. Despite the stabilization of CASP3, we hypothesize that D₁ stimulation triggers caspase-independent Apoptosis Inducing Factor (AIF), and it is through this mechanism that D₁ stimulation results in cl. PARP and apoptosis. Solid lines are representative of data generated in this work. Dashed lines have not been proven in this study but are representative of working hypothesis and targets for future work.

CHAPTER 4

GLOBAL DISCUSSION AND FUTURE DIRECTION

Global Discussion

The goal of this mechanistic-based study was to identify specific cellular macromolecules involved in DA-induced neurotoxicity that could potentially serve as targets for pharmacological intervention aimed at attenuating MA-associated striatal toxicity. By utilizing basic biomedical science, we developed an *in vitro* model to investigate molecular mechanisms responsible for the long-term, possibly irreversible neurotoxicity seen following MA abuse. Our hopes were that this research and associated findings would provide information relevant to the development of possible therapeutic options, including but not limited to the following: 1) macromolecular changes associated with enhanced reactive oxygen/nitrogen species and the effect of antioxidant supplementation, 2) identification of specific enzymes that contribute to or protect against MA/DA toxicity, 3) modulation of pro-apoptotic cell-signaling and gene expression following DA exposure, as well as 4) the role of D₁-mediated vs. non-D₁-mediated DA stimulation in apoptosis and associated downstream signaling.

Through this work we collected molecular evidence for pro-(nitro)oxidative protein changes within SK-N-MC following 25 and/or 50 μ M DA treatment. Previous studies in this model reported a DA-facilitated increase in nitrite levels as well as attenuation of cytotoxicity following antioxidant supplementation (Chen et al., 2003; 2004, Moussa et al., 2006). We are the first, however, to show protein alterations consistent with an environment rich in RO/NS following exposure to [DA] equivalent to that seen after MA use. We propose that DA-mediated activation of iNOS contributes to the enhanced (nitro)oxidative stress; and thereby providing support for the role of iNOS \gg nNOS in MA/DA-induced RO/NS production (Itzhak et al.,

2000; Chen et al., 2003; reviewed in Kita et al., 2003). Although studies demonstrate cell death following 16-24 h of DA treatment with concentrations as low as 50 μ M (Chan et al., 2007; Chen et al., 2003; Moussa et al., 2006), we are the first to report evidence of apoptosis after exposure to half of the lowest reported concentration (25 μ M); and we are the first to demonstrate that apoptosis occurred, at least in part, through the mitochondrial-mediated pathway involving CASP9 cleavage in SK-N-MC. Given the evidence for RO/NS and mitochondrial-mediated apoptosis in DA-treated SK-N-MC, we assessed the expression and activity of the mitochondrial, antioxidant enzyme MnSOD. Studies report a protective role for MnSOD overexpression in MA-induced apoptosis (Maragos et al., 2000), but we are the first to establish that following 50 μ M DA treatment in a model of methamphetamine neurotoxicity: 1) MnSOD expression is enhanced, 2) despite an elevation in MnSOD expression there is not a concurrent increase in activity, and 3) MnSOD is nitrated.

We identified several key proteins involved in DA-mediated signaling within SK-N-MC. Conflicting reports create an uncertain picture of the individual involvement of the mitogen activated protein kinases in this system (Chan et al., 2007; Chen et al., 2004; Zhen et al., 1998). We observed p38 and ERK1/2 phosphorylation following 25-50 and 50 μ M DA, respectively, without noting JNK phosphorylation after 6 h. We are the first to report activation of p38 through both D₁-dependent and DA-mediated, D₁-independent mechanisms. Further, we postulate that p38 is the “molecular switch” of DA-stimulated SK-N-MC cells based on its modulation of caspase 3 stabilization versus caspase 3 cleavage following D₁ stimulation or non-D₁ activation, respectively. We examined two transcription factors, NF κ B and AP-1 known not only for their regulatory role in iNOS and MnSOD expression, but also for their activation following ROS-derived neuronal injury (Alderton et al., 2001; Flora et al., 2002; Kinningham et

al., 1997; Pautz et al., 2010). This is the first report to demonstrate that NF κ B reporter activity was not increased after 0-100 μ M DA treatment, which is above the EC₅₀ of 75 μ M DA for D₁ receptors in SK-N-MC (Moussa et al., 2006). Unlike NF κ B, AP-1 reporter activity was significantly increased following a 6 h treatment of SK-N-MC cells with 25-100 μ M DA. Additional studies allowed us to be the first to report that in this model AP-1 is: 1) activated through a non-D₁-mediated pathway following DA stimulation, 2) dependent upon upstream p38 phosphorylation, and 3) a heterodimer containing cfos (Shaulian & Karin, 2001; 2002).

Although the above findings further the understanding of MA/DA-mediated mechanisms of neurotoxicity, perhaps our most important contribution lies in the discovery of multiple ways to prevent DA-induced apoptosis in our model. We identified three ways to prevent apoptosis in this model of DA-induced neurotoxicity which mimics that caused by MA abuse. The current study shows that by: 1) providing exogenous SOD supplementation prior to treatment, 2) simultaneously blocking the D₁ receptor and p38 phosphorylation, or 3) using a dominant negative to cfos we can prevent PARP fragmentation following 24 h treatment with 50 μ M DA. The original goal in the present study was to identify intracellular processes that may be responsible for the stereotyped neurotoxicity and functional impairment sustained by MA abusers. The implications of these findings may be extended to translational studies; and ultimately into clinical research. As stated previously, taking into account that the neurotoxicity experienced by MA abusers has negative, long-term functional sequelae with no effective treatment (Barr et al., 2006; Brackins et al., 2011; Chang et al., 2002; Salo et al., 2005; 2007; Volkow et al., 2001a, b), then perhaps the best “treatment” would be during MA abuse to prevent these from occurring.

Future Direction

Integrating the findings from this current work, it appears that SK-N-MC cells execute a dual response following DA treatment. The initiation of apoptosis clearly suggests SK-N-MC cells undergo programmed cell death in response to noxious stimuli. Conversely, an adaptive response is also initiated within SK-N-MC as evidenced by increased MnSOD protein expression, phosphorylation of HSP27, and stabilization of caspase 3. We decided to determine the status of HSP32, otherwise known as heme oxygenase-1 (HO-1), given that HO-1 expression is considered a neuroprotective response (Jazwa and Cuadrado, 2010; reviewed in Maines et al., 2000;) and is upregulated following DA stimulation or (nitro)oxidative stress (Calabrese et al., 2004; Naughton et al., 2002; reviewed in Schipper, 2004).

Figure 31 shows time-dependent expression of HO-1 in SK-N-MC following 0-50 μ M DA treatment for 8, 16, and 24 h. The magnitude of HO-1 protein upregulation at 12-24 h prompted the investigation of potentially harmful consequences from HO-1 overexpression.

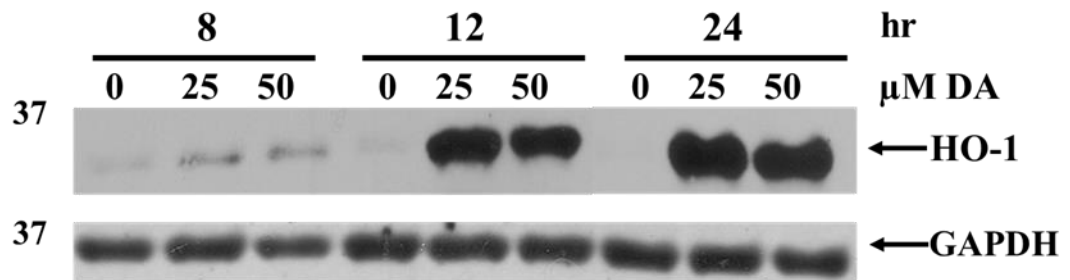


Figure 30: Dopamine Increases Heme Oxygenase 1 Expression in a Time-Dependent Manner

Western analysis of heme oxygenase-1 (HO-1; at 37 kDa) following 8, 16, or 24 h treatment with 0-50 μ M DA. Heme oxygenase-1 expression was noted within 8 h of DA treatment. A marked increase in protein expression was observed between 8-16 h DA treatments. The figure is representative of findings repeated at least twice.

Reports suggest that enhanced HO-1 activity may contribute to and exacerbate, rather than ameliorate, neurodegenerative disorders such as Alzheimer's disease, Parkinson's disease,

Huntington's disease, and multiple sclerosis (Mehindate et al., 2001; Schipper et al., 2000, 2006, 2009; Song, L. et al., 2007; Song, W. et al., 2006;). Interestingly, the *Hmox1* gene, which codes for the HO-1 protein, is induced in rat striatum after 2 h MA treatment (Jayanthi et al., 2009), but the study did not address if the upregulation of HO-1 is protective or deleterious. A study using cortical neuron/glia co-cultures reported that p38 inhibition decreases MA-induced HO-1 expression and subsequently exacerbates toxicity when compared to MA treatment alone. The study also showed inhibition of HO-1 activity by tin protoporphyrin IX increased MA-induced neurotoxicity (Huang et al., 2009).

Although these results suggest a protective role for HO-1, caution must be taken when analyzing data subsequent to p38 inhibition. As we have shown, p38 may play multiple roles within the same system; thus the decrease in HO-1 expression may not be causal for the increased toxicity noted in the study, rather it may be from inhibition of a p38-mediated protective pathway following MA administration. Likewise, carbon monoxide (CO) is a by-product of HO-1-facilitated heme breakdown as well as an upstream modulator of p38 phosphorylation (reviewed in Chung et al., 2008); therefore, the attenuation in HO-1 activity by tin protoporphyrin IX may indirectly hinder any protective effects from p38 signaling through decreased CO production. In opposition to the last two points, MA-induced HO-1 expression may be neuroprotective as suggested (Huang et al., 2009).

Based on preliminary data generated in our laboratory, we hypothesize the existence of a “feed-forward” loop between HO-1 and iNOS expression that leads to MnSOD inactivation and generation of massive (nitro)oxidative stress. The abundance of RO/NS overwhelms the cell's antioxidant capacity and neuronal death ensues (see Figure 32). We have established that in this cell system: 1) DA generates RO/NS; 2) both HO-1 and iNOS are upregulated upon DA

treatment in a time-sensitive manner; 3) footmarkers for peroxynitrite, such as 3-nitrotyrosine, are present following DA administration; 4) MnSOD is nitrated and fails to mount an adaptive response; 5) cellular apoptosis occurs as evidenced by stereotypical, microscopic, morphological appearance and PARP cleavage. The centerpiece to this hypothesis is the relationship of HO-1 activity to iNOS protein expression. Heme oxygenase-1 is upregulated by RO/NS and DA (reviewed in Schipper, 2004), but its modulation is particularly sensitive to iNOS-generated RNS (Datta and Lianos, 1999; Kitamura et al, 1998; Immenschuh et al., 1999). Furthermore, CO, a known by-product of HO-1 mediated heme breakdown, upregulates iNOS expression (Calabrese et al., 2004). As depicted in Figure 32, it is plausible that HO-1 has a deleterious role through its relationship with iNOS regulation in this cell system.

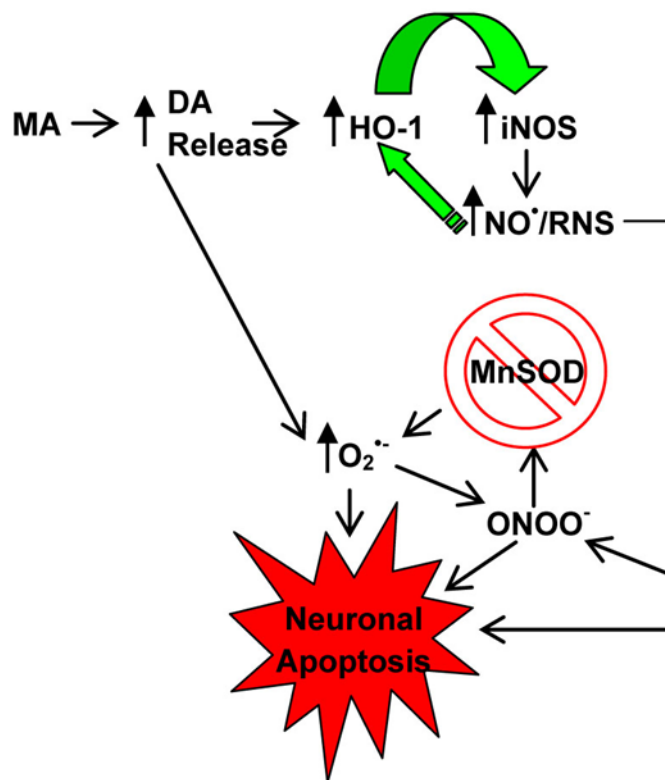


Figure 31: Proposed Mechanism of Action of Methamphetamine Neurotoxicity

Methamphetamine (MA) administration releases supraphysiological concentration of dopamine (DA) from the striatum. Heme oxygenase-1 (HO-1) expression is enhanced by DA, and its enzymatic by-product, CO, upregulates iNOS protein. The increased iNOS activity produces nitric oxide (NO[•]) that can: 1) combine with superoxide radicals (O₂^{•-}) from DA autoxidation and form highly reactive peroxynitrite (ONOO⁻), and 2) further upregulate HO-1 resulting in greater CO production and enhanced iNOS expression. The resulting ONOO⁻ renders MnSOD susceptible to nitration and subsequent inactivation, thus the system becomes overwhelmed with (nitro)oxidative stress and neuronal apoptosis ensues. Given the cyclic, feed-forward system between HO-1 and iNOS, we hypothesize that inhibition of HO-1 or its activity may avert MA-mediated DA neurotoxicity.

Future studies in our laboratory will be aimed at determining the role of HO-1 in DA-induced SK-N-MC toxicity as well as the modulation of its upstream signaling. Poly (ADP-ribose) polymerase fragmentation will serve as the indicator for apoptosis with and without the use of a blood brain barrier-permeable HO-1 inhibitor, such as Sn (IV) mesoporphyrin IX, following DA treatment. Analysis of HO-1 expression following treatment with a D₁ agonist,

co-treatment with DA and a D₁ antagonist, MAPK inhibitors, or A-Fos will provide information critical to understanding its DA-mediated signaling.

In regard to every past or present finding from this research, the ultimate goal is to conduct similar studies in vivo using a murine model. The first step will be to gather initial data on protein alterations within the striatum of MA-exposed mice such as: nitro(oxidative) changes, verification of apoptosis in the system, and up/down regulation of key enzymes. If the results from the MA treated murine studies reveal nitration of MnSOD, then we would administer MnSOD mimetics or other antioxidant treatment prior to MA and then reassess MnSOD and neurotoxic parameters. If HO-1 is expressed in the striatum following MA administration, then pre-treatment with a HO-1 inhibitor and analysis of neurotoxic parameters would be appropriate to evaluate if HO-1 is protective or deleterious. Studies in HO-1 knockout mice, to which we have access, would also help identify the role of MA-induced HO-1 expression. The findings from the murine research would hopefully serve as a bridge to translational studies--perhaps in primates--and with an ultimate goal of reaching clinical relevance.

REFERENCES

- Albertson, T. E., Derlet, R. W., & Van Hoozen, B. E. (1999). Methamphetamine and the expanding complications of amphetamines. *Western Journal of Medicine*, 170(4), 214-219.
- Alderton, W. K., Cooper, C. E., & Knowles, R. G. (2001). Nitric oxide synthases: structure, function, and inhibition. *Biochemistry Journal*, 357(3) 593-615.
- Anantharaman, M., Tangpong, J., Keller, J. N., Murphy, M. P., Markesbery, W. R., Kinningham, K. K., & St Clair, D. K. (2006). Beta-amyloid mediated nitration of manganese superoxide dismutase: implication for oxidative stress in a APPNLH/NLH X PS-1P264L/P264L double knock-in mouse model of Alzheimer's disease. *The American Journal of Pathology*, 168(5), 1608-18. DOI: 10.2353/ajpath.2006.051223.4.
- Ares-Santos, S., Granado, N., & Moratalla, R. (2013). The role of dopamine receptors in the neurotoxicity of methamphetamine. *Journal of Internal Medicine*, 273,437-553. DOI: 10.1111/joim.12049.
- Ares-Santos, S., Granado, N., Oliva, I., O'Shea, E. Martin, E.D., Colado, M.I., & Moratalla, R. (2012). Dopamine D(1) receptor deletion strongly reduces neurotoxic effects of methamphetamine. *Neurobiology of Disease*, 45(2), 810-820. DOI: 10.1016/j.nbd.2001.11.005.
- Badiani, A., Oates, M. M., Day, H. E., Watson, S. J., Akil, H., & Robinson, T. E. (1999). Environmental modulation of amphetamine-induced c-fos expression in D1 versus D2

- striatal neurons. *Behavioural Brain Research*, 103(2):203-209. DOI: 10.1016/S0166-4328(99)00041-8.
- Barr, A. M., Panenka, W. J., MacEwan, G. W., Thornton, A. E., Lang, D. J., Honer, W. G., & Lecomte, T. (2006). The need for speed: an update on methamphetamine addiction. *Journal of Psychiatry & Neuroscience*, 31(5), 301-313.
- Beauvais, G., Jayanthi, S., McCoy, M. T., Ladenheim, B., & Cadet, J. L. (2010). Differential effects of methamphetamine and SCH23390 on the expression of members of IEG families of transcription factors in the rat striatum, *Brain Research*, 1318(8), 1-10. DOI: 10.1016/j.brainres.2009.12.083.
- Berlett, B., & Stadtman, E. (1997). Protein oxidation in aging, disease, and oxidative stress. *Journal of Biological Chemistry*, 272(33), 20313-20316.
- Brackins, T., Brahm, N. C., & Kissack, J. C. (2011). Treatments for methamphetamine abuse: a literature review for the clinician. *Journal of Pharmacy Practice*, 24(6), 541-550. DOI: 10.1177/08971990011426557.
- Breckenridge, G. G., Germain, M., Mathai, J. P., Ngyren, M., & Shore, G., C. (2003). Regulation of apoptosis by endoplasmic reticulum pathways. *Oncogene*, 22, 8606-8618. DOI: 10.1038/sj.onc.1207108.
- Bronstein, D. M., & Hong, J. S. (1995). Effects of sulpiride and SCH 23390 on methamphetamine-induced changes in body temperature and lethality. *Journal of Pharmacology and Experimental Therapeutics*, 274(2), 943-950.

- Bruey, J. M., Ducasse, C., Bonniaud, P., Ravagnan, L., Susin, S. A., Diaz-Latoud, C., ... Garrido, C. (2000). Hsp27 negatively regulates cell death by interacting with cytochrome c. *Nature Cell Biology*, 2, 645-652. DOI: 10.1038/35023595.
- Cadet, J. L., Jayanthi, S., McCoy, M. T., Vawter, M., & Ladenheim, B. (2001). Temporal profiling of methamphetamine-induced changes in gene expression in the mouse brain: evidence from cDNA array. *Synapse*, 41(1), 40-48. DOI: 10.1002/syn.1058.
- Cadet, J. L., Ordonez, S. V., & Ordonez, J. V. (1997). Methamphetamine induces apoptosis in immortalized neural cells: protection by the proto-oncogene, bcl-2. *Synapse*, 25(2):176-184. DOI: 10.1002/(SICI)1098-2396(199702)25:2<176::AID-SYN8>3.0.CO;2-9.
- Cadet, J. L., Sheng, P., All, S., Rothman, R., Carlson, E., & Epstein, C. (1994). Attenuation of methamphetamine-induced neurotoxicity in copper/zinc superoxide dismutase transgenic mice. *Journal of Neurochemistry*, 62(1), 380-383. DOI:10.046/j.1471-4159.1994.62010380.x.
- Calabrese, V., Stella, A., M., Butterfield, D., A., & Scapagnini, G. (2004). Redox regulation in neurodegeneration and longevity: role of the heme oxygenase and HSP70 systems in brain stress tolerance. *Antioxidants & Redox Signaling*, 6(5), 858-913. DOI: 10.1089/ars.2004.6.895.
- Cass, W. A., Bowman, J. P., & Elmund, J., K. (1989). Behavior, striatal and nucleus accumbens field potential patterns and dopamine levels in rats given amphetamine continuously. *Neuropharmacology*, 28(3), 217-227.

- Cavanaugh, J. E., Jaumotte, J. D., Lakoski, J. M., & Zigmond, M., J. (2006). Neuroprotective role of ERK1/2 and ERK in a dopaminergic cell line under basal conditions and in response to oxidative stress. *Journal of Neuroscience Research*, *84*(6), 1367-1375. DOI: 10.1002/jnr.21024.
- Chan, A. S., Ng, L. W., Poon, L. W., Chan, W. W., & Wong, Y. H. (2007). Dopaminergic and adrenergic toxicities on SK-N-MC human neuroblastoma cells are mediated through G protein signaling and oxidative stress. *Apoptosis*, *12*(1), 167-179. DOI: 10.1007/s10495-006-0524-8.
- Chang, L., Ernst, T., Speck, O., Patel, H., DeSilva, M., Leonido-Yee, M., & Miller, E. N. (2002). Perfusion MRI abnormalities and computerized cognitive deficits in abstinent methamphetamine users. *Psychiatry Research: Neuroimaging*, *114*(2), 65-79. DOI: 10.1016/S0925-4927(02)00004-5.
- Chang, L., Alicata, D., Ernst, T., & Volkow, N. (2007). Structural and metabolic brain changes in the striatum associated with methamphetamine abuse. *Addiction*, *102*(1):16-32. DOI: 10.1111/j.1360-0443.2006.01782.x.
- Chen, J., Rusnak, M., Luedtke, R. R., & Sidhu, A. (2004). D1 dopamine receptor mediates dopamine-induced cytotoxicity via the ERK signal cascade. *Journal of Biological Chemistry*, *279*(38), 39317-39330. DOI: 10.1074/jbc.M403891200.

- Chen, J., Wersinger, C., & Sidhu, A. (2003). Chronic stimulation of D1 dopamine receptors in human SK-N-MC neuroblastoma cells induces nitric-oxide synthase activation and cytotoxicity. *Journal of Biological Chemistry*, 278(30), 28089-28100. DOI: 10.1074/jbc.M303094200.
- Chung, H.T., Choi, B. M., Kwon, Y. G., & Kim, Y. M. (2008). Interactive relations between nitric oxide (NO) and carbon monoxide (CO): heme oxygenase-1/CO pathway is a key modulator in NO-mediated antiapoptosis and anti-inflammation. *Methods in Enzymology*, 441, 328-38. DOI: 10.1016/S0076-6879(08)01218-4.
- Cregan, S. P., Fortin, A., MacLaurin, J. G., Callaghan, S. M., Cecconi, F., Yu, S. W., ...Slack, R. S. (2002). Apoptosis-inducing factor is involved in the regulation of caspase-independent neuronal cell death. *Journal of Cell Biology*, 158(3), 507-517. DOI: 10.1083/jcb.200202130.
- Cunha-Oliveira, T., Rego, A. C., Caroso, S. M., Borges, F., Swerdlow, R., H., Macedo, T., & de Oliveira, C. R. (2006). Mitochondrial dysfunction and caspase activation in rat corticalneurons treated with cocaine or amphetamine. *Brain Research*, 1089(1), 44-54. DOI: 10.1016/j.brainres.2006.03.061.
- D'Acquisto, F., & Ianaro, A. (2006). From willow bark to peptides: the ever-widening spectrum of NF- κ B inhibitors. *Current Opinion in Pharmacology*, 6(4), 387-392. DOI: 10.1016/j.coph.2006.02.009.

- Datta, P. K., & Lianos, E. A. (1999). Nitric oxide induces heme oxygenase-1 gene expression in mesangial cells. *Kidney International*, 55(5), 1734-1739. DOI: 10.1046/j.1523-1755.1999.00429.x.
- Davidson, C., Chen, Q., Zhang, X., Xiong, X., Lazarus, C., & Ellinwood. (2007). Deprenol treatment attenuates long-term pre- and post-synaptic changes evoked by chronic methamphetamine. *European Journal of Pharmacology*, 573(1-9), 100-110. DOI: 10.1016/j.ejphar.2007.06.046.
- Deng, X., & Cadet, J. L. (2000). Methamphetamine-induced apoptosis is attenuated in the striata of copper-zinc superoxide dismutase transgenic mice. *Brain Research*, 83(1-2), 121-124. DOI: 10.1016/S0169-328X(00)00169-8.
- Deng, X., Cai, N. S, McCoy, M. T., Chen, W., Trush, M. A., & Cadet, J. L. (2002a). Methamphetamine induces apoptosis in an immortalized rat striatal cell line by activating the mitochondrial cell death pathway. *Neuropharmacology*, 42(6):837-845. DOI: 10.1016/S0028-3908(02)00034-5.
- Deng, X., Jayanthi, S., Ladenheim, B., Krasnova, I. N., & Cadet, J. L. (2002b). Mice with partial deficiency of c-Jun show attenuation of methamphetamine-induced neuronal apoptosis. *Molecular Pharmacology*, 62(5), 993-1000. DOI: 10.1124/mol.62.5.993.
- Deng, X., Ladenheim, B., Tsao, L. II., & Cadet, J. L. (1999). Null mutation of c-fos causes exacerbation of methamphetamine-induced neurotoxicity. *Journal of Neuroscience*, 19(22), 10107-10115. DOI: 10.1523/JNEUROSCI.19-22-10107.1999.

- Derlet, R.W., & Heischober, B. (1990). Methamphetamine. Stimulant of the 1990s? *Western Journal of Medicine*, 153(6), 625-628.
- De Vito, M. J., & Wagner, G. C. (1989). Methamphetamine-induced neuronal damage: a possible role for free radicals. *Neuropharmacology*, 28(10), 1145-1150.
- Dietrich, J., Mandeol, A., Revel, M. O., Burgun, C., Anuis, D., & Zwiller, J. (2005). Acute or repeated cocaine administration generates reactive oxygen species and induces antioxidant enzyme activity in dopaminergic rat brain structures. *Neuropharmacology*, 48(7), 965-974. DOI: 10.1016/j.neuropharm.2005.01.018.
- Di Monte, D.A., Royland, J. E., Jakowec, M. W., Langston, J. W. (1996). Role of nitric oxide in methamphetamine neurotoxicity: protection by 7-nitroindazole, an inhibitor of neuronal nitric oxide synthase. *Journal of Neurochemistry*, 67(6), 2443-2450. DOI: 10.1046/j.1471-4159.1996.67062443.x.
- Drevets, W.C., Gautier, C., Price, J. C., Kupfer, D. J., Kinahan, P. E., Grace, A. A.,...Mathis, C. A. (2001). Amphetamine-induced dopamine release in human ventral striatum correlates with euphoria. *Biological Psychiatry*, 49(2), 81-96. DOI:10.1016/S0006-3223(00)01038-6.
- Feldman, R. S., Meyer, J. S, & Quenzer, L. F. (1997). Stimulants: amphetamine and cocaine. In *Principles of Neuropsychopharmacology* (549-590). Sunderland, MA: Sinauer Associates Inc.

Finnegan, K. T., Ricaurte, G., Seiden, L. S., & Schuster, C. R. (1982). Altered sensitivity to d-methylamphetamine, apomorphine, and haloperidol in rhesus monkeys depleted of caudate dopamine by repeated administration of d-methylamphetamine.

Psychopharmacology (Berl), 77(1):43-52.

Fischman, M. W., & Schuster, C. R. (1974). Tolerance development to chronic methamphetamine intoxication in the rhesus monkey. *Pharmacology and Biochemistry and Behavior*, 2(4), 503-508. DOI:10.1016/0091-3057(74)90010-0.

Flora, G., Lee, Y. W., Nath, A., Maragos, W., Henning, B., & Toborek, M. (2002). Methamphetamine-induced TNF-alpha gene expression and activation of AP-1 in discrete regions of mouse brain: potential role of reactive oxygen intermediates and lipid peroxidation. *Neuromolecular Medicine*, 2(1):71-85. DOI: 10.1385/NMM:2:1:71.

Fowler, J. S., Volkow, N. D., Logan, J., Alexoff, D., Telang, F., Wang, G. J., ...Apelskog, K. (2008). Fast uptake and long-lasting binding of methamphetamine in the human brain: comparison with cocaine. *NeuroImage*, 43(4), 756-763. DOI: 10.1016/j.neuroimage.2008.07.020.

Giovanni, A., Liang, L. P., Hastings, T. G., & Zigmond, M. J. (1995). Estimating hydroxyl radical content in rat brain using systemic and intraventricular salicylate: impact of methamphetamine. *Journal of Neurochemistry*, 64(4), 1819-1825. DOI: 10.1046/j.1471-4159.1995.64041819.x.

- Gluck, M. R., Moy, L. Y., Jayatilleke, E., Hogan, K. A., Manzano, L., & Sonsalla, P. K. (2001). Parallel increases in lipid and protein oxidative markers in several mouse brain regions after methamphetamine treatment. *Journal of Neurochemistry*, *79*(1), 152-160. DOI: 10.1046/j.1471-4159.2001.00549.x.
- Goldstein, R. Z., Nolkow, N. D., Chang, L., Wang, G. J., Fowler, J. S., Depue, R. A., & Gur, R. C. (2002). The orbitofrontal cortex in methamphetamine addiction: involvement in fear. *Neuroreport*, *13*(17), 2253-2257. DOI: 10.1097/01.wnr0000044215.09266.bf
- Graham, D. G. (1978). Oxidative pathways for catecholamines in the genesis of neuromelanin and cytotoxic quinines. *Molecular Pharmacology*, *14*(4), 663-643.
- Graham, F. L., & van der Eb, A. J. (1973). A new technique for the assay of infectivity of human adenovirus 5 DNA. *Virology*, *52*(2), 456-467.
- Gross, N. B., & Marshall, J. F. (2009). Striatal dopamine and glutamate receptors modulate methamphetamine-induced cortical Fos expression. *Neuroscience*, *161*(4), 1114-1125. DOI: 10.1016/j.neuroscience.2009.04.023.
- Halazonetis, T. D., Georgopoulos, K., Greenburg, M. E., & Leder, P. (1988). c-Jun dimerizes with itself and with c-Fos, forming complexes of different DNA binding affinities. *Cell*, *55*(5), 917-924. DOI: 10.1016/0092-8674(88)90147-X.
- Harvey, D. C., Lacan, G., & Melegan, W. P. (2000). Regional heterogeneity of dopaminergic deficits in vervet monkey striatum and substantia nigra after methamphetamine exposure. *Experimental Brain Research*, *133*(3):348-58.

- Heikkila, R. E., Orlansky, H., Mytilineou, C., & Cohen, C. (1975). Amphetamine: evaluation of *d*- and *l*-isomers as releasing agents and uptake inhibitors for 3H-dopamine and 3H-NE in slices of rat neostriatum and cerebral cortex. *Journal of Pharmacology and Experimental Therapeutics*, *194*(1), 47-56.
- Herceg, Z., & Wang, Z. Q. (1999). Failure of poly(ADP-ribose) polymerase cleavage by caspases leads to induction of necrosis and enhanced apoptosis, *Molecular and Cellular Biology*, *19*(7), 5124-5133. DOI: 10.1128/MCB.19.7.5124.
- Herdman, M., Marcelo, A., Huang, Y., Niles, R. M., Dhar, S., & Kinningham, K. K. (2006). Thimerosal induces apoptosis in a neuroblastoma model via the cJun N-terminal kinase pathway. *Toxicological Sciences*, *92*(1), 246-53. DOI: 10.1093/toxsci/kfj205.
- Holley, A. K., Dhar, S. K., & St. Clair, D. K. (2010). Manganese superoxide dismutase versus p53: the mitochondrial center. *Annals of the New York Academy of Sciences*, *10*(6), 649-661. DOI: 10.1016/j.mito.2010.06.003.
- Huang, Y. N., Wu, C. H., Lin, T. C., & Wang, J. Y. (2009). Methamphetamine induces heme oxygenase-1 expression in cortical neurons and glia to prevent its toxicity. *Toxicology and Applied Pharmacology*, *240*(3), 315-326. DOI: 10.1016/j.taap.2009.06.021.
- Humphrey, M. L., Cole, M. P., Pendergrass, J. C., & Kinningham, K. K. (2005). Mitochondrial mediated thimerosal-induced apoptosis in a human neuroblastoma cell line (SK-N-SH). *Neurotoxicology*, *26*(3), 407-416. DOI: 10.1016/j.neuro.2005.03.008.

- Imam, S.Z., Newport, G. D., Itzhak, Y., Cadet, J. L., Islam, F., Slikker, W., & Ali, S. F. (2001). Peroxynitrite plays a role in methamphetamine-induced dopaminergic neurotoxicity: evidence from mice lacking neuronal nitric oxide synthase gene or overexpressing copper-zinc superoxide dismutase. *Journal of Neurochemistry*, 76(3), 745-749.
- Immenschuh, S., Tan, M., & Ramadori, G. (1999). Nitric oxide mediates the lipopolysaccharide dependent upregulation of the heme oxygenase-1 gene expression in cultured rat Kupfer cells. *Journal of Hepatology*, 30(1), 61969. 10.1016/S0168-8278(99)80008-7.
- Ito, M., Numachi, Y., Ohara, A., & Sora, I. (2008). Hyperthermic and lethal effects of methamphetamine: roles of dopamine D1 and D2 receptors. *Neuroscience Letters*, 438(3), 327-329. DOI: 10.1016/j.neulet.2008.04.034.
- Itzhak, Y., & Ali, S. F. (1996). The neuronal nitric oxide synthase inhibitor, 7-nitroindazole, protects against methamphetamine-induced neurotoxicity in vivo. *Journal of Neurochemistry*, 67(4), 1770-1773. DOI: 10.1046/j.1471-4159.1996.67041770.x.
- Itzhak, Y., Ghandia, C., Huang, P L., & Ali, S. F. (1998). Resistance of neuronal nitric oxide synthase-deficient mice to methamphetamine-induced dopaminergic neurotoxicity. *The Journal of Pharmacology and Experimental Therapeutics*, 284(3), 1040-1047.
- Itzhak, Y., Martin, J. L., & Ali, S. F. (1999). Methamphetamine-and 1 methyl-4-phenyl-1,2,3,6-tetrahydropyridine-induced dopaminergic neurotoxicity in inducible nitric oxide synthase-deficient mice. *Synapse*. 34(4): 305-312. DOI: 10.1002/(SICU)1098-2396(19991215)34:4,305::AID-SYN6>3.0.CO;2#.

Itzhak, Y., Martin, J. L., & Ali, S. F. (2000). Comparison between the role of the neuronal and inducible nitric oxide synthase in methamphetamine-induced neurotoxicity and sensitization. *Annals of the The New York Academy of Sciences*, *914*(1), 104-111. DOI: 10.1111/j.1749-6632.2000.tb05188.x.

Jayanthi, S., Deng, X., Ladenheim, B., McCoy, M. T., Cluster, A., Cai, N. S., & Cadet, J. L. (2005). Calcineurin/NFAT-induced up-regulation of the Fas ligand/Fas death pathway is involved in methamphetamine-induced neuronal apoptosis. *Proceedings of the National Academy of Science*, *102*(3), 868-873. DOI: 10.1073/pnas.0404990101.

Jayanthi, S., Deng, X., Naoilles, P. A., Ladenheim, B., & Cadet, J. L. (2004). Methamphetamine induces neuronal apoptosis via cross-talks between endoplasmic reticulum and mitochondria-dependent death cascades. *FASEB Journal*, *18*(2), 238-251. DOI: 10.1096/fj.03-0295com.

Jayanthi, S., Ladenheim, B., Andrews, A. M., & Cadet, J. L. (1998). Overexpression of human copper/zinc superoxide dismutase in transgenic mice attenuates oxidative stress caused by methylenedioxymethamphetamine (Ecstasy). *Neuroscience*, *91*(4), 1379-1387. DOI: 10.1016/S0306-4522(98)00696-8.

Jayanthi, S., McCoy, M. T., Beauvais, G., Ladenheim, B., Gilmore, K., Wood, W., & Cadet, J. L. (2009). Methamphetamine induces dopamine D1 receptor-dependent endoplasmic reticulum stress-related molecular events in the rat striatum. *PLoS One* *4*(6), e6092. DOI: 10.1371/journal.pone.0006092.

- Jazwa, A., & Cuadrado, A. (2010). Targeting heme oxygenase-1 for neuroprotection and neuroinflammation in neurodegenerative diseases. *Current Drug Targets*, 11(12), 1517-1531.
- Jones, S. R., Gainetdinov, R. R., Jaber, M., Giros, B., Wightman, R. M., & Caron, M. G. (1998). Profound neuronal plasticity in response to inactivation of the dopamine transporter. *Proceedings of the National Academy of Sciences of the United States of America*, 95(7), 4029-4034. DOI: 10.1073/pnas.95.7.4029.
- Jung, Y., Nakano, K., Liu, W., Gallick, G. E., & Ellis, L. M. (1999). Extracellular Signal-related Kinase Activation Is Required for Upregulation of Vascular Endothelial Growth Factor by Serum Starvation in Human Colorectal Cancer Cells. *Cancer Research*, 59(19), 4804-4807.
- Junn, E., & Mouradian, M. M. (2001). Apoptotic signaling in dopamine-induced cell death: the role of oxidative stress, p38 mitogen-activated protein kinase, cytochrome c and caspases. *Journal of Neurochemistry*, 78(2), 374-383. DOI: 10.1046/j.1471-4159.2001.00425.x.
- Karila, L., Weinstein, A., Aubin, H. J., Benyamina, A., Renaud, M., & Batki, S. L. (2010). Pharmacological approaches to methamphetamine dependence: a focused review. *British Journal of Clinical Pharmacology*, 69(9), 578-592. DOI: 10.1111/j.1365-2125.2010.03639.x.

Keller, J. N., Kindy, M. S., Holtsberg, F. W., St Clair, D. K., Yen, H. C. Germeyer, A.,...Mattson, M. P. (1998). Mitochondrial manganese superoxide dismutase prevents neural apoptosis and reduces ischemic brain injury: suppression of peroxynitrite production, lipid peroxidation, and mitochondrial dysfunction. *Journal of Neuroscience*, 18(2), 3414-3422. DOI: 10.1523/JNEUROSCI.18-02-00687.1998.

Kinningham, K. K., Oberley, T. D., Sin, S., Mattingly, C. A., & St Clair, D. K. (1999). Overexpression of manganese superoxide dismutase protects against mitochondrial-initiated poly(ADP-ribose) polymerase-mediated cell death. *FASEB Journal*, 13(12), 1601-1610.

Kinningham, K., & St. Clair, D. K. (1997). Overexpression of manganese superoxide dismutase selectively modulates the activity of Jun-associated transcription factors in fibrosarcoma cells. *Cancer Research*, 57(23), 5265-5271.

Kinningham, K. K., Xu, Y., Daosukho, C., Popova, B., & St Clair, D. K. (2001). NF- κ B dependent mechanisms coordinate the synergistic effect of TPA and cytokines on SOD2 induction. *Biochemistry Journal*, 353(Pt 1), 147-156.

Kita, T., Wagner, G. C., & Nakashima, T. (2003). Current research on methamphetamine-induced neurotoxicity: animal models of monoamine disruption. *Journal of Pharm* 92(3), 178-195. DOI: 10.1254/jphs.92.178.

- Kitamura, Y., Furukawa, M., Matsuoka, Y., Tooyama, I., Kimura, H., Nomura, Y., & Taniguchi, T. (1998). In vitro and in vivo induction of heme oxygenase-1 in rat glial cells: possible involvement of nitric oxide production from inducible nitric oxide synthase. *Glia*, 22(2), 138-148. DOI: 10.1002/(SICU)1098-1136(199802)22:2<138::AID-GLIA5>3.0.CO;2-3.
- Klivenyi, P., St Clair, D., Wemer, M., Yen, H. C., Oberley, T., Yang, L., & Flint Beal, M. (1998). Manganese superoxide dismutase overexpression attenuates MPTP toxicity. *Neurobiology of Disease*, 5(4), 253-258. DOI: 10.1006/nbdi.1998.0191.
- Komjáti, K., Mabley, J. G., Viraq, L., Southan, G. J., Salzman, A. L., & Szabo, C. (2004). Poly(ADP-ribose) polymerase inhibition protect neurons and the white matter and regulates the translocation of apoptosis-inducing factor in stroke. *Internal Journal of Molecular Medicine*, 13(3), 373-382. DOI: 10.3892/ijmm.13.3.373.
- Krasnova, I. N., & Cadet, J. L. (2009). Methamphetamine toxicity and messengers of death. *Brain Research Review*, 60(2), 379-407. DOI: 10.1016/j.brainresrev.2009.03.002.
- Laemmli, U. K. (1970). Cleavage of structural proteins during the assembly of the head of bacteriophage T4. *Nature* 227(5259), 680-685.
- Landry, J., & Huot, J. (1995). Modulation of actin dynamics during stress and physiological stimulation by a signaling pathway involving p38 MAP kinase and heat-shock protein 27. *Biochemistry and Cell Biology*, 73(9-10), 703-707. DOI: 10.1139/o95-078.

- Larson, E. B., Akkenti, F., Edwards, S., Graham, D. L., Simmons, D. L., Alibhai, I. N., . . . Self, D. W. (2010). Striatal regulation of Δ FosB, FosB, and cFos during cocaine self-administration and withdrawal. *Journal of Neurochemistry*, *115*(1), 112-122. DOI: 10.1111/j.1471-4159.2010.06907.x.
- Laruelle, M., Abi-Dargham, A., van Dyck, C. H., Rosenblatt, W., Zea-Ponce, Y., Zoghbi, S. S., . . . Kung, H. F. (1995). SPECT imaging of striatal dopamine release after amphetamine challenge. *Journal of Nuclear Medicine*, *36* (7):1182-1190.
- LaVoie, M. J., Card, J. P., & Hastings, T. G. (2004). Microglial activation precedes dopamine terminal pathology in methamphetamine-induced neurotoxicity. *Experimental Neurology*, *187*(1), 47-57. DOI: 10.1016/j.expneurol.2004.01.010.
- LaVoie, M., & Hastings, T. (1999). Peroxynitrite- and nitrite-induced oxidation of dopamine: implications for nitric oxide in dopaminergic cell loss. *Journal of Neurochemistry*, *73*(6), 2546-2554. DOI: 10.1046/j.1471-4159.1999.0732546.x.
- Lazebnik, Y. A., Kaufmann, S. H., Desnoyers, S., Poirier, G. G., & Earnshaw, W. C. (1994). Cleavage of poly(ADP-ribose) polymerase by a proteinase with properties like ICE. *Nature*, *37*(6495), 346-347. DOI: 10.1038/371346a0.
- Lee, K. W., Kim, Y., Kim, A. M., Kelmin, D., Nairn, A. C., Greengard, P. (2006). Cocaine-induced dendritic spine formation in D1 and D2 dopamine receptor-containing medium spiny neurons in nucleus accumbens. *Proceedings of the National Academy of Sciences in the United States of America*, *103*(9), 3399-3404. DOI: 10.1073/pnas.0511244103.

- Li, P., Nijhawan, D., Budihardjo, I., Srinivasula, S. M., Ahmad, M., Alnemri, E. S., & Wang, X. (1997). Cytochrome c and dATP-dependent formation of Apaf-1/caspase-9 complex initiates an apoptotic protease cascade. *Cell*, *91*(4):479-489. DOI:10.1016/S0092-8674(00)80434-1.
- Li, Y., Huang, T. T., Carlson, E. J., Melov, S., Ursell, P. C., Olson, J. L., . . . Epstein, C. J. (1995). Dilated cardiomyopathy and neonatal lethality in mutant mice lacking manganese superoxide dismutase. *Nature Genetics*, *11*(4), 376-381. DOI: 10.1038/np1295-376.
- Liu, L., Cavanaugh, J. E., Wang, Y., Sakagami, H., Mao, Z., & Mia, Z. (2003). ERK5 activation of MEF2-mediated gene expression plays a critical role in BDNF-promoted survival of developing but not mature cortical neurons. *Proceedings of the National Academy of Sciences in the United States of America*, *100*(14), 8532-8537. DOI: 10.1073/pnas.1332804100.
- MacMillan-Crow, L. A., Crow, J. P., & Thompson, J. A. (1998). Peroxynitrite-mediated inactivation of manganese superoxide dismutase involves nitration and oxidation of critical tyrosine residues. *Biochemistry*, *37*(6), 1613-1622. DOI: 10.1021/bi971894b.
- MacMillan-Crow, L. A., & Thompson, J. A. (1999). Tyrosine modifications and inactivation of active site manganese superoxide dismutase mutant (Y34F) by peroxynitrite. *Archives of Biochemistry and Biophysics*, *366*(1), 82-88. DOI: 10.1006/abbi.1999.1202.
- Maines, M. D. (2000). The heme oxygenase system and its functions in the brain. *Cellular and Molecular Biology*, *46*(3):573-85.

- Maragos, W. F., Jakel, R., Chesnut, D., Pocernich, C. B., Butterfield, D. A., St Clair, D., & Cass, W. A. (2000). Methamphetamine toxicity is attenuated in mice that overexpress human manganese superoxide dismutase. *Brain Research*, 878(1-2), 218-222. DOI: 10.00068993.
- Marks-Konczalik, J., Chu, S. C., & Moss, J. (1998). Cytokine-mediated transcriptional induction of the human inducible nitric oxide synthase gene requires both activator protein 1 and nuclear factor kappaB-binding sites. *Journal of Biological Chemistry*, 273(35), 22201-22208. DOI: 10.1074/jbc.273.35.22201.
- Martin, T. A., Jayanthi, S., McCoy, M. T., Brannock, C., Ladenheim, B., Garrett, T., . . . Cadet, J. L. (2012). Methamphetamine causes differential alterations in gene expression and patterns of histone acetylation/hypoacetylation in the rat nucleus accumbens. *PLoS One*, 7(3):e34236. DOI: 10.1371/journal.pone.0034236.
- McCann, U. D., Wong, D. F., Yokoi, F., Villenmagne, V., Dannals, R. F., & Ricaurte, G. A. (1998). Reduced striatal dopamine transporter density in abstinent methamphetamine and methcathinone users: evidence from positron emission tomography studies with [11C]WIN-35,428. *Journal of Neuroscience*, 18(20), 8417-8420. DOI: 10.1523/JNEUROSCIE.18-20-08417.1998.
- McCann, U. D., Kuwabara, H., Kumar, A., Palermo, M., Abbey, R., Brasic, J., . . . Ricaurte, G. A. (2008). Persistent cognitive and dopamine transporter deficits in abstinent methamphetamine users. *Synapse*, 62(2), 91-100. DOI: 10.1002/syn.20471.

- McLeman, E. R., Warsh, J. J., Ang, L., Li, P. P., Kalasinsky, K. S., Ross, B. M., . . . Kish, S. J. (2008). The human nucleus accumbens is highly susceptible to G protein down-regulation by methamphetamine and heroin. *Journal of Neurochemistry*, *74*(5), 2120-2126. DOI: 10.1046/j.1471-4159.2000.0742120.x.
- Mearow, K. M., Dodge, M. E., Rahimtula, M., & Yegappan, C. (2002). Stress-mediated signaling in PC12 cells - the role of the small heat shock protein, Hsp27, and Akt in protecting cells from heat stress and nerve growth factor withdrawal. *Journal of Neurochemistry*, *83*(2), 452-462. DOI:10.1046/j.1471-4159.2002.01151.x.
- Mehindate, K., Sahlas, D. J., Frankel, D., Mawai, Y., Liberman, A., Corcos, J., . . . Schipper, H. M. (2001). Proinflammatory cytokines promote glial heme oxygenase-1 expression and mitochondrial iron deposition: implications for multiple sclerosis. *Journal of Neurochemistry*, *77*(5):1386-1395. DOI: 10.1046/j.1471-4159.2001.00354.x.
- Mirecki, A., Fitzmaurice, P., Ang, L., Kalasinsky, D. S., Peretti, F. J., Aiken, S. S., . . . Kish, S. J. (2004). Brain antioxidant systems in human methamphetamine users. *Journal of Neurochemistry*, *89*(6), 1396-1408. DOI: 10.1111/j.1471-4159.2004.02434.x.
- Missale, C., Nash, S. R., Ribinson, S. W., Jaber, M., & Caron, M. G. (1998). Dopamine receptors: from structure to function. *Physiology Reviews*, *78*(1), 189-225. DOI: 101152/physrev.199878.1.189.
- Morgan, D., Grant, K. A., Gage, H. D., Mach, R. H., Kaplan, J. R. Prioleau, O., . . . Nader, M. A. (2002). Social dominance in monkeys: dopamine D2 receptors and cocaine self-administration. *Nature Neuroscience*, *5*(2), 169-174. DOI: 10.1038/nn798.

- Moussa, C. E., Tomita, Y., & Sidhu, A. (2006). Dopamine D1 receptor-mediated toxicity in human SK-N-MC neuroblastoma cells. *Neurochemistry International*, 48(3), 226-234. DOI: 10.1016/j.neuint.2005.09.007.
- Naughton, P. Foresti, R., Bains, S. K., Hoque, M., Green, C. J., & Motterlini, R. (2002). Induction of heme oxygenase 1 by nitrosative stress. A role for nitroxyl anion. *Journal of Biological Chemistry*, 277(43), 40666-4074. DOI: 10.1074/jbc.M203863200.
- O'Dell, S. J., Weihmuller, F. B., & Marshall, J. F. (1991). Multiple methamphetamine injections induce marked increases in extracellular striatal dopamine which correlate with subsequent neurotoxicity. *Brain Research*, 564(2), 256-260. DOI: 10.1016/0006-8993(91)91461-9.
- O'Dell, S. J., Weihmuller, F. B., & Marshall, J. F. (1993). Methamphetamine-induced dopamine overflow and injury to striatal dopamine terminals: attenuation by dopamine D1 or D2 antagonists. *Journal of Neurochemistry*, 60(5):1792-9. DOI: 10.1111/j.1471-4159.1993.tb13405.x.
- Olive, M., Krylov, D., Echlin D. R., Gardner, D., Taparowsky, E., & Vinson, D. (1997). A dominant negative to activation protein-1 that abolishes DNA binding and inhibits oncogenesis. *Journal of Biological Chemistry*, 272(30), 18586-18594. DOI: 10.1074/jbc.272.30.18586.
- Oliver, F. J., de la Rubia, G., Roli, V., Ruiz-Ruiz, M. C., de Murcia, G., & Murcia, J. M. (1998). Importance of poly(ADP-ribose) polymerase and its cleavage in apoptosis. Lesson from an uncleavable mutant. *Journal of Biological Chemistry*, 273(50):33533-33539.

- Pandey, P., Farber, R., Nakazawa, A., Kumar, S., Bharti, A., Nalin C., . . . Kharbanda, S. (2000). Hsp27 functions as a negative regulator of cytochrome c-dependent activation of procaspase-3. *Oncogene*, *19*(16), 1975-1981. DOI: 10.1038/sj.onc.1203531.
- Parcellier, A., Gurvuxani, S., Schmitt, E., Solary, E., & Garrido, C. (2003). Heat shock proteins, cellular chaperones that modulate mitochondrial cell death pathways. *Biochemical and Biophysical Research Communications*, *304*(3), 505-512. DOI: 10.1016/S0006-291X(03)00623-5.
- Pautz, A., Art, J., Hahn, S., Nowag, S., Voss, C., & Kleinert, H. (2010). Regulation of the expression of inducible nitric oxide synthase. *Nitric Oxide* *23*(2), 75-93. DOI: 10.1016/niox.2010.04.007.
- Pramanik, R., Qi, X., Borowicz, S., Choubey, D., Schultz, R. M., Han, J., & Chen, G. (2003). p38 isoforms have opposite effects on AP-1-dependent transcription through regulation of c-Jun. The determinant roles of the isoforms in the p38 MAPK signal specificity. *Journal of Biological Chemistry*, *278*(7):4831-4839. DOI: 10.1074/jbc.M207732200.
- Preston, K. L., Wagner, G. C., Schuster, C. R., & Seiden, L. S. (1985). Long-term effects of repeated methylamphetamine administration on monoamine neurons in the rhesus monkey brain. *Brain Research*, *338*(2), 243-248. DOI: 10.1016/0006-8993(85)90153-2.
- Risco, A., & Cuedna, A. (2012). New insights into the p38 γ and p38 δ MAPK pathways. *Journal of Signal Transduction*, 520289. DOI: 10.1155/2012/520289.

- Roberts-Lewis, J. M., Roseboom, P. H., Iwaniec, L. M., & Gnegy, M. E. (1986). Differential down-regulation of D1-stimulated adenylate cyclase activity in rat forebrain after in vivo amphetamine treatments. *Journal of Neuroscience*, *6*(8), 2245-51. DOI: 10.1523/JNEUROSCI.06-08-02245.1986.
- Robinson, A. J., & Nestler, E. J. (2011). Transcriptional and epigenetic mechanisms of addiction. *Nature Review Neuroscience*, *12*(11), 623-637. DOI: 10.1038/nrn3111.
- Robinson, T. E., & Berridge, K. C. (1993). The neural basis of drug craving: an incentive-sensitization theory of addiction. *Brain Research Reviews*, *18*(3), 247-291. DOI: 10.1016/0165-0173(93)90013-P.
- Rojo, A., Innamorato, N. G., Martin-Moreno, A. M., De Ceballos, M. L., Yamamoto, M., & Cuadrado, A. (2010). Nrf2 regulates microglial dynamics and neuroinflammation in experimental Parkinson's disease. *Glia*, *58*(5):588-598. DOI: 10.1002/glia.20947.
- Rosenberg, P. A. (1988). Catecholamine toxicity in cerebral cortex in dissociated cell culture. *Journal of Neuroscience*, *8*(8), 2887-2894. DOI: 10.1523/JNEUROSCI.08-08-02887.1988.
- Salo, R., Nordahl, T. E., Moore, C., Waters, C., Natsuaki, Y., Galloway, G. P., . . . Sullivan, E. V. (2005). A dissociation in attentional control: evidence from methamphetamine dependence. *Biological Psychiatry* *57*(3), 310-313. DOI: 10.1016/j.biopsych.2004.10.035.

- Salo, R., Nordahal, T. E., Natsuaki, Y., Leamon, M. H., Galloway, G. P., Waters, C., . . .
Buonocore, M. H. (2007). Attentional control and brain metabolite levels in
methamphetamine abusers. *Biological Psychiatry*, *61*(11), 1272-1280. DOI:
10.1016/j.biopsych.2006.07.031.
- Schipper, H. M. (2004). Heme oxygenase expression in human central nervous system disorders.
Free Radical Biology and Medicine, *37*(12), 1995-2011. DOI:
10.1016/j.freeradbiomed.2004.09.015.
- Schipper, H. M., Bennett, D. A., Liberman, A., Vienias, J. L., Schneider, J. A., Kelly, J., &
Arvanitakis, Z. (2006). Glial heme oxygenase-1 expression in Alzheimer disease and
mild cognitive impairment. *Neurobiology of Aging*, *27*(2):252-261. DOI:
10.1016/j.neurobiolaging.2005.01.016.
- Schipper, H. M., Chertkow, H., Mehindate, K., Frankel, D., Melmed, C., & Bergman, H. (2000).
Evaluation of heme oxygenase-1 as a systemic biological marker of sporadic AD.
Neurology, *54*(6), 1297-1304.
- Schipper, H. M., Song, W., Zukor, H., Hascalovici, J. R., & Zeligman, D. (2009). Heme
oxygenase-1 and neurodegeneration: expanding frontiers of engagement. *Journal of
Neurochemistry*, *110*(2), 469-485. DOI: 10.1111/j.1471-4159.2009.06160.x.
- Schmidt, C. J., Ritter, J. K., Sonsalla, P. K., Hanson, G. R., & Gibb, J. W. (1985). Role of
dopamine in the neurotoxic effects of methamphetamine. *Journal of Pharmacology and
Experimental Therapeutics*, *233*(3), 539-544.

- Schreiber, M. A., & McIntire, S. L. (2011). A *Caenorhabditis elegans* p38 MAP kinase pathway mutant protects from dopamine, methamphetamine, and MDMA toxicity. *Neuroscience Letter*, *498*(1), 99-103. DOI: 10.1016/j.neulet.2011.04.071.
- Seiden, L. S., Fischman, M. W., & Schuster, C. R. (1976). Long-term methamphetamine induced changes in brain catecholamines in tolerant rhesus monkeys. *Drug and Alcohol Dependence*, *1*(3), 215-9.
- Seiden, L. S., & Vosmer, G. (1984). Formation of 6-hydroxydopamine in caudate nucleus of rat brain after a single large dose of methamphetamine. *Pharmacology Biochemistry and Behavior*, *21*(1), 29-31.
- Sekine, Y., Ouchi, Y., Sigihara, G., Takei, N., Yoshikawa, E., Nakamura, K., . . . Cadet, J. L. (2008). Methamphetamine causes microglial activation in the brains of human abusers. *Journal of Neuroscience*, *28*(22), 5756-5761. DOI: 10.1523/JNEUROSCI.1179-08.2008.
- Shaulian, E., & Karin, M. (2001). AP-1 in cell proliferation and survival. *Oncogene*, *20*(19), 2390-2400. DOI: 10.1038/sj.onc.1204383.
- Shaulian, E., & Karin, M. (2002). AP-1 as a regulator of cell life and death. *Nature Cell Biology*, *4*(5), 131-136. DOI: 10.1038/ncb0502-e131.
- Shi, G., Jin, L., & Andres, D. A. (2011). A rit GTPase-p38 mitogen-activated protein kinase survival pathway confers resistance to cellular stress. *Molecular and Cellular Biology*, *31*(10), 1938-1948. DOI: 10.1128/MCB.01380-10.

- Shuto, T., Kuroiwa, M., Hamamura, M., Yabuuchi, K., Shimazoe, T. Watanabe, S., . . . Yamamoto, T. (2006). Reversal of methamphetamine-induced behavioral sensitization by repeated administration of a dopamine D1 receptor agonist. *Neuropharmacology*, *50*(8), 991-997. DOI: 10.1016/j.neuropharm.2006.01.009.
- Sidhu, A., & Fishman, P. (1990). Identification and characterization of functional D1 dopamine receptors in a human neuroblastoma cell line. *Biochemical and Biophysical Research Communication*, *166*(2), 574-579. DOI: 10.1016/0006-291X(90)90847-G.
- Smeyne, R. J., Vendrell, M., Hayward, M., Baker, S. J., Miao, G. G., Schilling, K., . . . Morgan, J. I. (1993). Continuous c-fos expression precedes programmed cell death in vivo. *Nature*, *363*(6425):166-169. DOI: 10.1038/363166a0.
- Song, L., Song, W., & Schipper, H. M. (2007). Astroglia overexpressing heme oxygenase-1 predispose co-cultured PC12 cells to oxidative injury. *Journal of Neuroscience Research*, *85*(10), 2186-2195.
- Song, W., Su, H., Song, S., Paudel, H. K., & Schipper, H. M. (2006). Over-expression of heme oxygenase-1 promotes oxidative mitochondrial damage in rat astroglia. *Journal of Cell Physiology*, *206*(3), 655-663. DOI: 10.1002/jcp.20509.
- Sonsalla, P. K., Gibb, J., & Hanson, G. R. (1986). Roles of D1 and D2 dopamine receptor subtypes in mediating the methamphetamine-induced changes in monoamine systems. *Journal of Pharmacology and Experimental Therapeutics*, *238*(3), 932-7.

- Spielewoy, C., Gonon, F., Roubert, C., Fauchey, V., Jaber, M., Caron, M. G., . . . Giros, B. (2000). Increased rewarding properties of morphine in dopamine-transporter knockout mice. *European Journal of Neuroscience*, *12*(5), 1827-1837.
- Spitz, D. R., Malcolm, R. R., & Roberts, R. J. (1990). Cytotoxicity and metabolism of 4-hydroxy-2-nonenal and 2-nonenal in H2O2-resistant cell lines. Do aldehydic by-products of lipid peroxidation contribute to oxidative stress? *Biochemistry Journal*, *267*(2), 453-459.
- Squadrito, G., & Pryor, W. (1998). Oxidative chemistry of nitric oxide: the roles of superoxide, peroxynitrite, and carbon dioxide. *Free Radical Biology and Medicine*, *25*(4-5), 392-403. DOI: 10.1016/S0891-5849(98)00095-1.
- St. Clair, D. K., Porntadavity, S., Xu, Y., Kinningham, K., (2002). Transcription regulation of human manganese superoxide dismutase gene. *Methods of Enzymology*, *349*, 306-12.
- Stokes, A. H., Hastings, T. G., & Vrana, K. E. (1999). Cytotoxic and genotoxic potential of dopamine. *Journal of Neuroscience Research*, *55*(6), 659-65. DOI: 10.1002/(SICI)1097-4547(19990315)55:6<659::AID-JNRI>3.0.CO;2-C.
- Sulzer, D., Chen, T. K., Lau, Y. Y., Kristensen, H., Rayport., & Ewing, A. (1995). Amphetamine redistributes dopamine from synaptic vesicles to the cytosol and promotes reverse transport. *Journal of Neuroscience*, *15*(5 pt 2), 4102-4108. DOI: 10.1523/JNEUROSCI.15-05-04102.1995.
- Sun, Y., & Oberley, L.W. (1996). Redox regulation of transcription factors. *Free Radical Biology and Medicine*, *21*(3), 335-348. DOI: 10.1016/0891-5849(96)00109-8.

- Susin, S. A., Daugas, E., Ravagnan, L., Samejima, K., Zamzami, N., Loeffler, M., ... Kroemer, G. (2000). Two distinct pathways leading to nuclear apoptosis. *The Journal of experimental medicine*, 192(4), 571-80. DOI: 10.1084/jem.192.4.571.
- Susin, S. A., Lorenzo, H. K., Zamzami, N., Marzo, I., Snow, B. E., Brothers, G. M., ... Kroemer, G. (1999). Molecular characterization of mitochondrial apoptosis-inducing factor. *Nature*, 397(6718), 441-446. DOI: 10.1038/17135.
- Tanno, M., Gorog, D. A., Bellachcne, M., Cao, X., Quinlan, R. A., & Marber, M. S. (2003). Tumor necrosis factor-induced protection of the murine heart is independent of p38-MAPK activation. *Journal of Molecular and Cellular Cardiology*, 35(12):1523-1527. DOI: 10.1016/j.yjmcc.2003.09.019.
- Theodore, M., Kawai, Y., Yang, J., Kleshchenko, Y., Reddy, S. P., Villalta, F., & Arinze, I. J. (2008). Multiple nuclear localization signals function in the nuclear import of the transcription factor Nrf2. *The Journal of biological chemistry*, 283(14), 8984-94. DOI: 10.1074/jbc.M709040200.
- Thomas, D. M., & Kuhn, D. M. (2005). MK-801 and dextromethorphan block microglial activation and protect against methamphetamine-induced neurotoxicity. *Brain Research*, 1050(1-2), 190-198. DOI: 10.1016/j.brainres.2005.05.049.
- Thomas, D. M., Walker, P. D., Benjamins, J. A., Geddes, T. J., & Kuhn, D. M., (2004). Methamphetamine neurotoxicity in dopamine nerve endings of the striatum is associated with microglial activation. *Journal of Pharmacology and Experimental Therapeutics*, 311(1), 1-7. DOI: 10.1124/jpet.104.070961.

- Thompson, P. M., Hayashi, K. M., Simon, S. L., Geaga, J. A., Hong, M. S., Sui, Y., . . . London, E.D. (2004). Structural abnormalities in the brains of human subjects who use methamphetamine. *Journal of Neuroscience*, *24*(26), 6028-6036. DOI: 10.1523/JNEUROSCI.0713-04.2004.
- Tong, J., Ross, B., M., Schmunk, G. A., Peretti, F. J., Kaasinsky, K. S., Furukawa, Y., . . . Kish, S. J. (2003). Decreased striatal dopamine D₁ receptor-stimulated adenylyl cyclase activity in human methamphetamine users. *American Journal of Psychiatry*, *160*(5), 896-903. DOI: 10.1176/appi.ajp.160.5.896.
- Torgerson, T. R., Colosia, A. D., Donahue, J. P., Lin, Y. Z., & Hawiger, J. (1998). Regulation of NF- κ B, AP-1, NFAT, and STAT1 nuclear import in T lymphocytes by noninvasive delivery of peptide carrying the nuclear localization sequence of NF- κ B. *Journal of Immunology*, *161*(11), 6084-6092.
- The United Nations Office on Drugs and Crime (2012). World Drug Report 2012. United Nations publication, Sales No. E.12.XI.1.
- Vanderschuren, L., Schoffelmeer, A. N., Mulder, A. H., & De Vries, T. J. (1999). Dopaminergic mechanisms mediating the long-term expression of locomotor sensitization following pre-exposure to morphine or amphetamine. *Psychopharmacology (Berl)*, *143*(3), 244-253.
- van Gaalen, M. M., Brueggeman, R. J., Bronium, P. F., Schoffelmeer, A. N., & Vanderschuren, L. J. (2006). Behavioral disinhibition requires dopamine receptor activation. *Psychopharmacology (Berl)*, *187*(1), 73-85. DOI: 10.1007/s00213-006-0396-1.

Veeneman, M. M., Broekhoven, M. H., Damsteegt, R., & Vanderschuren, L. J. (2011). Distinct contributions of dopamine in the dorsolateral striatum and nucleus accumbens shell to the reinforcing properties of cocaine. *Neuropsychopharmacology: official publication of the American College of Neuropsychopharmacology*, 37(2), 487-98. DOI: 10.1038/npp.2011.209.

Villemagne, V., Yuan, H., Wong, D. F., Dannals, R. F., Hatzidimitriou, G., Mathews, W. B., . . . Ricaurte, G. A. (1998). Brain dopamine neurotoxicity in baboons treated with doses of methamphetamine comparable to those recreationally abused by humans: evidence from [11C]WIN-35,428 positron emission tomography studies and direct in vitro determinations. *Journal of Neuroscience*, 18(1), 419-27. DOI: 10.1523/JNEUROSCI.18-01-00419.1998.

Volkow, N. D., Chang, L., Wang, G., J., Fowler, J. S., Ding, Y. S., Sedler, M., . . . Pappas, N. (2001c). Low level of brain dopamine D₂ receptors in methamphetamine abusers: association with metabolism in the orbitofrontal cortex. *American Journal of Psychiatry*, 158(12), 2015-2021. DOI: 10.1176/appi.ajp.158.12.2015.

Volkow, N. D., Chang, L., Wang, G., J., Fowler, J. S., Franceschi, D., Sedler, M., . . . Logan, J. (2001b). Loss of dopamine transporters in methamphetamine abusers recovers with protracted abstinence. *Journal of Neuroscience*, 21(23), 9414-9418. DOI: 10.1523/JNEUROSCI.21-23-09414.2001.

- Volkow, N. D., Chang, L., Wang, G. J., Fowler, J. S., Leonido-Yee, M., Franceschi, D., . . . Miller, E. N. (2001a). Association of dopamine transporter reduction with psychomotor impairment in methamphetamine abusers. *American Journal of Psychiatry*, *158*(3), 377-382. DOI: 10.1176/appi.ajp.158.3.377.
- Volkow, N. D., Fowler, J. S., Wang, G. J., Shumay, E., Telang, F., Thanos, P. K., & Alexoff, D. (2010). Distribution and pharmacokinetics of methamphetamine in the human body: clinical implications. *PloS one*, *5*(12), e15269. DOI:10.1371/journal.pone.0015269.
- Volkow, N. D., Fowler, J. S., Wang, G. J., & Swanson, J. M. (2004). Dopamine in drug abuse and addiction: results from imaging studies and treatment implications. *Molecular Psychiatry*, *9*(6), 557-569. DOI: 10.1038/sj.mp.4001507.
- Wagner, G. C., Carelli, R. M., & Jarvis, M. F. (1985). Pretreatment with ascorbic acid attenuates the neurotoxic effects of methamphetamine in rats. *Research Communications in Chemical Pathology and Pharmacology*, *47*(2), 221-228.
- Wang, M., Wong, A. H., & Liu, F. (2012) Interactions between NMDA and dopamine receptors: A potential therapeutic target. *Brain Research*, *2*(1476), 154-163. DOI: 10.1016/j.brainres.2012.03.029.
- Wang, S. F., Yen, J. C., Yin, P. H., Chi, C. W., & Lee, H. E. (2008). Involvement of oxidative stress-activated JNK signaling in the methamphetamine-induced cell death of human SH-SY5Y cells. *Toxicology*, *246*(2-3), 234-241. DOI: 10.1016/j.tox.2008.01.020.

- Wilson, J. M., Kalasinsky, K. S., Levey, A. I., Bergeron, C., Reiber, G., Anthony, R. M., . . . Kish, S. J. (1996). Striatal dopamine nerve terminal markers in human, chronic methamphetamine users. *Nature Medicine*, 2(6), 699-703.
- Woolverton, W. L., Ricaurte, G. A., Forno, L. S., & Seiden, L. S. (1989). Long-term effects of chronic methamphetamine administration in rhesus monkeys. *Brain Research*, 486(1), 73-78. DOI: 10.1016/0006-8993(89)91279-1.
- Worsley, J. N., Moszczynska, A., Falardeau, P., Kalasinshky, K. S., Schmunk, G., Guttman, M., & Kish, S. J. (2000). Dopamine D1 receptor protein is elevated in nucleus accumbens of human, chronic methamphetamine users. *Molecular Psychiatry*, 5(6), 664-72.
- Wu, C. W., Ping, Y. H., Yen, J. C., Chang, C. Y. Wang, S. F., Yeh, C. L., . . . Lee, H. C. (2007). Enhanced oxidative stress and aberrant mitochondrial biogenesis in human neuroblastoma SH-SY5Y cells during methamphetamine induced apoptosis. *Toxicology and Applied Pharmacology*, 220(3), 243-51. DOI: 10.1016/j.taap.2007.01.011.
- Xu, W., Zhu, J. P., & Angulo, J. A. (2005). Induction of striatal pre- and postsynaptic damage by methamphetamine requires the dopamine receptors. *Synapse (New York, N.Y.)*, 58(2), 110-121. DOI: 10.1002/syn.20185.
- Yamamoto, B. K., and Zhu, W. (1998). The effects of methamphetamine on the production of free radicals and oxidative stress. *Journal of Pharmacology and Experimental Therapeutics*, 287(1), 107-114.

- Zafar, K. S., Inayat-Hussain, S. H., Siegel, D., Bao, A., Shieh, B., & Ross, D. (2006). Overexpression of NQO1 protects human SK-N-MC neuroblastoma cells against dopamine-induced cell death. *Toxicology Letter*, *166*(3), 261-267. DOI: 10.1016/j.toxlet.2006.07.340.
- Zhen, X., Uryu, K., Want, H. Y., & Friedman, E. (1998). D1 dopamine receptor agonists mediate activation of p38 mitogen-activated protein kinase and c-Jun amino-terminal kinase by a protein kinase A-dependent mechanism in SK-N-MC human neuroblastoma cells. *Molecular Pharmacology*, *54*(3), 453-458. DOI: 10.1124/mol54.3.453.
- Zhou, G., Bao, Z., & Dixon, J. (1995). Components of a new human protein kinase signal transduction pathway. *Journal of Biological Chemistry*, *270*, 12665-9. DOI: 10.1074/jbc.270.21.12665.
- Zhu, J. P., Xu, W., & Angulo, J. A. (2006). Methamphetamine-induced cell death: selective vulnerability in neuronal subpopulations of the striatum in mice. *Neuroscience*, *140*(2), 607-22. DOI: 10.1016/j.neuroscience.2006.02.055.

APPENDIX A: APPROVAL LETTER



Office of Research Integrity

November 7, 2018

Melinda L. Asbury
2114 Sunset Ave
Durham, NC 27705

Dear Ms. Asbury:

This letter is in response to the submitted dissertation abstract entitled "*Mechanisms of Dopamine-Induced Methamphetamine Neurotoxicity*." After assessing the abstract it has been deemed not to be human subject research and therefore exempt from oversight of the Marshall University Institutional Review Board (IRB). The Code of Federal Regulations (45CFR46) has set forth the criteria utilized in making this determination. Since the study does not involve human subjects as defined in DHHS regulation 45 CFR §46.102(f) it is not considered human subject research. If there are any changes to the abstract you provided then you would need to resubmit that information to the Office of Research Integrity for review and determination.

I appreciate your willingness to submit the abstract for determination. Please feel free to contact the Office of Research Integrity if you have any questions regarding future protocols that may require IRB review.

Sincerely,

Bruce F. Day, ThD, CIP
Director

WE ARE... MARSHALL.

One John Marshall Drive • Huntington, West Virginia 25755 • Tel 304/696-4303
A State University of West Virginia • An Affirmative Action/Equal Opportunity Employer

APPENDIX B: ABBREVIATIONS

$\cdot\text{OH}$ —hydroxyl radical

3-NT—3-nitrotyrosine

4-HNE—4-hydroxy-2-nonenal

AIF—apoptosis-inducing factor

AMPH—amphetamine

ANOVA—analyses of data and variance

AP-1—activator protein 1

ATS—amphetamine type stimulants

CASP3—caspase 3

CASP9—caspase 9

CO—carbon monoxide

Cu/ZnSOD—copper/zinc superoxide dismutase

DA—dopamine

DAT—dopamine transporters

eNOS—endothelial nitric oxide synthase

ERK1/2—extracellular signal-related kinases 1 and 2

GAPDH—glyceraldehyde 3-phosphate dehydrogenase

H^+ —hydrogen ion

H_2O_2 —hydrogen peroxide

HO-1—heme oxygenase-1

HSP27—heat shock protein 27

HSP70—heat shock protein 70

iNOS—inducible nitric oxide synthase

JNK—c-Jun N-terminal kinase

MA—methamphetamine

MAO-A/B—monoamine oxidase A or B

MAPK—mitogen activated protein kinase

MnSOD—manganese superoxide dismutase

MTT —3-(4,5-dimethylthiazol-2-yl)-2,5-dephenyl tetrazolium bromide

NFκB—nuclear factor kappa B

nNOS—neuronal nitric oxide synthase

NOS—nitric oxide synthase

Nrf-2—nuclear factor E2-related factor

O₂—molecular oxygen

O₂^{•-}—superoxide radical

ONOO⁻—peroxynitrite

P-ERK 1/2—phosphorylated extracellular signal-related kinases 1 and 2

P-p38—phosphorylated p38

PARP—poly (ADP-ribose) polymerase

PEG-SOD—polyethylene glycol superoxide dismutase

RO/NS—reactive oxygen/nitrogen species

SB203580—inhibitor of p38 phosphorylation

SCH-23390—selective dopamine D1 receptor antagonist

S.E.M.—standard error of the mean

SKF-38393—selective dopamine D1 receptor agonist

SOD—superoxide dismutase

STAT—signal transducer and activator of transcription

TNF—tumor necrosis factor

TPA—tissue plasma activator or 12-O-tetradecanoylphorbol-13-acetate or phorbol ester

TUNEL—deoxynucleotidyl transferase-mediated dUTP nick-end labeling